HAPTIC SPATIAL UPDATING

Ahmed Nadeem

A THESIS SUBMITTED TO

THE FACULTY OF GRADUATE STUDIES

IN PARTIAL FULFILLMENT OF THE REQUIREMENTS

FOR THE DEGREE OF

MASTER OF SCIENCE

GRADUATE PROGRAM IN BIOLOGY

YORK UNIVERSITY

TORONTO, ONTARIO

August 2026

© Ahmed Nadeem, 2026

Abstract

Spatial updating refers to the process of updating representations of object locations as observers move. Yet spatial representations are not always updated perfectly. During visually simulated self-motion, visual updating errors occur in the direction of travel (Kim & Harris, 2024). However, reports of haptic updating errors are sparse. This thesis examines haptic spatial updating during active translation. Blindfolded participants haptically located an object on a tabletop, then remained stationary or moved laterally or anteroposteriorly by 30 or 60 cm before replacing the object at its remembered location. Self-motion produced overcompensatory biases opposite to the direction of travel, which increased with translation magnitude to approximately 5–20cm after 60cm steps. Placement precision also declined following self-motion. These findings show that haptic spatial updating during active translation systematically overestimates self-motion, diverging from reported visual updating patterns, and may reflect distortion introduced during transformation between haptic, self-motion, and response reference frames.

Acknowledgements

First and foremost, I would like to thank Dr. Laurence R. Harris for his truly unending support, wise counsel, thoughtful feedback, and remarkable patience with all my ideas and experiments. I cannot imagine, nor have I found any empirical evidence for, a kinder, more knowledgeable, or more extraordinary professor. His mentorship has been fundamental in shaping both this thesis and the person I am today.

I would also like to thank Dr. Laurie Wilcox for her thoughtful advice and for welcoming me into her lab meetings, where I had the opportunity to share my work, receive valuable feedback, and think more deeply about the project as it developed. I am also grateful to the members of my committee for their time, care, and dedication in reviewing this lengthy document and helping bring the thesis to its final form.

I am also deeply grateful to all the Harris Lab members, who first welcomed me as a volunteer in the lab and then helped me grow into an actual scientist. Thank you to Björn for all of the statistics and R help; to John for his poignant questions during lab meetings; and to Ambika for helping me learn how to read the literature and find my footing in the field. Thank you as well to Fatemeh, Rachel, and Cecilia for being present in lab meetings, listening patiently to my long presentations, and making the lab such a supportive place to learn and work.

I would also like to thank Connected Minds, and NSERC for supporting this research and for the scholarship funding that helped sustain me throughout these two years.

I am sincerely grateful to all the participants who volunteered their time for these experiments. Without their willingness to take part, this work would not have been possible.

Last, but certainly not least, I would like to thank my family for their unending support, patience, and advice; for listening to me babble endlessly about hands; and for allowing me to measure arm lengths and recruit them into multiple makeshift versions of the experiments that eventually became part of this thesis.

Table of Contents

Abstract ii

Acknowledgements iii

Table of Contents iv

List of Tables viii

List of Figures ix

1.0 Introduction 1

1.1 Visual localisation 1

1.2 Haptic localisation 3

1.3 Updating studies 5

1.3.1 Visual Updating 6

1.3.2 Haptic Updating 7

1.4 Outlined Plan of Experiments 8

2.0 Methods 11

2.1 Overview 11

2.2 Equipment 11

2.2.1 Setup and Stimuli 11

2.2.2 Table 13

2.2.3 OptiTrack System 13

2.2.4 Walkable Platform 13

2.2.5 Godot Program 15

2.2.5.1 Godot and OptiTrack Synchronization 15

2.3 Participants and Recruitment 16

2.4 Procedure 17

2.4.1 Training 17

2.4.2 Trial Sequence 17

2.4.3 Block Structure and Trial Counts 19

2.4.4 Experiment Specific Trial Structure 22

2.4.4.1 Experiment 1 22
2.4.4.2 Experiment 2 22
2.4.4.3 Experiment 3 23
2.4.4.4 Experiment 4 24
2.4.5 Post-experiment measures 25
2.5 Data Processing *25*
2.5.1 Data cleaning 25
2.5.2 Accuracy Analysis 26
2.5.3 Precision Analysis 28
2.5.4 Inferential Statistics 28
2.5.4.1 Linear Mixed-Effects Models for Experiments 1 and 2 29
2.5.4.2 Linear Mixed-Effects Models for Experiments 3 and 4 29
2.5.4.3 Relative Reach Analysis 30
3.0 Experiment 1 - Lateral self-motion (one step) **32**
3.1 Accuracy *32*
3.1.1 Accuracy of Control Conditions 32
3.1.2 Accuracy Post-Self-Motion Left/Right 33
3.1.3 Differences Across Depth Within Lateralities 37
3.1.4 Relative Reach and Lateral Bias 37
3.2 Precision *38*
3.2.1 Precision of Controls 38
3.2.2 Precision Post-Self-Motion Left/Right 39
3.3 Summary *41*
4.0 Experiment 2 Anteroposterior self-motion (one step) **42**
4.1 Accuracy *42*
4.1.1 Accuracy of Control Conditions 42
4.1.2 Accuracy Post Anteroposterior Self-Motion 43
4.1.3 Across lateralities 47
4.1.4 Relative Reach and Anteroposterior Bias 48
4.2 Precision *50*
4.2.1 Precision of Controls 50
4.2.2 Precision Post Anteroposterior Self-Motion 50

4.3 Summary 53

5.0 Experiment 3 - Lateral self-motion (multistep) **54**

5.1 Accuracy *54*

5.1.1 Accuracy of Control Conditions 54

5.1.2 Accuracy Post Multistep Self-Motion Left/Right 55

5.1.2.1 Effect of Target Position on Lateral Bias 57

5.1.2.2 Effect of Starting Position on Lateral Bias at Each Target Position 59

5.1.2.3 Effect of Step Magnitude on Lateral Bias 60

5.1.3 Relative Reach and Lateral Bias 62

5.2 Precision *63*

5.2.1 Precision of Controls 63

5.2.2 Precision Post-Self-Motion Left/Right 64

5.3 Summary *67*

6.0 Experiment 4 - Anteroposterior Self-motion (multistep) **69**

6.1 Accuracy *69*

6.1.1 Accuracy of Control Conditions 69

6.1.2 Accuracy Post Anteroposterior Self-motion 70

6.1.2.1 Forward Self-motion Anteroposterior Bias 72

6.1.2.2 Backward Self-motion Anteroposterior Bias 74

6.1.3 Relative Reach and Anteroposterior Bias 75

6.2 Precision *76*

6.2.1 Precision of Controls 76

6.2.2 Precision Post Anteroposterior Self-Motion 77

6.3 Summary *79*

7.0 Discussion **81**

7.1 General Summary of Findings *81*

7.1.1 Bias Findings 81

7.1.2 Precision Findings 82

7.2 Evaluation of the Hypotheses *83*

7.2.1 Bias Hypotheses (H1 and H2) 83

7.2.2 Precision Hypotheses (H3 and H4) 83

7.3 Direction of Bias and the Transformation of the Haptic Reference Frame After Self-Motion *84*
7.3.1 Stationary haptic replacement was relatively stable 84
7.3.2 Active self-motion introduced a directional updating error 85
7.3.3 Self-Motion Overestimation Is a Useful but Insufficient Explanation 86
7.3.3.1 Constraints on a Simple Self-Motion Overestimation Account 87
7.3.4 Comparison to Visual Experiments 88
7.3.4.1 – Comparison to Spatiotopic Visual studies 88
7.3.4.2 – Comparison with gaze and head-centered sensorimotor updating 89
7.3.5 Transformations of Reference Frames 90
7.4 Bias's Magnitude *94*
7.4.1 Initial Position 94
7.4.2 Movement Magnitude 95
7.4.3 Relative Reach's Contribution 95
7.5 Precision Loss After Self-Motion *96*
7.6 Limitations *97*
7.7 General Conclusion *99*
7.8 Future Directions *100*
References **102**
Appendix A: Post Experiment Surveys **117**
Post-Study Participant Experience *117*
Participant Background Questionnaire for Haptic Perception Study *118*

List of Tables

Table 3.1: Stationary control condition lateral bias across target positions:..... 33
Table 3.2: Experiment 1 stance-matched contrasts in signed lateral bias 35
Table 3.3: Experiment 1 across-target contrasts in signed lateral bias..... 36
Table 3.4: Experiment 1 stationary-control precision across target positions 39
Table 3.5: Experiment 1 self-motion versus stationary-control precision contrasts 39
Table 4.1: Experiment 2 stationary-control anteroposterior bias across target positions43
Table 4.2: Experiment 2 stance-matched contrasts in signed anteroposterior bias..... 46
Table 4.3: Experiment 2 across-depth contrasts in signed anteroposterior bias..... 47
Table 4.4: Experiment 2 stationary-control precision across target positions 50
Table 4.5: Experiment 2 self-motion versus stationary-control precision contrasts 52
Table 5.1: Experiment 3 stationary-control lateral bias across target positions 55
Table 5.2: Experiment 3 across-target contrasts in signed lateral bias..... 58
Table 5.3: Experiment 3 starting-position contrasts in signed lateral bias 59
Table 5.4: Experiment 3 step-magnitude contrasts in signed lateral bias 61
Table 5.5: Experiment 3 stationary-control precision across target positions 64
Table 5.6: Experiment 3 self-motion versus stationary-control precision contrasts 66
Table 5.7: Experiment 3 step-magnitude contrasts in precision 66
Table 6.1: Experiment 4 stationary-control anteroposterior bias across target positions69
Table 6.2: Experiment 4 (forward) anteroposterior bias contrasts 72
Table 6.3: Experiment 4 (forward) across-target contrasts in anteroposterior bias..... 73
Table 6.4: Experiment 4 (backward) anteroposterior bias contrasts..... 74
Table 6.5: Experiment 4 stationary-control precision across target positions 77
Table 6.6: Experiment 4 (forward) precision contrasts..... 78
Table 6.7: Experiment 4 (backward) precision contrasts 79
Table 7.1: Summary of the outcomes of the original hypotheses 84

List of Figures

Figure 1.1: Stylized summary of characteristic stationary localisation biases 5
Figure 1.2: Possible spatial updating outcomes after self-motion: 6
Figure 1.3: Schematic summary of the four hypotheses 10
Figure 2.1: Photograph of the experimental room and apparatus 12
Figure 2.2: Walkable platform configurations 14
Figure 2.3: Trial-sequence schematic..... 19
Figure 2.4: Spatial layouts and coordinate conventions for Experiments 1 and 2 20
Figure 2.5: Spatial layouts and coordinate conventions for Experiments 3 and 4 21
Figure 2.6: Accuracy and precision measures used across experiments 27
Figure 3.1: Experiment 1 object placement 34
Figure 3.2 Experiment 1 Lateral Bias 36
Figure 3.3 Experiment 1 relative reach and lateral bias 38
Figure 3.4: Experiment 1 stance-matched contrasts in endpoint variability 40
Figure 4.1: Experiment 2 object placements and anteroposterior bias..... 44
Figure 4.2: Experiment 2 across-laterality contrasts in signed anteroposterior bias..... 48
Figure 4.3: Experiment 2 Relative Reach and Anteroposterior Bias..... 49
Figure 4.4: Experiment 2 stance-matched contrasts in endpoint variability 51
Figure 5.1: Experiment 3 object placements and lateral bias 56
Figure 5.2: Experiment 3 lateral bias after self-motion 58
Figure 5.3: Experiment 3 step-magnitude contrasts in signed lateral bias 61
Figure 5.4: Experiment 3 Relative Reach and Lateral Bias 63
Figure 5.5: Experiment 3 self-motion versus stationary-control endpoint variability 65
Figure 6.1: Experiment 4 object placements and anteroposterior bias..... 71
Figure 6.2: Relative Reach and Anteroposterior Bias..... 76
Figure 6.3: Experiment 4 endpoint variability 77
Figure 7.1: Proposed transformation-chain account of apparent overestimation during haptic spatial updating..... 92

1.0 Introduction

A fundamental capacity of humans that is often treated as self-evident is the ability to determine the location of a point in space relative to oneself (also known as egocentric localisation) and to keep track of such a point before, during and after self-motion. In humans, spatial location can be described in three dimensions using Cartesian coordinates, which specify an object's position in metric terms relative to the body. Despite its common framing as a predominantly visual behaviour (Klier et al., 2008; Li & Angelaki, 2005; Toni et al., 1996), localisation of objects in the world encountered during our daily life often uses a combination of multiple sensory modalities including vision, as mentioned previously, audition (S. R. Oldfield & Parker, 1984), and haptics (Klatzky & Lederman, 1988) working together to enable us to localize objects in the world accurately and precisely. For the purposes of this thesis, haptic perception can be considered in terms of two relevant components: (i) tactile information which is based on stimuli contacting the skin, including cues related to pressure, texture, vibration, and temperature (Dassonville, 1995; Dijkerman & Medendorp, 2021), and (ii) proprioceptive information about the position and of the exploring limb (Kennedy, 1993; Strong, 1994). During active exploration, these tactile and proprioceptive signals may also be accompanied by kinaesthetic information about limb movement, allowing object properties and locations to be inferred relative to the body (Blumenfeld, 1937). In this thesis I will be looking at the limitations of haptic localisation in maintaining such a representation of an object's location after self-motion.

1.1 Visual localisation

In visual localisation tasks, participants briefly view a target and, after its removal, indicate its remembered location by touching the previously seen position (Forster et al., 2023; Henriques et al., 1998), adjusting a visual marker to the remembered position with a joystick (Kim & Harris, 2024), or pointing toward the remembered direction as a measure of position (Adamovich et al., 1998; Medendorp et al., 1999). Accuracy is typically quantified as displacement from the true target location along an axis of interest (Kim & Harris, 2024), as Euclidean distance (Adamovich et al., 2001), as a gain factor (Klier et

al., 2008; Medendorp, Tweed, et al., 2003), or as angular deviation relative to the body's midline (Hollins & Kelley, 1988; Newport et al., 2002). This accuracy is commonly assessed in terms of systematic bias, whereas response dispersion reflects precision (Soechting & Flanders, 1989). Visual localisation studies commonly examine targets within reachable space, which extend to ~75 cm from the participant (Fernández-Díaz & Travieso, 2011; Parseihian et al., 2014; Serino, 2019). For briefly presented targets at relatively near reachable distances, subsequent memory-guided localisations are often close to veridical, with responses typically dispersed by approximately 1–3 cm around the true target location and showing only a slight egocentric bias, such that positions are set slightly closer to the self (Adamovich et al., 1998; Westwood et al., 2003). Within a comparable near-range localisation distance, McIntyre et al. (1997, 1998) showed that increasing the response delay (0.5–8 s) produces a systematic egocentric drift, such that remembered target locations shift progressively closer to the self, with a pronounced change emerging after ~5 s reflecting a type of delay dependent distortion in visually encoded spatial memory.

When targets lie beyond reaching distance and responses are given by pointing rather than directly touching the same position, there is an even stronger bias towards the self with deviations of up to 15 cm towards the body when targets are further than 50 cm from the participant (Parseihian et al., 2014; Soechting & Flanders, 1989). This phenomenon of an increased bias towards the self when distance from the body increases will be referred to as a *positive egocentric bias* from here on in the context of remembered localisation. Based on these results, visual localisation appears not to be uniformly veridical: performance is typically accurate at short/no delays and nearer distances (Adamovich et al., 1998; Soechting & Flanders, 1989) but shows a robust tendency toward a positive egocentric bias when targets are farther away and/or must be remembered across delays in time (McIntyre et al., 1997). Thus, memory-guided visual localisation is often accurate under favourable spatial and temporal conditions, but it remains susceptible to systematic egocentric distortions under greater distance or memory demands.

1.2 Haptic localisation

In the haptic modality, localisation experiments use a similar methodology as visual localisation experiments: participants encode a target's location or orientation which is done via exploration with their hand to find the object without visual or auditory cues (Klatzky & Lederman, 1993). After contact with the target, participants encode its location, withdraw to a neutral position, and then attempt to reproduce the remembered location by returning the object (or the hand) to the original site (Nelson et al., 2018; Shimono et al., 2001), or by rotating a pointer to point to the target (Kappers & Schakel, 2011; Zuidhoek et al., 2004). Some haptic studies also investigate remembered spatial locations using open-loop pointing tasks analogous to those used in visual localisation research (Dassonville, 1995; Giudice et al., 2011, 2017). Because these paradigms share similar task demands, their findings can be compared to examine modality-specific differences in remembered spatial localisation.

Unfortunately, haptic localisation findings are less uniform than those reported in visual localisation. In the haptic domain, positive angular egocentric biases are frequently observed, often expressed as angular deviations toward the self (Kappers, 2007; Kappers & Schakel, 2011; Postma et al., 2008; Szubielska et al., 2024; Szubielska & Möhring, 2019; Volcic & Kappers, 2008), and a smaller subset reports significant positive egocentric localisation biases (towards the body) in Euclidean space, which can reach up to ~5 cm toward the self (Rincon-Gonzalez et al., 2011), particularly when stimuli are placed nearer the limits of reachable space (Jones et al., 2010, 2012; Kuling et al., 2016; Mugge et al., 2016). In contrast, placement-focused paradigms have reported distal (negative) localisation biases that can reach ~6–7 cm *away* from the veridical object location (Jones et al., 2012; Wako & Ayabe-Kanamura, 2016; Weast & Proffitt, 2018), with such effects often emerging when targets are positioned closer to the body (de Grave et al., 2011; Shimono et al., 2001).

Unlike visual localisation, where systematic deviations are often discussed primarily in relation to target distance and retention interval, haptic localisation biases appear to be shaped by a broader array of spatial, bodily, and task-specific factors (Kappers & Koenderink, 1999). The direction and magnitude of these biases have been

reported to vary with the object's position relative to the body, with more positive egocentric biases near the limits of reach (Beek et al., 2014; Jones et al., 2012) and more distal, negative biases for positions closer to the self (McGuire & Sabes, 2009; Volcic et al., 2007; Wako & Ayabe-Kanamura, 2016). Biases can also be altered by the presence or arrangement of other objects in the workspace (Hollins & Kelley, 1988), the initial position of the hand (Volcic et al., 2007), the spatial hemifield in which the target is located (Dassonville, 1995), the nature of the tactile experience itself (Van Dijk et al., 2013), and the specific demands imposed by the localisation task (Jones et al., 2012). Notably, in contrast to the delay-dependent distortions often reported in visual localisation, several haptic studies have found little or no additional decline in localisation accuracy across the retention intervals examined (Faineteau et al., 2005; Zuidhoek et al., 2003), both visual and haptic response patterns are summarized in Fig. 1.1.

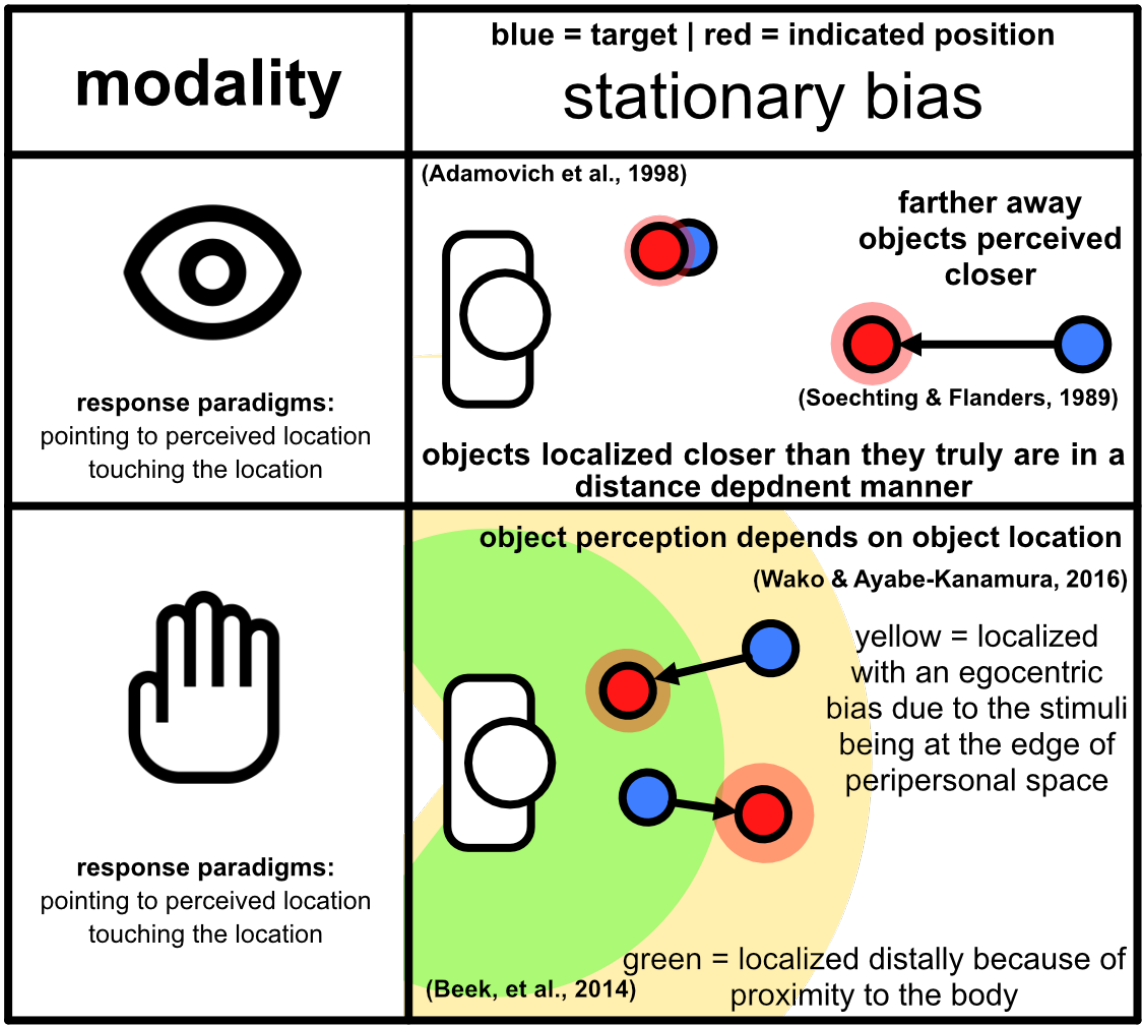

Figure 1.1: Stylized summary of characteristic stationary localisation biases: Blue markers denote target locations and red markers denote remembered (reproduced) locations; arrows indicate the direction of systematic bias, and translucent red circles around remembered locations indicate relative response variability. In vision, an egocentric bias is always present and distance-dependent, with farther targets judged closer than veridical. In haptics, localisation biases are either egocentric or distal which depends on the initial target distance relative to the maximum reach of a participant, with distal biases for nearer targets and egocentric biases near the limits of reach.

1.3 Updating studies

A key fact to note in both visual and haptic localisation studies is that they are normally studied under stationary conditions and across a broad range of locations around an observer (Adamovich et al., 1998; Kappers, 1999; Medendorp et al., 1999; Sheth & Shimojo, 2001; Shimono et al., 2001). However, when translation and/or rotation of the observer are introduced, these movements change a previously encoded target's direction and distance which then needs to be updated relative to the new position and orientation of the body (Medendorp, Tweed, et al., 2003). This process of maintaining or revising a remembered object's location relative to the self as the body moves is termed spatial updating (Hollins & Kelley, 1988; Presson & Montello, 1994), a perfect spatial update can be seen in Fig. 1.2A, conversely, a failure to update a location can be seen in Fig. 1.2B. Under- and over-updating are illustrated in Fig. 1.2C and D, respectively; although such errors may arise from several sources, visual studies often interpret them in relation to misestimation of the observer's travelled distance (Kim & Harris, 2024; Medendorp et al., 1999). Updating a remembered target's coordinates in reference to a translation and/or rotation allows objects to be localized even after the sensory signal is removed and intervening movement has occurred. Everyday behaviour routinely involves walking, turning, and remembering the locations of previously seen and interacted-with objects, making updating behaviour and its characterization essential to an understanding of human perception.

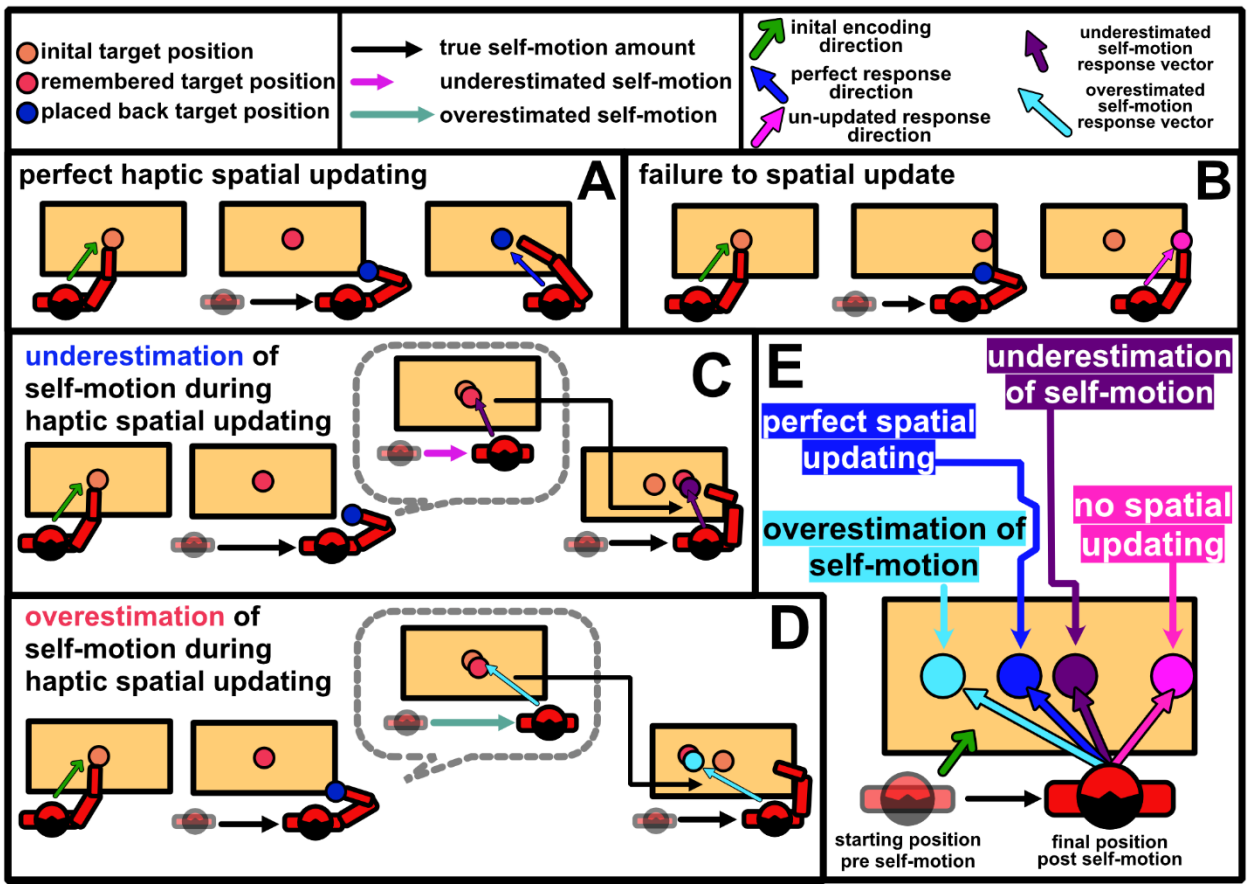

Figure 1.2: Possible spatial updating outcomes after self-motion: Panel A shows perfect updating, in which the remembered object location is adjusted appropriately after movement and the object is replaced at its true position. Panel B shows no updating, in which the participant effectively reproduces the original body-relative action despite having moved. Panel C shows undercompensation, in which the participant behaves as though less self-motion occurred than actually did, producing a placement shifted in the direction of travel. Panel D shows overcompensation, in which the participant behaves as though more self-motion occurred than actually did, producing a placement shifted opposite to the direction of travel. The present findings most closely resemble this overcompensatory pattern shown in Panel D. Panel E summarizes these possible updating outcomes across movement directions and provides a visual framework for interpreting the observed displacement errors.

1.3.1 Visual Updating

To study localisation and its updating during self-motion in a controlled laboratory setting, the behaviour is typically structured into separate phases. Participants first encode a target location, then undergo self-motion, and finally indicate the remembered target location from their new position and/or orientation. However, only a few studies have examined memory-guided localisation of briefly viewed targets after controlled

whole-body self-motion, particularly for lateral translations. Studies that have investigated this phenomenon have mainly been confined to the visual modality. Representative works include step-based self-displacements in darkness (Medendorp et al., 1999; Van Pelt & Medendorp, 2007). More recently, virtual-reality (VR) has been used to simulate visual translations (Kim & Harris, 2024), motion platforms have been used to apply controlled passive self-motion (Kim & Harris, 2024; Perdreau et al., 2019), and visually simulated rotations have been examined in related paradigms (Segen et al., 2023).

A consistent outcome across visual spatial-updating studies is that self-motion induces systematic localisation errors that depend on the direction of the observer's displacement, with remembered targets typically indicated as shifted toward the observer (positive displacements) relative to their true world-fixed location, visualised in Fig.1.2C (Kim & Harris, 2024; Medendorp et al., 1999; Van Pelt & Medendorp, 2007). This error pattern is widely interpreted as reflecting incomplete compensation for self-motion: the updating process underestimates the magnitude of the displacement executed, such that the target's updated position is computed as less shifted than it should be (Kim & Harris, 2024; Medendorp et al., 1999). As a result, when observers respond from their post-motion position, they indicate the target is closer to the body than would be expected under stationary visual localisation, producing an apparent amplification of egocentric bias relative to no-motion.

1.3.2 Haptic Updating

Spatial updating has been examined far less extensively in the haptic domain than in vision, and the available paradigms are not directly aligned with visual whole-body translation studies. Existing haptic work has largely focused on changes in position around a tabletop (Giudice et al., 2011, 2017; Hollins & Kelley, 1988), or on imagined shifts in viewpoint relative to a tabletop layout (Martolini et al., 2021). By contrast, voluntary straight-line body translations, such as lateral or anteroposterior stepping while maintaining a remembered target location, do not appear to have been studied haptically in a manner directly analogous to visual translation paradigms such as that of Medendorp et al. (1999). Moreover, haptic spatial-updating performance is often quantified either as angular error (Giudice et al., 2017; Hollins & Kelley, 1988) or through layout-matching

and recognition judgments (Martolini et al., 2021; Pasqualotto & Newell, 2007). In the latter tasks, participants encode a haptic layout, undergo actual or imagined self-motion, and then judge whether a subsequently explored layout matches the previously encoded one from the new perspective. Although these paradigms are important for assessing whether spatial relations are preserved across viewpoint changes, they do not reveal whether remembered object locations are replaced with systematic metric bias or altered precision after self-motion.

Existing haptic updating studies have also tended to emphasize population differences rather than metric characterization of post-motion localisation. Blind participants, for example, show better layout-recognition performance than sighted participants after self-motion around a table (Martolini et al., 2021). On the other hand, older adults show larger egocentric pointing biases after self-motion than younger adults (Bennett et al., 2017).

Accordingly, a direct psychophysical characterization of haptic localisation ability after self-motion, quantifying both systematic bias (accuracy) and response dispersion (precision) within a memory-guided object replacement paradigm in a neurologically typical (“normally sighted”) sample, appears to lack a clear empirical precedent in the published literature. This gap motivates a focused investigation that isolates linear whole-body self-motion while evaluating haptic spatial updating with metric measurements of both bias and precision after self-motion.

1.4 Outlined Plan of Experiments

Based on the localisation literature in the visual and haptic domains reviewed above, in conjunction with the identified gap in the haptic literature; I plan to investigate how a linear displacement generated by a participant moving along the edge of a table (via an active step) might affect haptic localisation. Based on findings from static haptic localisation research and post-self-motion localisation visual research, I expected no major differences in haptic performance after self-motion from visual performance after self-motion. Accordingly, I predicted that post-self-motion replacements would be displaced in the direction of self-motion, consistent with an amplified positive egocentric

bias when remembered targets were reconstructed from a new body position in visual spatial updating. 1.5 Hypotheses of Experiments

H1: self-motion will produce systematic placement bias parallel to the axis of translation. Specifically, placements post-translation will be shifted in the direction of travel for forward, backward, leftward, and rightward translations. That is, I hypothesize that, as in visual updating, haptic spatial updating will take into account less than 100% of the observer's movement resulting in an egocentric bias, as seen in Fig. 1.3A.

H2: longer translations (e.g., two steps) will yield larger directional biases than shorter translations (e.g., one step). This is because more self-motion is harder for an observer to take into account (Kim & Harris, 2024). I also hypothesize this because more self-motion or translation away from an object would logically result in that object being further into the extremities of the reach where larger biases manifest (Soechting & Flanders, 1989), both of which will result in systematic biases that are greater after larger displacements, as seen in Fig. 1.3B.

H3: self-motion will reduce response precision relative to equally timed stationary control trials in a haptic localisation task. As illustrated in Fig. 1.3A, this prediction corresponds to the smaller green dispersion circle in the stationary condition (left) and the larger green dispersion circle in the self-motion condition (right). This hypothesis is motivated by the visual updating literature, in which self-motion is often estimated imprecisely, increasing uncertainty about the remembered target location and thereby reducing post-movement localisation precision (Kim & Harris, 2024).

H4: larger self-motion magnitudes will produce lower response precision. As illustrated in Fig. 1.3B, this prediction corresponds to the larger green dispersion circle after two steps, relative to the smaller dispersion associated with the shorter translation. Parallel to H2, H4 formalizes a dose–response prediction for variability: as displacement magnitude increases, greater accumulated noise in self-motion estimation should yield more variable, and therefore less precise, object placements.

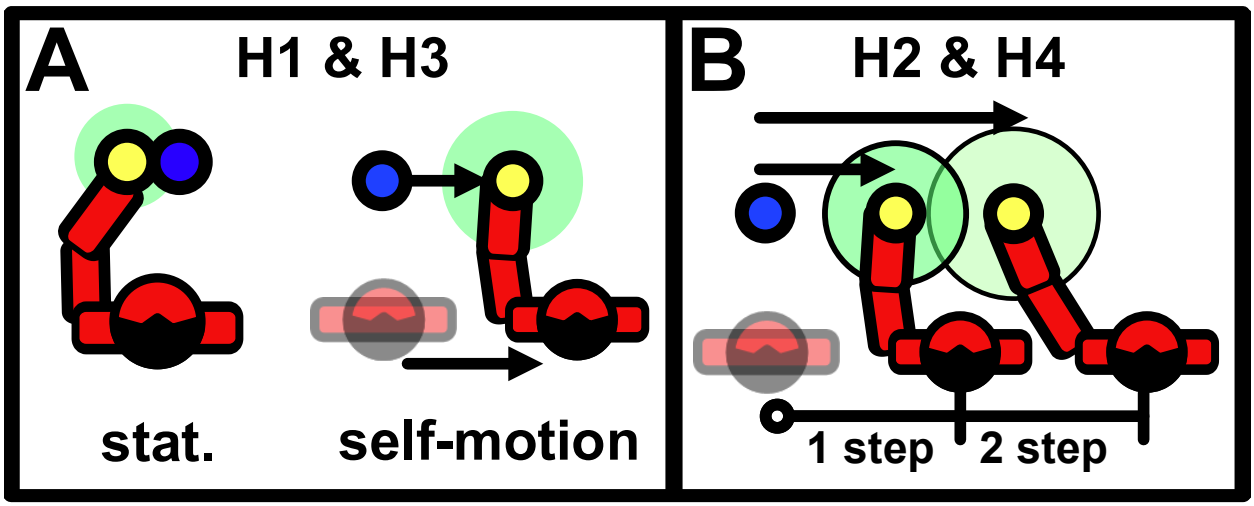

Figure 1.3: Schematic summary of the four hypotheses: The blue circle denotes the encoded target location; the yellow circle denotes the participant's remembered replacement, and the green halo indicates response dispersion (lower precision). Left panel (H1 & H3): relative to stationary trials, self-motion produces a systematic shift in replacements parallel to the translation axis and increases variability. Right panel (H2 & H4): increasing translation magnitude (two steps vs one step) yields larger directional bias and further reduces precision. (Illustrations are not to scale. In the right panel, the two-step response position is depicted schematically and does not indicate that the target lay beyond reachable space).

This thesis addresses the gap in knowledge regarding haptic localisation biases after self-motion by examining haptic localisation under experimentally controlled active, linear self-motion. Specifically, blindfolded participants picked up an object from a table in front of them and either remained standing at a designated position for 5 s (stationary control) or executed an active linear translation in a specified direction, over a specified distance, and using a specified number of steps (self-motion condition). They then attempted to replace the object at its original location. Bias, defined as the signed positional difference along the axis of motion, and response precision, defined as the average distance of each participant's placements from that participant's mean placement, were quantified from calibrated motion-tracking data expressed within a common spatial reference frame across the experimental setup.

This thesis reports four experiments designed to assess how haptic spatial updating varies as a function of (i) target distance from the body, (ii) the direction of self-motion (leftward, rightward, forward, backward), and (iii) self-motion distance (e.g., 30 cm, 60 cm).

2.0 Methods

2.1 Overview

Across four experiments, blindfolded participants performed a haptic object localisation task under experimentally controlled active whole-body linear self-motion. In each trial, participants initially encoded the target location of a magnetic object on a table via a haptic search. Then they retrieved the object from the tabletop and either remained stationary for 5 s or performed an active translation in a specified direction for a specified number of steps before attempting to replace the object at its original location. Bias was quantified as the signed positional difference along the axis of motion, and precision was quantified as the average dispersion of each participant's placements around their own mean placement. These measures were derived from motion-tracking data recorded within a common calibrated reference frame across all experiments.

2.2 Equipment

2.2.1 Setup and Stimuli

All four experiments were conducted using the experimental setup shown in Fig. 2.1. Participant and object movements were recorded by the OptiTrack motion-capture cameras distributed around the experimental room (Fig. 2.1A). The tabletop workspace, on which the haptic localisation task was performed, is shown in Fig. 2.1B. Participants wore a blindfold fitted with a nose flap to eliminate residual downward vision (Fig. 2.1Ba). The primary task object was a motion-tracked magnetic stick (Fig. 2.1Bb), designed to support stable haptic grasping and reliable tracking: its handle measured 2 cm in diameter and 14 cm in height, a Neodymium disk magnet was embedded within the 3D-printed housing to allow stable placement on the magnetic tabletop, and a larger circular top piece, approximately 12 cm in diameter, supported three infrared reflective markers. Participants also wore marker-fitted headwear to permit tracking of head position during the task (Fig. 2.1Bc). The computer-related components of the setup are shown in Fig. 2.1C, although the laptop is not shown, the platform where the laptop running the Godot task program is shown (Fig. 2.1Ca) and the separate computer running the OptiTrack acquisition software (Fig. 2.1Cb). Finally, participants stood and translated along a raised

wooden platform adjacent to the table, which supported the blindfolded self-motion component of the task (partially visible in Fig. 2.1D, fully visible in Fig. 2.1).

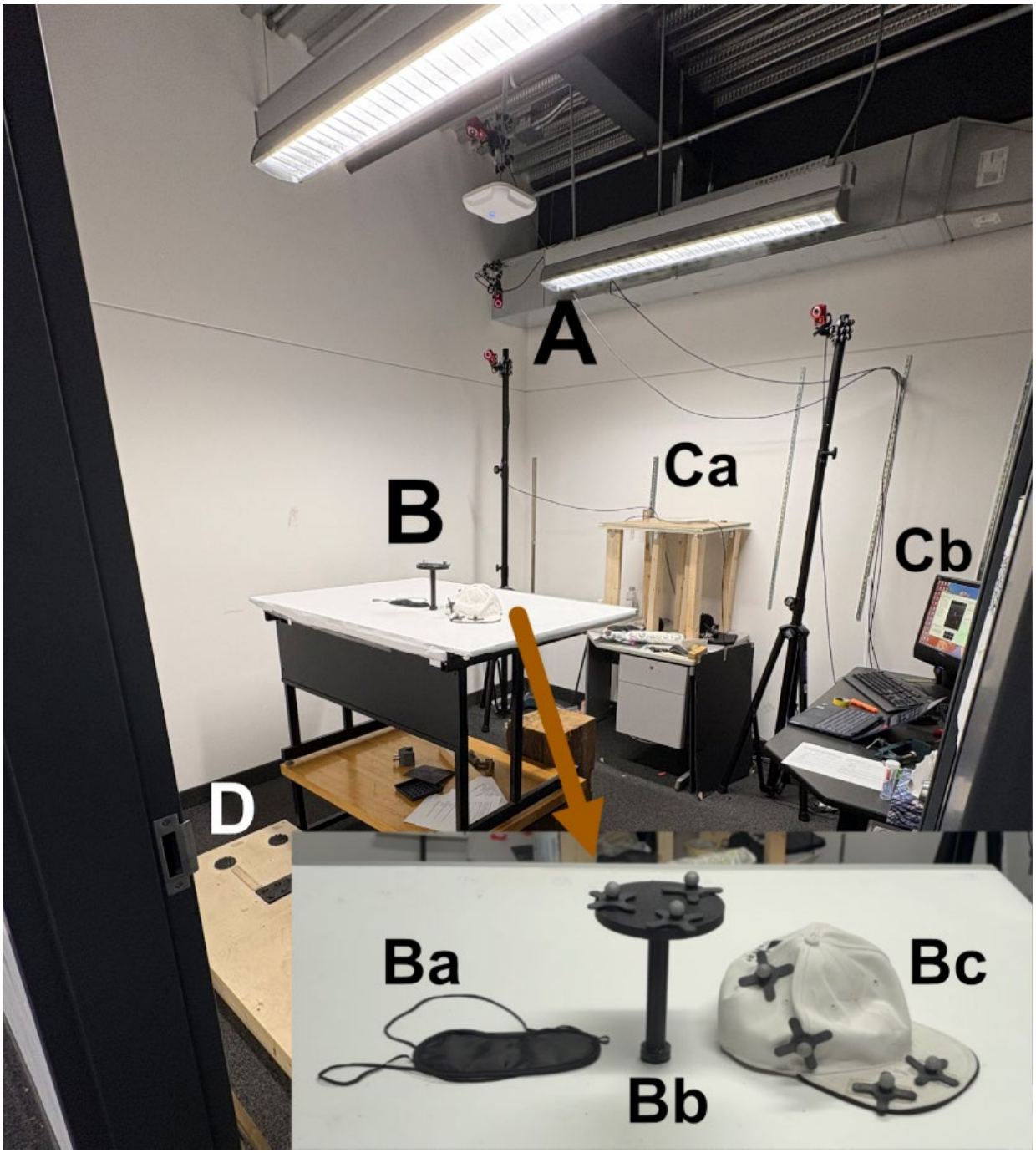

Figure 2.1: Photograph of the experimental room and apparatus: (A) OptiTrack motion-capture cameras. (B) Tabletop workspace. Inset: (Ba) blindfold, (Bb) motion-tracked magnetic stimulus, and (Bc) marker-fitted headwear. (Ca) Location of the laptop running the Godot task program. (Cb) Computer running OptiTrack acquisition software. (D) Raised walkable platform with tactile stops.

2.2.2 Table

The tabletop workspace (Fig. 2.1B) consisted of a magnetic whiteboard surface measuring 124.46 cm (width) × 91.44 cm (depth) × 1.1 cm (thickness), positioned centrally on a stable standing-desk platform with a total height of 111 cm from the floor. The desk structure was formed by two four-legged tables stacked to produce a rigid, non-wobbling surface during haptic exploration and replacement. The whiteboard was covered with poster paper cut to size, which reduced visible seams and surface irregularities, facilitated cleaning, and provided a lower-friction matte surface relative to the draggy native glossy finish of the whiteboard.

2.2.3 OptiTrack System

Participant movements and magnetic stick locations were recorded using an OptiTrack motion-capture system. Data acquisition was performed on a Windows 7 workstation (shown in Fig 2.1Cb) running OptiTrack software (Tracking Tools v2.3.4) with six 1.9-megapixel infrared cameras (V100:R2) distributed around the room (Fig. 2.1A). The calibrated tracking volume encompassed both the tabletop workspace and the walkable platform. Prior to data collection, the capture volume was calibrated using the OptiTrack recommended tri-point wand procedure, yielding an estimated spatial accuracy of 0.84 mm per marker.

Three infrared reflective markers were affixed to each tracked object, as visible on the magnetic stick and marker-fitted headwear in Fig. 2.1Bb and Bc. Within the OptiTrack software, each three-marker configuration was defined as a rigid body, allowing the system to track both the individual marker positions and the estimated spatial position of the corresponding object on each recorded frame.

2.2.4 Walkable Platform

A raised walkable platform was installed adjacent to the long side of the tabletop to support blindfolded self-motion and to provide stable positional anchoring through foot contact (partially visible in Fig. 2.1D, with the three experiment-specific layouts shown in Fig. 2.2). The platform was constructed from a 62 cm × 122 cm wooden panel elevated approximately 5.08 cm by a supporting frame made from 2.54 cm × 5.08 cm lumber. 3D-

printed tactile stops with raised bumps were fixed at predefined locations to indicate standing positions; the spacing between stops was 60 cm in Experiment 1, 40 cm in Experiment 2, and 30 cm in Experiments 3 and 4. These markers provided distinct tactile cues through footwear, enabling participants to locate start and end positions without visual input. When needed, brief corrective verbal guidance was given to maintain safe alignment with the intended standing location based on experimenter judgement.

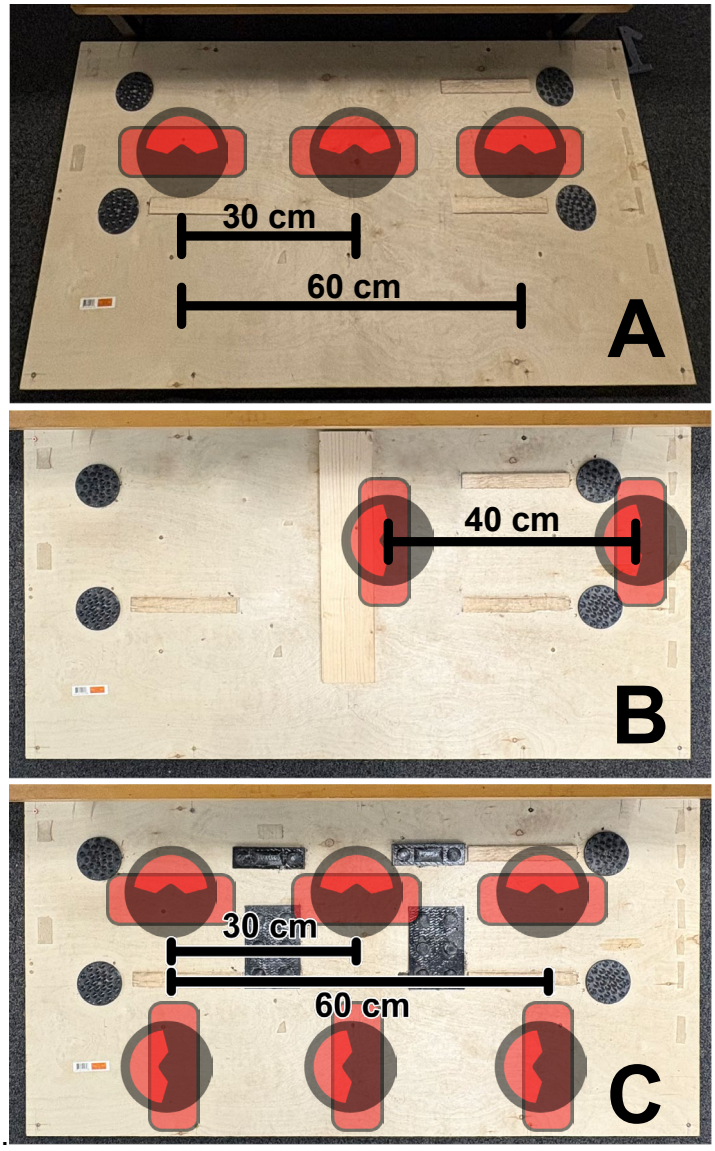

Figure 2.2: Walkable platform configurations: These configurations were used to define standing locations and intended self-motion distances across experiments. Black tactile pads indicate foot-placement locations, while wooden shims or planks provided structural support and alignment cues. Overlaid participant icons indicate the approximate standing

locations and facing directions used during the task. Bracket labels show the intended displacement distances between standing positions. (A) Experiment 1: lateral stepping between two standing positions, with a 60 cm translation between the left and right locations; the 30 cm label indicates the intermediate centre position used for the centre stationary condition. (B) Experiment 2: anteroposterior stepping after a 90° counterclockwise reorientation relative to Experiment 1, with front and back standing positions separated by 40 cm and a central plank serving as a toe stop. (C) Experiments 3 and 4 shared the same walkable platform configuration. The upper half of Panel C shows participant icons in the lateral orientation for Experiment 3, whereas the lower half shows the anteroposterior orientation used in Experiment 4. Adjacent standing positions were separated by 30 cm, and the two outer positions by 60 cm.

2.2.5 Godot Program

Trial randomization, auditory cue delivery, and event timestamping were implemented in a custom program developed in Godot (v4.3) and run on a computer independent of the OptiTrack system. The program generated experiment-specific trial sequences across target locations and self-motion conditions. In Experiments 3 and 4, it additionally controlled the progression between standing locations required by the movement design. Based on the current movement configuration, an appropriate corresponding auditory cue was presented, and this occurred in synchrony with the event timestamps collected for later analysis. These timestamps corresponded to the key moments illustrated in Fig. 2.3: A marked the moment at which the experimenter placed the object, B marked the start of the participant's search before object retrieval, C marked completion of object retrieval, Da marked the end of the movement period, Db marked the end of the 5 s stationary delay, and Ea or Eb marked the object replacement event following the movement or delay interval, respectively.

2.2.5.1 Godot and OptiTrack Synchronization

Since the Godot program and the OptiTrack system operated on separate computers, synchronization was achieved by starting both systems' recording processes simultaneously. In Godot, this consisted of initiating the program timer, whereas in OptiTrack it consisted of starting the motion-capture recording. At the beginning of each recording sequence, the experimenter verified that the two systems were aligned; if synchronization differed by more than 0.1 s, the process was restarted. This alignment was necessary to synchronize Godot event timestamps with the motion-capture video during data processing and cleanup.

2.3 Participants and Recruitment

All procedures complied with the Declaration of Helsinki. Participants were recruited through York University's Undergraduate Research Participant Pool (URPP), provided written informed consent prior to testing, and received course credit for participation. Across Experiments 1–4, 87 individuals were tested. The final analytic sample comprised 72 sighted, predominantly right-handed participants, with 18 participants included in each experiment. Participants were retained only if they achieved a score of 50 or higher on the Edinburgh Handedness Inventory (R. C. Oldfield, 1971), indicating a predominantly right-handed preference, and if they completed the task in a manner consistent with the experimental instructions and tracking requirements.

Fifteen participants were excluded prior to analysis. Seven participants did not complete a usable experimental session, either because they did not finish the task or because trial progression was too slow to complete the experiment within the available testing period of 1 hour. Two participants were excluded because their behaviour indicated that they had not adequately understood or implemented the required spatial-updating task despite instruction and passing the initial training. Two additional participants were excluded because they repeatedly used their arm to gauge the tabletop or spatial distances while blindfolded, despite being instructed not to use such compensatory strategies. Finally, four participants were excluded because their height prevented reliable tracking of the head marker within the calibrated OptiTrack capture volume. Procedures were approved by the York University Research Ethics Board (e2025-023).

- Experiment 1: 18 participants (mean age = 19.9 years, SD = 2.94; mean Edinburgh Handedness Inventory score = 82.1; 7 males, 11 females)
- Experiment 2: 18 participants (mean age = 19.7 years, SD = 2.33; mean Edinburgh Handedness Inventory score = 82.0; 6 males, 12 females)
- Experiment 3: 18 participants (mean age = 19.4 years, SD = 2.97; mean Edinburgh Handedness Inventory score = 55.6; 4 males, 14 females)
- Experiment 4: 18 participants (mean age = 18.8 years, SD = 1.68; mean Edinburgh Handedness Inventory score = 87.2; 5 males, 13 females)

2.4 Procedure

Participants were tested individually under blindfolded conditions. Before data collection began, standardized verbal instructions describing the task sequence were provided by the experimenter, along with an acted-out procedure of the experiment. The participant then proceeded through a training phase, followed by the main blocked task and post-task questionnaires.

2.4.1 Training

Training was used to familiarize participants with the task sequence and to ensure that blindfolded stepping on the walkable platform could be performed safely and confidently. Participants first completed two practice trials with vision, followed by at least two practice trials with the eyes closed and at least one practice trial while blindfolded. Each practice trial followed the same acted-out version of the experimental procedure and used the same auditory cues as the main experiment. Participants were asked to pick up the object, either wait for 5 s, or move in a specified direction by a specified number of steps and then replace the object at its original location. After the initial five practice trials, participants were asked whether they wished to complete additional practice to improve comfort maneuvering on the walkable platform. Additional sets of five trials were also administered when the participant appeared hesitant or unstable in the experimenter's judgment. Before proceeding to the experimental blocks, participants had to confirm that they could not see through the blindfold and verbally describe the task sequence accurately. These criteria were used to determine whether training was complete.

2.4.2 Trial Sequence

Across all experiments, each trial followed the same core sequence (Fig. 2.3A–C), although specific events differed depending on whether the trial involved self-motion (Fig. 2.3Da–Ea) or was stationary (Fig. 2.3Db–Eb). At the beginning of each trial, the researcher placed the motion-tracked magnetic stick at the target location specified by the Godot program. Following a spacebar press by the experimenter, participants then heard an auditory instruction to search for the object, retrieve it using the right hand only,

and bring it to a standardized home position. Participants were not permitted to use the left hand to contact either the table or the object. Once located, the object was lifted and held near the body midline, just anterior to the navel and without contacting the tabletop. Participants then received an auditory instruction either to remain stationary for 5 s (Db) or, on movement trials (Da), to execute a specified translation. In Experiments 1 and 2, movement cues specified direction only, instructing participants to “take a step to the left,” “take a step to the right,” “take a step forward,” or “take a step backward,” as appropriate. In Experiments 3 and 4, the auditory cues specified both direction and movement magnitude, instructing participants to take either one or two steps in the required direction (e.g., “take 1 step to the right”, “take two steps forward”). On movement trials, movement completion was judged by the experimenter once the participant had come to a complete stop, and this event was marked by an additional spacebar press. After the stationary delay or movement phase, participants were instructed to replace the object at its original location on the tabletop. Trial completion was defined as the end of the replacement response, after which the event was time-stamped by the experimenter.

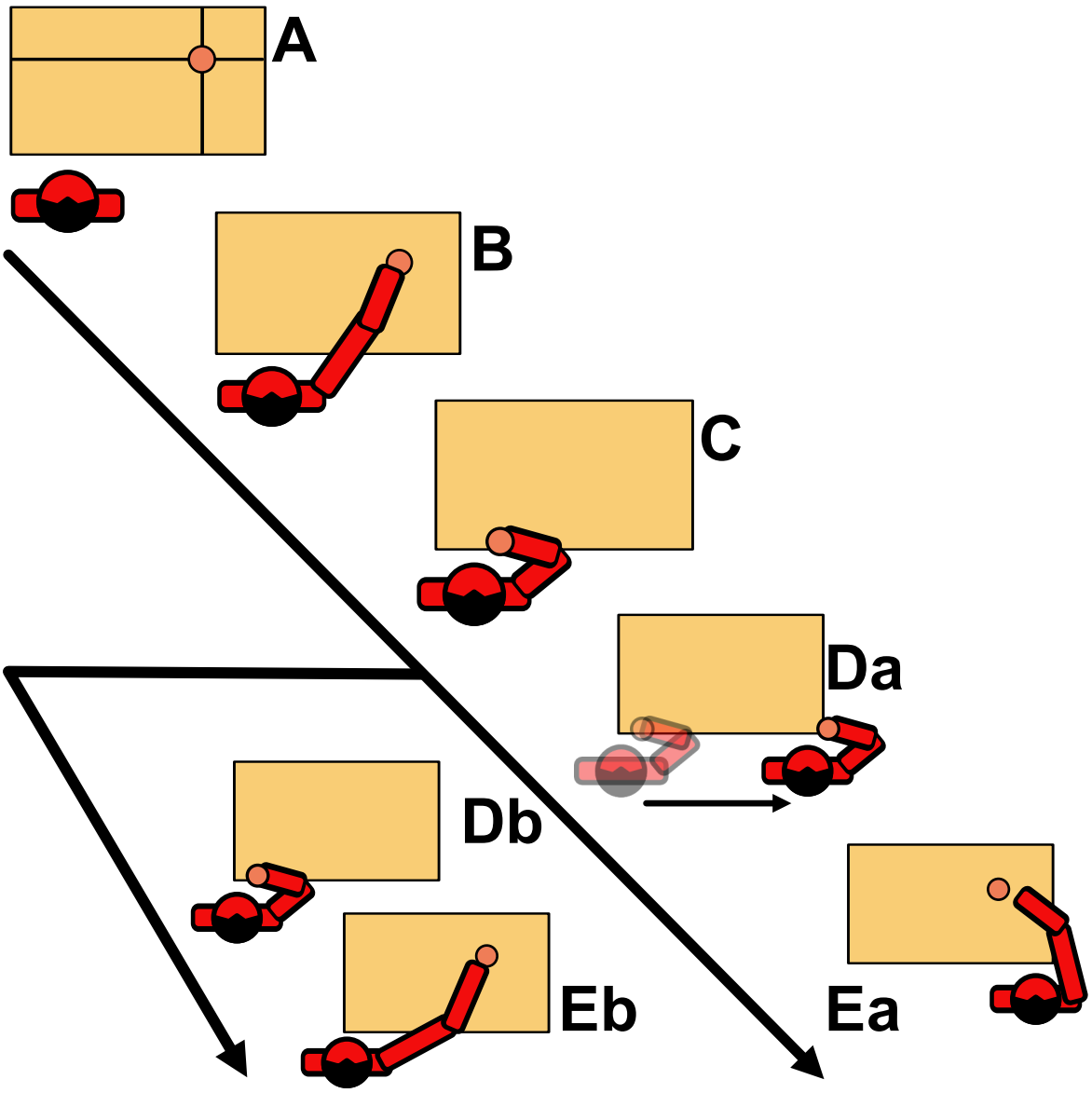

Figure 2.3: Trial-sequence schematic: Steps A–C were identical across conditions: (A) the motion-tracked magnetic stick was placed at a predefined target location; (B) the blindfolded participant haptically searched the tabletop; and (C) the object was retrieved and held at a standardized home position near the body midline. (D) Condition manipulation: (Da) a cued whole-body translation to a new standing position, or (Db) a stationary delay with no self-motion. (E) Response phase: (Ea) the participant replaced the object at the remembered target location after self-motion, or (Eb) after the stationary delay.

2.4.3 Block Structure and Trial Counts

Each experiment was administered in a blocked format, with a certain number of trials defining a block, and brief rest periods between blocks. In Experiment 1 (Fig. 2.4A),

each block corresponded to a single motion condition, with 6 target locations, each target position being repeated 3 times in 1 block, yielding 18 trials per block. Experiment 1 comprised 5 blocks, including 3 stationary and 2 movement conditions, for a total of 90 trials. Experiment 2 (Fig. 2.4B) comprised 4 blocks, including 2 stationary and 2 movement conditions, for a total of 72 trials. Individual blocks typically lasted 5–10 min, and break durations of approximately 1–3 min, full sessions lasted approximately 40-50 minutes, rarely going to or over 60 minutes.

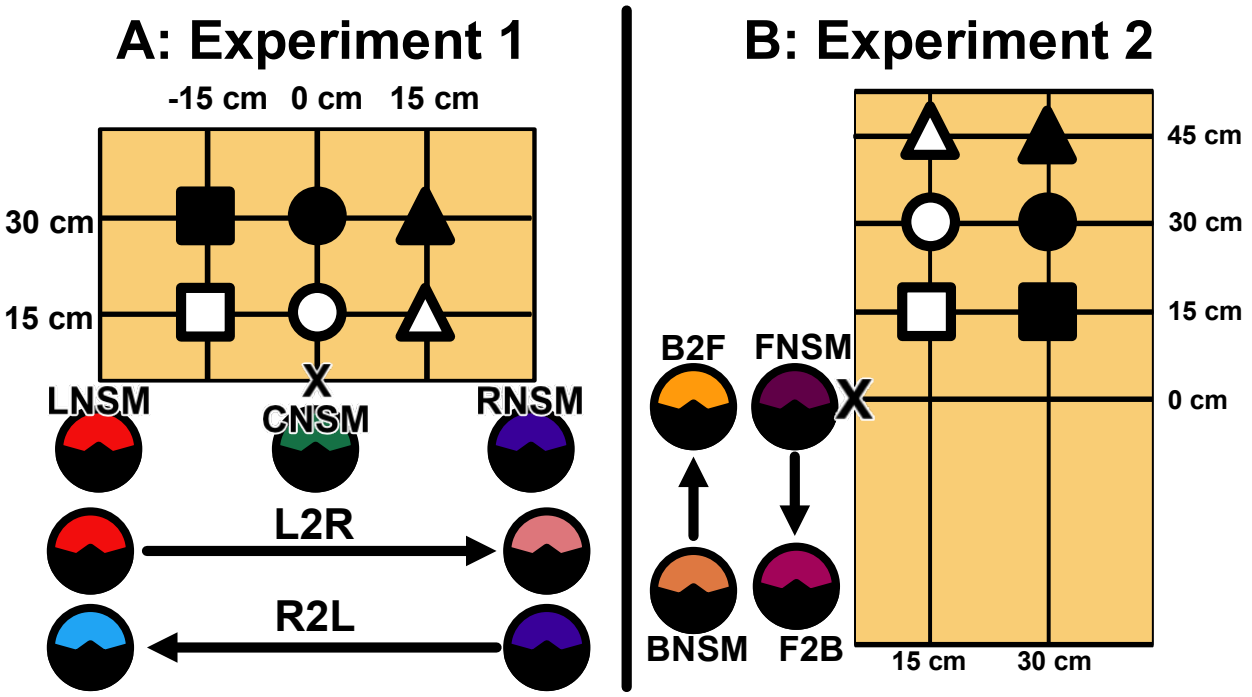

Figure 2.4: Spatial layouts and coordinate conventions for Experiments 1 and 2: Each panel shows the tabletop workspace, experiment-specific coordinate origin, target locations, participant standing positions, and permitted movement directions. Target positions are shown as black or white shapes with black outlines on the yellow rectangular table. Head icons indicate participant standing positions and facing direction, with the black hairline peak marking the direction faced. The black X outlined in white denotes the coordinate origin, and arrows indicate the direction of self-motion between standing positions. (A) Experiment 1 used a six-target array with three lateral target locations at each of two depths, three stationary conditions, and two lateral movement conditions. (B) Experiment 2 used a six-target array with two stationary conditions and two anteroposterior movement conditions, allowing replacement bias and precision to be assessed following forward and backward self-motion. Movement condition acronyms follow a consistent coding rule: L, C, R, F, and B denote left, centre, right, front, and back positions, respectively; NSM denotes no self-motion; and "2" denotes movement from one position to another, as in L2R for left-to-right movement or F2B for front-to-back movement.

In Experiments 3 and 4, each block sampled all 9 motion conditions, comprising 6 translation conditions and 3 stationary conditions, across 3 target positions 1 repetition each, yielding 27 trials per block. Participants completed 3 such blocks, giving 81 trials in total and 3 repetitions per target location and motion condition. Rest breaks were provided between blocks, with block durations of approximately 5–10 min and break durations of approximately 1–3 min. Across experiments, total session duration did not exceed approximately 50-55 minutes and rarely went over 60 minutes.

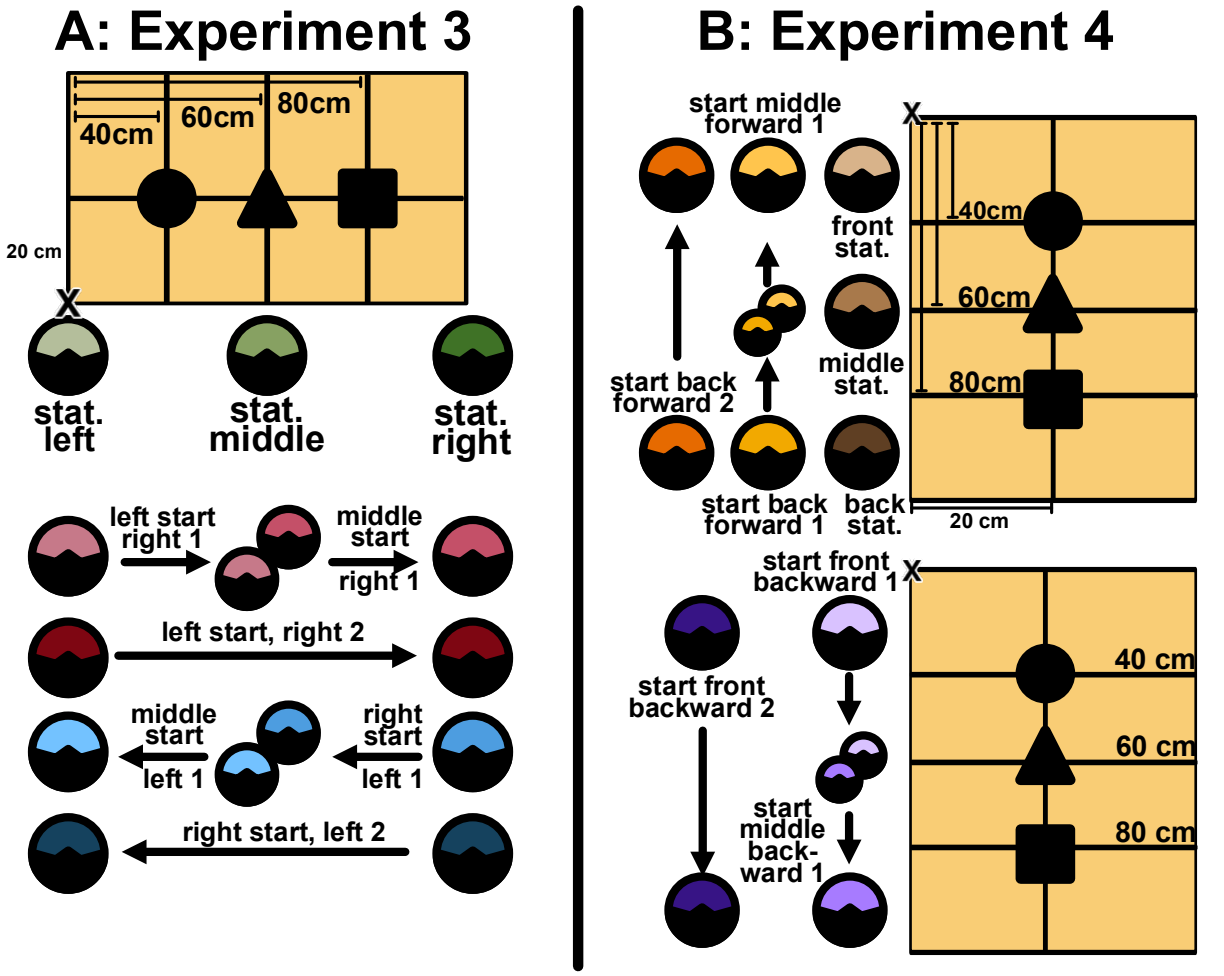

Figure 2.5: Spatial layouts and coordinate conventions for Experiments 3 and 4: Each panel shows the tabletop workspace, experiment-specific coordinate origin, target locations, participant standing positions, and permitted movement directions. Target locations are shown as black shapes or black outlines with white fill on the yellow rectangular table. Head icons indicate participant standing positions and facing direction, with the black hairline peak marking the direction faced. The black X outlined in white denotes the coordinate origin, and arrows indicate the direction of self-motion between standing positions. (A) Experiment 3 examined lateral self-motion across a three-target

linear array, with three stationary conditions and six translation conditions corresponding to one-step and two-step leftward or rightward movements. (B) Experiment 4 applied the same movement-magnitude structure to anteroposterior self-motion, with three stationary conditions and six translation conditions across a workspace that included target locations in front of and behind the participant.

2.4.4 Experiment Specific Trial Structure

2.4.4.1 Experiment 1

Experiment 1 used a rectangular six-target array and a blocked design in which each block was organized around a fixed starting position on the walkable platform. As shown in Fig. 2.4A, participants began trials from the left, centre, or right side of the table, depending on the stationary or self-motion condition assigned to that block. To preserve this block-specific starting stance, participants were verbally guided back to the appropriate tactile stop after each trial so that every subsequent trial began from the intended standing location. The intended self-motion displacement was 60 cm, and the movement interval was designed to approximate the 5 s delay used in the stationary control conditions. Recorded movement distances closely matched this intended displacement: participants travelled 60.7 ± 0.59 cm SEM during right-to-left self-motion (R2L) and 59.7 ± 0.60 cm SEM during left-to-right self-motion (L2R). Mean movement durations were likewise close to the stationary delay, at 4.90 ± 0.10 s SEM for R2L and 5.13 ± 0.11 s SEM for L2R. Movement duration did not differ significantly from the 5 s stationary delay, indicating that the temporal interval between object retrieval and replacement was adequately matched across stationary and self-motion conditions. In addition, R2L and L2R did not differ significantly from one another in either displacement distance or movement duration.

2.4.4.2 Experiment 2

Experiment 2 preserved the general blocked structure of Experiment 1 but shifted the self-motion manipulation to the anteroposterior axis. As in Experiment 1, each block was organized around a fixed starting position, and participants were verbally guided back to the appropriate tactile platform marker after each trial so that subsequent trials began from the intended front or back standing location, as shown in Fig. 2.4B. Since Experiment 2 was designed to examine one-step anteroposterior self-motion, the intended

displacement was set to 40 cm, rather than 60 cm as in Experiment 1, to ensure that the forward and backward translations could be performed comfortably, reliably and safely. Recorded movement distances closely matched this intended displacement: participants travelled 37.0 ± 0.99 cm SEM during back-to-front self-motion (B2F) and 37.7 ± 1.23 cm SEM during front-to-back self-motion (F2B). Mean movement durations were 4.25 ± 0.20 s SEM for B2F and 4.05 ± 0.13 s SEM for F2B. Although these movement durations were somewhat shorter than the 5 s stationary delay, they remained sufficiently close to preserve a broadly comparable retrieval-to-replacement interval across conditions. In addition, B2F and F2B did not differ significantly from one another in either displacement distance or movement duration.

2.4.4.3 Experiment 3

Experiment 3 used a linear three-target array and manipulated self-motion magnitude. Rather than making a single 60 cm translation as in Experiment 1, participants took either one 30 cm step or two successive 30 cm steps, yielding intended total displacements of 30 cm or 60 cm to the left or right (see Fig. 2.5A). This change also altered the spatial relationship between the participant's starting and ending positions and the remembered target location. Whereas movement in Experiment 1 always carried the participant across the body midline, and movement in Experiment 2 was always directed toward or away from the body, Experiment 3 included conditions in which participants moved toward, away from, or across the remembered object location. Unlike Experiments 1 and 2, trials proceeded continuously from the participant's current standing location rather than resetting to a fixed start position after each trial. This procedure was adopted to reduce total session time and minimize participant fatigue.

In addition, because Experiment 3 trials progressed continuously from the participant's current standing location rather than resetting after each trial, the Godot program dynamically determined the next feasible trial. After each trial, the program evaluated the participant's current position, the movement conditions already completed, and the remaining untested condition combinations, then selected a subsequent trial that could begin naturally from that standing location whenever possible. Thus, for example, after a participant moved from the left position to the middle position, the next trial was

preferentially selected from conditions that could begin at the middle position, allowing the sequence to continue without unnecessary repositioning. In the rare cases where no compatible remaining trial could begin from the participant's current location, the program instructed the participant to move to the required starting position before object search began. These brief repositioning events were procedural only and were not treated as distinct experimental conditions.

Furthermore, Experiment 3 was designed to manipulate movement magnitude, rather than to match the temporal interval of the stationary conditions, the primary movement check concerned displacement distance. Recorded head displacement was approximately 27–28 cm for the one-step conditions and approximately 52–55 cm for the two-step conditions. Specifically, one-step rightward movements averaged 28.1 ± 1.11 cm SEM from the left start and 26.9 ± 1.00 cm SEM from the middle start, while one-step leftward movements averaged 28.4 ± 1.22 cm SEM from the middle start and 28.0 ± 0.88 cm SEM from the right start. Two-step movements averaged 51.7 ± 2.01 cm SEM for rightward translation and 54.7 ± 1.80 cm SEM for leftward translation. Although the two-step displacements were somewhat shorter than the nominal 60 cm target, they were substantially and significantly greater than the corresponding one-step displacements in both movement directions, confirming that the intended self-motion magnitude manipulation was successfully implemented. One-step movements did not differ significantly across starting positions within the same direction, and the two-step leftward and rightward movements did not differ significantly from one another in total displacement.

2.4.4.4 Experiment 4

Experiment 4 applied the multistep movement logic of Experiment 3 to the anteroposterior task orientation used in Experiment 2. As in Experiment 3, trials progressed continuously from the participant's current standing location rather than returning to a fixed start position after every trial, allowing forward and backward movements to proceed stepwise across the three-position platform. The same dynamic Godot trial-selection procedure used in Experiment 3 was implemented in Experiment 4. Two target conditions were omitted because they would have required participants

standing at the most anterior position to replace targets located 30 cm and 50 cm behind the body, which exceeded comfortable posterior reach (see Fig. 2.5B).

Experiment 4 was designed around intended one-step and two-step anteroposterior displacements of approximately 30 cm and 60 cm, respectively. The recorded differences between standing adjacent positions were approximately 33 cm whereas separations between the two outer standing positions were approximately 66–68 cm. For example, adjacent-position separations included 33.05 ± 1.03 cm SEM between the two one-step backward starting configurations and 33.28 ± 0.79 cm SEM between the two one-step forward starting configurations, whereas outer-position separations included 66.81 ± 1.23 cm SEM and 67.68 ± 1.13 cm SEM across the corresponding two-step spatial spans. These one-step and two-step spatial separations differed significantly, confirming that the intended anteroposterior movement-magnitude manipulation was successfully implemented in Experiment 4.

2.4.5 Post-experiment measures

After completion of all experimental blocks, participants completed two questionnaires (Appendix A: Post Experiment Surveys). The first was a brief self-report questionnaire assessing perceived task difficulty, enjoyability, and understanding on a 5-point Likert scale. The second collected background information such as prior experience with sports, musical instruments, video games, and other haptic or tactile activities. As well as biological information such as age, gender, sex, arm length, and height. The second questionnaire also included within it the Edinburgh Handedness Inventory, which was used as a background measure of handedness.

2.5 Data Processing

2.5.1 Data cleaning

Each experimental block produced two raw data files: a Godot output file and an OptiTrack motion-capture file. The Godot file recorded the event structure for the experimental block, which included timestamps for key events during the trials and block. The OptiTrack file recorded continuous three-dimensional positions of the tracked objects

at 100 frames per second. Since the two systems were initiated nearly simultaneously at the beginning of each block, their timestamps could be aligned directly. Data cleaning was then performed in Python 3.10 using a script that paired each Godot file with its corresponding OptiTrack file and produced a single participant data file for each block.

For each Godot event timestamp, the temporally nearest OptiTrack frame was identified, and the corresponding spatial coordinates of the tracked hat rigid body (defined from the 3 points on the hat) and magnetic stick rigid body were extracted. These coordinates, together with the associated event labels and condition information, were compiled into a trial-level dataset for later analysis. During this process, OptiTrack coordinates were also transformed into a simplified orthogonal reference frame to make the resulting datasets easier to interpret and analyze in R. The same cleaning procedure was applied across all four experiments.

2.5.2 Accuracy Analysis

Accuracy was assessed as signed endpoint bias along the task-relevant axis of motion. Following data cleaning, trial-level datasets were imported into R, and two spatial events were extracted for each trial: the experimenter-defined target location and the participant's final replacement location, each expressed in X and Z coordinates. Signed endpoint bias was calculated as the participant's replacement coordinate minus the corresponding target coordinate on the analysed axis.

For Experiments 1 and 3, the primary accuracy measure was signed lateral bias along the X-axis, shown in pink in Fig. 2.6A. For Experiments 2 and 4, the primary measure was signed front–back bias along the Z-axis, shown in pink in Fig. 2.6B. Although total endpoint error could be decomposed into orthogonal spatial components, only the component parallel to the relevant self-motion axis was used for the primary accuracy analysis. This same axis-specific measure was applied to stationary and movement trials, allowing stationary baselines to be evaluated first and then compared directly with their corresponding self-motion conditions.

Statistical differences between condition mean displacements along the axis of motion were evaluated using a linear mixed-effects model (Section 2.5.4, Inferential

Statistics). Additional control measures, including object-displacement and head-movement vectors, were derived to assess whether observed effects could be attributed to extraneous variation in trial execution. In Experiments 3 and 4, composite condition labels were further separated into start-position and movement-condition components to support the planned spatial-updating analyses.

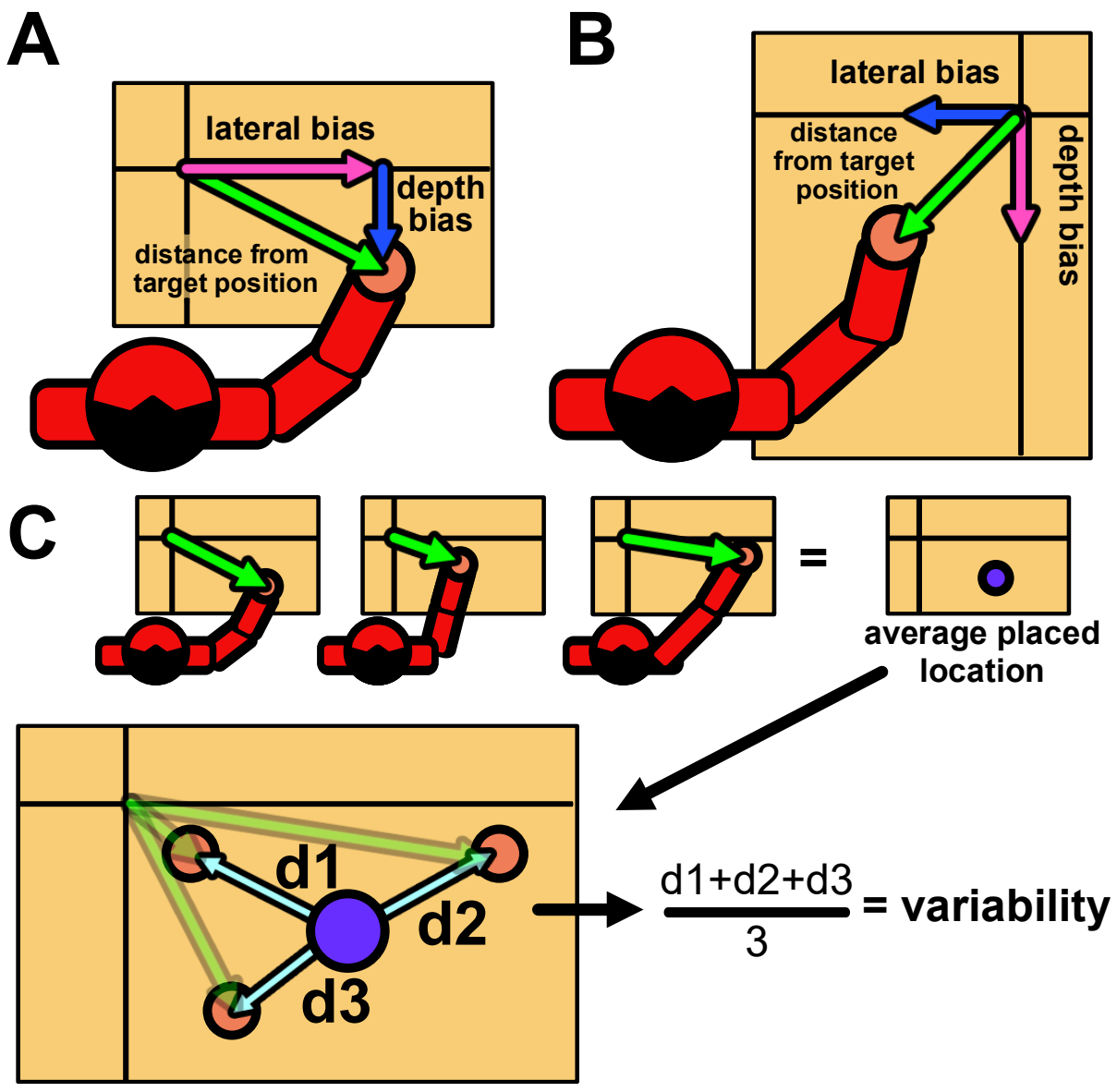

Figure 2.6: Accuracy and precision measures used across experiments: (A) Endpoint-error decomposition for Experiments 1 and 3; the signed component highlighted in pink was used as the primary accuracy measure. (B) Equivalent decomposition for Experiments 2 and 4; the signed component highlighted in pink was used as the primary accuracy measure. In both panels, the black-line intersection marks the original target

location, the orange circle marks the replacement location, and the green vector denotes total endpoint error. (C) Precision measure based on repeated placements of the same target within a participant and condition. The purple point indicates the participant's mean endpoint, and d1-d3 represent the Euclidean distances from each individual placement to that mean. Precision was defined as the average of these distances.

2.5.3 Precision Analysis

Precision was quantified as within-participant endpoint variability. As illustrated in Fig. 2.6C, repeated placements were grouped within each participant, condition, and target-location combination, and a participant-specific mean endpoint was calculated from those repeated responses. The Euclidean distance from each individual placement to that mean endpoint was then computed, and these distances were averaged to yield the precision measure.

This measure was therefore independent of the original target location and indexed the dispersion of repeated responses around a participant's own mean endpoint. Lower values indicated tighter clustering of responses, whereas higher values indicated greater within-participant variability.

2.5.4 Inferential Statistics

Inferential analyses were conducted using linear mixed-effects models (R Core Team, 2021). Separate models were fitted for signed bias and precision within each experimental design family. For bias analyses, the dependent variable was each participant's mean signed endpoint error, computed within each condition and target-location combination along the axis relevant to that experiment. For precision analyses, the dependent variable was each participant's mean within-participant endpoint variability score, computed within each condition and target-location combination. Precision values were log-transformed prior to inferential modelling. In all models, participant was included as a random intercept to account for stable between-participant differences in overall response tendency. Planned follow-up comparisons were performed using estimated marginal means, with Holm adjustment applied to control for multiple comparisons.

2.5.4.1 Linear Mixed-Effects Models for Experiments 1 and 2

Experiments 1 and 2 used rectangular six-target arrays in which target location varied along two spatial dimensions. Accordingly, the bias and precision models for these experiments included self-motion condition, the target's X position, the target's Z position, and all corresponding interaction terms. In Experiment 1, the outcome variable for the bias model was signed lateral bias, whereas in Experiment 2 it was signed anteroposterior bias. The same two-dimensional target-location structure was used for the precision analyses.

$$Bias \sim Movement\ Condition * X\ Position\ of\ Object * Z\ Position\ of\ Object + (1\ |Participant)$$

Equation 1: Linear mixed model used for experiments 1-4, bias analysis

$$Precision \sim Movement\ Condition * X\ Pos\ of\ Object * Z\ Pos\ of\ Object + (1|Participant)$$

Equation 2: Linear mixed model used for experiments 1-4 precision analysis

These models tested whether bias or precision differed across self-motion conditions, whether they varied across the two-dimensional target array, and whether the effect of self-motion depended on the target's spatial location.

2.5.4.2 Linear Mixed-Effects Models for Experiments 3 and 4

Experiments 3 and 4 used linear three target position and introduced a more complex multistep movement structure. For analysis, movement direction, movement magnitude, and starting position were therefore combined into a composite variable, referred to as *motion condition*. This variable was required to distinguish, one-step movements in the same direction which began from different positions on the platform, allowing each experimentally distinct movement configuration to be retained in the model. Because target location varied along only one spatial dimension in Experiments 3 and 4, the primary bias and precision models included motion condition, target position (x position only), and their interaction.

$$Bias \sim Motion\ Condition * Target\ Position + (1|Participant)$$

Equation 3: Linear mixed-effects model used for signed bias analyses in Experiments 3 and 4.

A secondary bias analysis was conducted in Experiment 3 in particular to examine the effect of movement magnitude more directly without starting position. In this follow-up model, compatible movement conditions were recoded into broader movement families that grouped movements by direction and step magnitude while collapsing across starting position. This analysis was used to compare one-step and two-step lateral translations within the same direction of movement.

$$Bias \sim Movement\ family\ * Target\ Position + (1|Participant)$$

Equation 4: Follow-up linear mixed-effects model used to examine step-magnitude effects on signed lateral bias in Experiment 3.

Finally, precision in Experiments 3 and 4 was modelled using the same primary motion-condition structure as the bias analysis, with log-transformed within-participant variability as the dependent variable.

$$Precision \sim Motion\ Condition * Target\ Position + (1|Participant)$$

Equation 5: Linear mixed-effects model used for precision analyses in Experiments 3 and 4.

These models tested whether post-self-motion bias and precision differed across the multistep movement configurations, whether these effects varied by target position, and, in the Experiment 3 follow-up analysis, whether larger lateral movement magnitudes produced stronger bias than smaller movement magnitudes.

2.5.4.3 Relative Reach Analysis

A further complementary analysis was performed to assess whether self-motion biases were related to the biomechanical extent of the replacement response. In short, investigating if was a factor in the bias observed. a *Relative Reach* measure was

calculated and correlated against lateral bias. For each trial, post-movement reach distance was defined as the Euclidean distance between the participant's head position and the final object replacement position at the replacement event. This value was then divided by the participant's measured arm length to produce a relative-reach ratio (Equation 6). Thus, a value below 1 indicated that the object was replaced within the participant's measured arm length, a value of 1 corresponded to arm length, and values above 1 would indicate that the replacement position exceeded the participant's measured arm length. Possibly due to some shifting or swaying of the body to adjust and reach.

$$Relative\ Reach = \frac{\sqrt{(object\ X\ pos - head\ X\ pos)^2 + (object\ Z\ pos - head\ Z\ pos)^2}}{arm\ length}$$

Equation 6: Relative-reach definition. All object and head coordinates were taken from the post-movement replacement event.

To test whether relative reach predicted the magnitude of lateral self-motion bias, a linear mixed-effects model (Equation 7) was fitted across the axis specific bias. The dependent variable was the mean bias, and relative reach was included as a continuous fixed-effect predictor. Participant was included as a random intercept to account for stable between-participant differences in overall bias. For each model, the fixed-effect slope estimate for relative reach was extracted to quantify the direction and magnitude of the relationship, and the associated p-value was used to assess statistical significance. Conditional R^2 values were also calculated to quantify the proportion of variance explained by the full model, including both the fixed effect of relative reach and the participant-level random effects.

$$Mean\ Axial\ Bias \sim Mean\ Relative\ Reach + (1 \mid participant)$$

Equation 7: Linear mixed-effects model used to test whether relative reach predicted lateral bias in Experiment 1.

3.0 Experiment 1 - Lateral self-motion (one step)

Experiment 1 examined whether a lateral self-motion step of 60 cm altered the ability to replace haptically explored objects accurately and precisely. On each trial, participants memorized one of six target locations, with three targets positioned at a depth of 15 cm and the remaining three at a depth of 30 cm from the participant. Within each depth, the central target was located at the centre of the table, corresponding to 60 cm from the left edge and to the participant's 0 cm lateral midline position. Before replacing the object, participants either remained stationary at the centre of the table with no self-motion (CNSM), on the left side of the table with no self-motion (LNSM), or on the right side of the table with no self-motion (RNSM), or they translated laterally from the left to right side of the table (L2R) or from right to left side of the table (R2L) on a walking platform (see Fig. 2.1, Chapter 2).

3.1 Accuracy

3.1.1 Accuracy of Control Conditions

Signed lateral bias did not differ reliably among the three stationary control conditions at either target depth (CNSM, LNSM, RNSM, Table 3.1). These comparisons were required to establish whether stationary changes in body position relative to the target array influenced lateral replacement performance, which would indicate a possible contribution of the distance from the participant to the target distance on lateral bias. Across the six target locations, the mean placement bias remained small in magnitude, ranging from -2.52 to 1.72 cm at 15 cm depth, with SEMs ranging from 0.49 to 1.61 cm, and from -2.73 to 1.23 cm at 30 cm depth, with SEMs ranging from 0.68 to 1.22 cm. All pairwise stationary-condition estimated marginal mean (EMM) comparisons were non-significant in the linear mixed-effects model for lateral bias (see Methods 2.5.4, Equation 1). In addition, none of the stationary control conditions showed reliable changes in lateral bias across the -15, 0, and 15 cm lateral target positions at either depth. Thus, standing position alone did not need to be considered as a source of lateral bias differences, and baseline lateral bias did not vary systematically across the stationary target array.

Table 3.1: Stationary control condition lateral bias across target positions: Values show mean signed lateral bias ± SEM in centimetres for each stationary control condition. Positive values indicate rightward bias, and negative values indicate leftward bias. Pairwise p-values are Holm-adjusted estimated marginal mean comparisons from the linear mixed-effects model fitted to signed lateral bias. All stationary-control contrasts were non-significant. pHolm refers to Holm-adjusted p-value

Target position	CNSM bias	LNSM bias	RNSM bias	CNSM vs RNSM pHolm	CNSM vs LNSM pHolm	RNSM vs LNSM pHolm
-15, 15 □	-0.44 ± 0.83	1.07 ± 0.81	1.73 ± 1.61	1.000 (ns)	1.000 (ns)	1.000 (ns)
0, 15 ○	0.03 ± 0.49	0.01 ± 0.75	0.56 ± 0.96	1.000 (ns)	1.000 (ns)	1.000 (ns)
15,15 △	0.31 ± 0.65	-0.75 ± 0.95	-2.52 ± 0.88	0.743 (ns)	0.937 (ns)	0.937 (ns)
-15, 30 ■	-1.41 ± 0.68	0.48 ± 0.88	1.23 ± 1.22	0.281 (ns)	0.439 (ns)	0.760 (ns)
0, 30 ●	-0.74 ± 0.93	0.39 ± 0.92	-0.12 ± 1.16	0.800 (ns)	0.642 (ns)	0.833 (ns)
15, 30 ▲	0.80 ± 0.86	-0.93 ± 1.06	-2.73 ± 0.79	0.149 (ns)	0.478 (ns)	0.462 (ns)

3.1.2 Accuracy Post-Self-Motion Left/Right

Given that stationary starting stance did not influence lateral bias, each self-motion condition was compared with its stance-matched stationary control, with left-to-right self-motion (L2R) compared against left no self-motion (LNSM) and right-to-left self-motion (R2L) compared against right no self-motion (RNSM). Across both comparisons, object replacement showed a systematic lateral bias opposite to the direction of self-motion. As shown in Fig. 3.1A, rightward self-motion produced leftward replacement errors across all target positions. Mean signed lateral bias was negative at both depths, ranging from -8.01 to -16.2 cm at 15 cm depth (SEMs: 1.68-3.17 cm) and from -6.16 to -13.0 cm at 30 cm depth (SEMs: 1.80-3.04 cm), depending on target position. By contrast, Fig. 3.1B shows that leftward self-motion produced rightward replacement errors, with mean signed lateral bias ranging from 7.20 to 13.4 cm at 15 cm depth (SEMs: 2.21-3.21 cm) and from 5.37 to 13.2 cm at 30 cm depth (SEMs: 1.91-3.21 cm). Thus, lateral self-motion produced systematic directional shifts in object replacement, with participants replacing objects leftward of the true location after rightward self-motion and rightward of the true location after leftward self-motion.

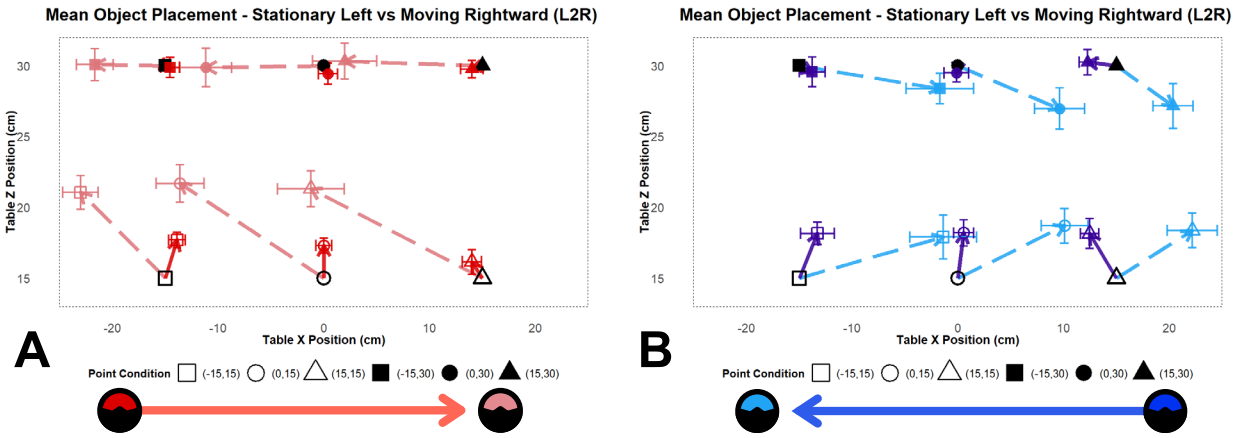

Figure 3.1: Experiment 1 object placement: Panel A shows mean object replacement locations for left-to-right self-motion (L2R; dashed light red) and its stance-matched stationary control, left no self-motion (LNSM; solid dark red). Panel B shows mean object replacement locations for right-to-left self-motion (R2L; dashed light blue) and its stance-matched stationary control, right no self-motion (RNSM; solid dark blue). Error bars indicate SEM along the table X- and Z-axes.

The lateral bias opposite to the direction of self-motion was a statistically significant effect. The linear mixed-effects model fitted to signed lateral bias in Experiment 1 confirmed this pattern, as described in Methods 2.5.4, Equation 1. The model showed a significant main effect of self-motion, $F(4, 520.11) = 119.11$, $p < 2.2 \times 10^{-16}$, a significant main effect of target lateral position, $F(2, 520.11) = 12.45$, $p = 5.243 \times 10^{-6}$, and a significant interaction between self-motion condition and target's lateral position, $F(8, 520.11) = 2.68$, $p = 6.764 \times 10^{-3}$. However, the depth of the target (15 cm vs 30 cm away from the participant) did not influence the lateral bias, $F(1, 520.12) = 0.04$, $p = 0.837$, and none of the interactions involving target depth were significant. Together, these findings show that self-motion reliably altered lateral bias, and that the magnitude of this effect depended on where the target was located laterally on the table, rather than on how far away it was in depth from the participant.

Given the significant effect of target lateral position, and the significant interaction between self-motion condition and lateral position, the contrasts were examined in two complementary ways. Table 3.2 reports the within-position stance-matched contrasts between each self-motion condition and its corresponding stationary control, whereas Table 3.3 reports the across-position contrasts within the self-motion conditions only. The within-position contrasts showed that lateral self-motion produced reliable displacement

at every target location. For L2R versus LNSM, all EMM differences were significant and negative, ranging from -6.68 to -15.47 cm, confirming that rightward self-motion shifted object replacement leftward relative to the stationary baseline. This effect became larger as targets were positioned farther rightward, with EMM differences increasing in magnitude from -9.07 cm at (-15, 15), to -13.60 cm at (0, 15), and -15.47 cm at (15, 15), with the same pattern at 30 cm depth from -6.68 cm at (-15, 30), to -11.54 cm at (0, 30), and -12.08 cm at (15, 30). For R2L versus RNSM, all EMM differences were also significant but positive, ranging from 8.10 to 11.95 cm, confirming that leftward self-motion shifted object replacement rightward relative to the stationary baseline. In this comparison, the largest differences occurred at the leftmost target positions, with EMM differences of 11.71 cm at (-15, 15) and 11.95 cm at (-15, 30), and smaller differences toward the right side of the table, particularly at (15, 30), where the EMM difference was 8.10 cm. Thus, Table 3.2 shows that both directions of lateral self-motion produced reliable bias opposite to the direction of movement, with the largest shifts generally occurring at target positions farthest from the stance-matched starting side.

Table 3.2: Experiment 1 stance-matched contrasts in signed lateral bias: Signed lateral bias contrasts between each self-motion condition and its stance-matched stationary control in Experiment 1. Mean signed lateral bias values are shown for the stationary and self-motion conditions at each target location. The contrast column reports pairwise estimated marginal mean differences from the linear mixed-effects model, calculated as self-motion minus stationary. Negative values indicate leftward bias; positive values indicate rightward bias. P-values are Holm-adjusted; all reported stance-matched contrasts reached statistical significance after correction

Comparison	Target Position	Stationary mean bias (cm)	Self-motion mean bias (cm)	EMM difference (cm)	Holm-Adjusted p value
L2R vs LNSM	-15, 15 □	1.07 ± 0.81	-8.01 ± 1.68	-9.07	2.24 × 10^-4 (***)
	0, 15 ○	0.01 ± 0.75	-13.60 ± 2.27	-13.60	7.95 × 10^-8 (***)
	15,15 △	-0.75 ± 0.95	-16.20 ± 3.17	-15.47	1.49 × 10^-9 (***)
	-15, 30 ■	0.48 ± 0.88	-6.16 ± 1.80	-6.68	0.00724 (**)
	0, 30 ●	0.39 ± 0.92	-11.10 ± 2.45	-11.54	5.87 × 10^-6 (***)
	15, 30 ▲	-0.93 ± 1.06	-13.00 ± 3.04	-12.08	3.00 × 10^-6 (***)
R2L vs RNSM	-15, 15 □	1.73 ± 1.61	13.40 ± 3.21	11.71	8.81 × 10^-6 (***)
	0, 15 ○	0.56 ± 0.96	10.10 ± 2.21	9.53	1.57 × 10^-4 (***)
	15,15 △	-2.52 ± 0.88	7.20 ± 2.37	9.72	1.57 × 10^-4 (***)
	-15, 30 ■	1.23 ± 1.22	13.20 ± 3.21	11.95	3.93 × 10^-6 (***)
	0, 30 ●	-0.12 ± 1.16	9.63 ± 2.36	9.75	1.48 × 10^-4 (***)
	15, 30 ▲	-2.73 ± 0.79	5.37 ± 1.91	8.1	9.76 × 10^-4 (***)

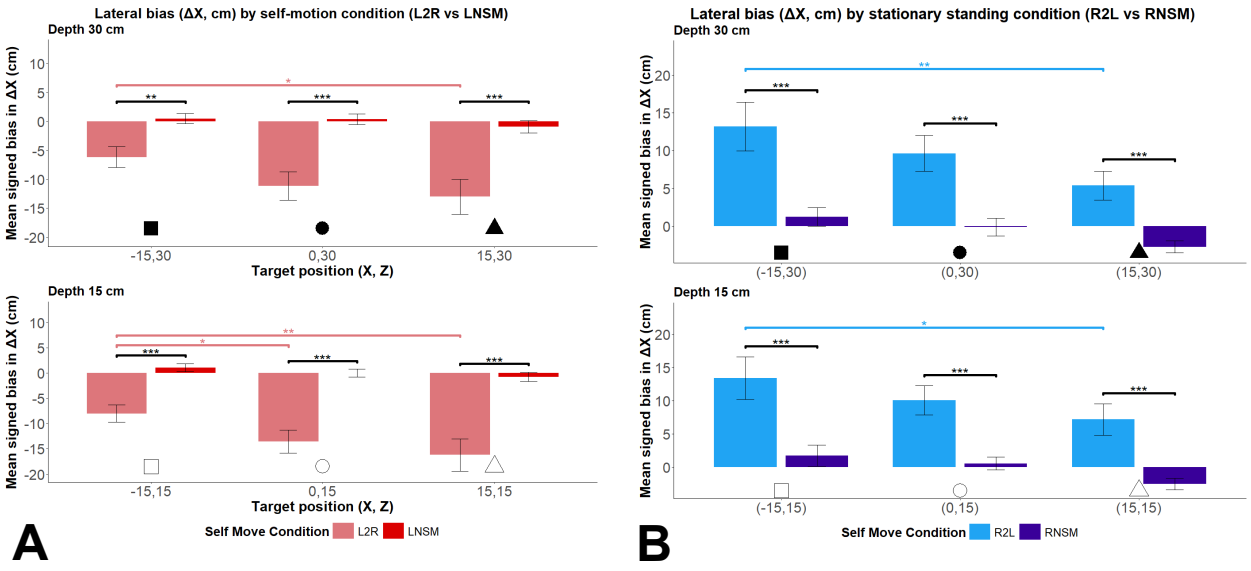

Figure 3.2 Experiment 1 Lateral Bias: Panels A and B show mean signed lateral bias for each target position at the two target depths, 15 cm and 30 cm. Black horizontal brackets indicate within-position contrasts between each self-motion condition and its stance-matched stationary control, whereas coloured brackets indicate across-target-position contrasts within a movement condition. All contrasts are based on estimated marginal means from the linear mixed-effects model with Holm-adjusted inferences; Asterisks denote Holm-adjusted significance levels: p ≤ 0.05 (*), p ≤ 0.01 (**), p ≤ 0.001 (***).

Table 3.3: Experiment 1 across-target contrasts in signed lateral bias: Pairwise contrasts in signed lateral bias (cm) between lateral target positions within each self-motion condition and depth, based on estimated marginal means from the lateral bias linear mixed-effects model for Experiment 1. Only the self-motion conditions are shown. Values represent model-estimated differences in signed lateral bias rather than mean differences. P-values are Holm-adjusted; significance levels are denoted as p ≤ .05 (*), p ≤ .01 (**), and non-significant (ns).

Self-motion Condition	Depth	X Position Contrast	Difference in EMM bias (cm)	Holm-Adjusted p-value
L2R	15	-15 vs 15 (□ vs △)	8.21	0.00250 (**)
		-15 vs 0 (□ vs ○)	5.59	0.0449 (*)
		0 vs 15 (○ vs △)	2.62	0.2847 (ns)
	30	-15 vs 15 (■ vs ▲)	6.82	0.0184 (*)
		-15 vs 0 (■ vs ●)	4.95	0.0929 (ns)
		0 vs 15 (● vs ▲)	1.87	0.4436 (ns)
R2L	15	-15 vs 15 (□ vs △)	6.23	0.0332 (*)
		-15 vs 0 (□ vs ○)	3.33	0.3464 (ns)
		0 vs 15 (○ vs △)	2.90	0.3464 (ns)
	30	-15 vs 15 (■ vs ▲)	7.81	0.00438 (**)
		-15 vs 0 (■ vs ●)	3.55	0.1628 (ns)
		0 vs 15 (● vs ▲)	4.26	0.1628 (ns)

The spatial pattern shown in Table 3.2 was then tested directly through the across-position contrasts within each self-motion condition, shown by the coloured brackets in Fig. 3.2A and B and detailed in Table 3.3. In the L2R condition, lateral bias differed significantly between the two outermost target positions at both depths, with a difference of 8.21 cm between -15 and 15 cm at 15 cm depth, $p = 0.00250$, and 6.82 cm at 30 cm depth, $p = 0.0184$. The -15 versus 0 cm contrast was also significant at 15 cm depth, difference = 5.59 cm, $p = 0.0449$, whereas the remaining intermediate contrasts were not significant. In the R2L condition, the same outermost-position contrast was significant at both depths, with a difference of 6.23 cm between -15 and 15 cm at 15 cm depth, $p = 0.0332$, and 7.81 cm at 30 cm depth, $p = 0.00438$. The other contrasts within R2L were not significant. Together, these across-position comparisons confirm that the magnitude of self-motion-induced lateral bias varied systematically across the table, with the clearest differences occurring between the leftmost and rightmost target positions.

3.1.3 Differences Across Depth Within Lateralities

Contrasts comparing the 15 and 30 cm depth positions within each lateral target position showed no significant differences in lateral bias for either self-motion condition or its stance-matched stationary control. Specifically, depth did not significantly alter bias at $x = -15$, 0, or +15 cm for L2R vs. LNSM, or R2L vs. RNSM conditions, with all Holm-adjusted pairwise comparisons non-significant, $p = 1.00$. Thus, lateral bias was statistically comparable across the two depth levels within each laterality.

3.1.4 Relative Reach and Lateral Bias

To assess whether the lateral bias observed after self-motion was related to participants' effective reaching demands, directional lateral bias was plotted as a function of relative reach, defined as the post-movement head-to-placement distance divided by participant arm length (Fig. 3.3). All observed reaches had relative-reach values below 1, indicating that placements remained within participants' arm length and did not require extra-personal reaching. Separate linear mixed models were then fitted for each self-motion condition to assess whether relative reach predicted lateral bias within each movement direction. These analyses showed no evidence of a reliable relationship between relative reach and lateral bias. For left-to-right self-motion (L2R), the slope was

not significant, slope = -2.71, SE = 7.38, t(104.87) = -0.37, p = 0.714, with a marginal R^2 of 0.001 and a conditional R^2 of 0.535. Similarly, for right-to-left self-motion (R2L), the slope was not significant, slope = -7.12, SE = 8.55, t(102.63) = -0.83, p = 0.407, with a marginal R^2 of 0.005 and a conditional R^2 of 0.524.

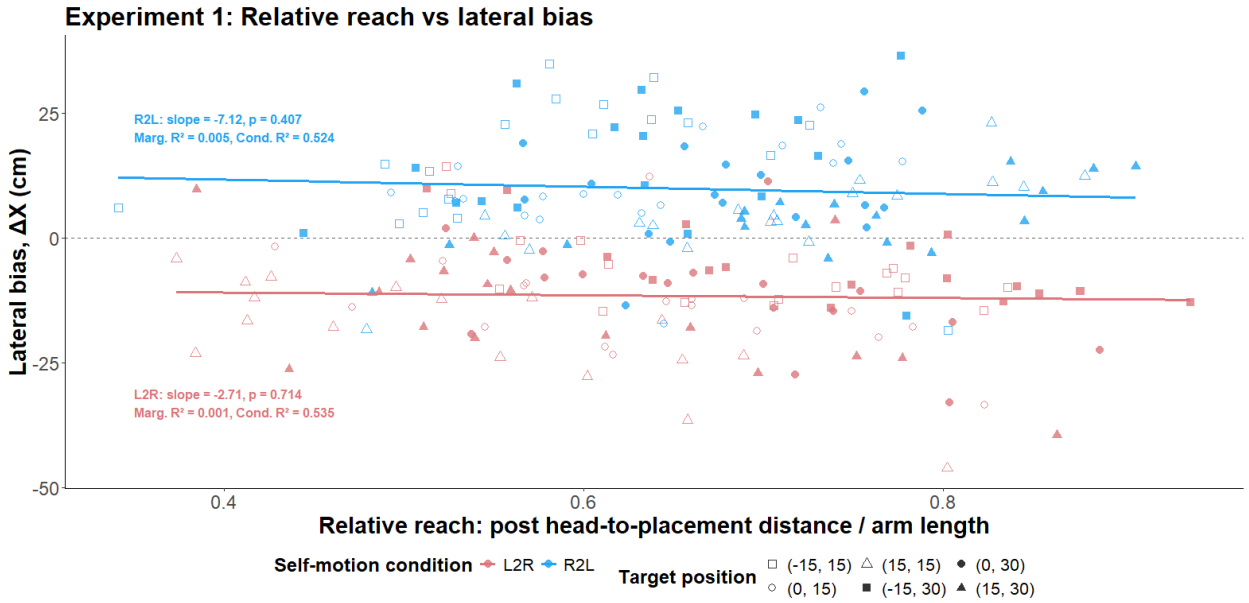

Figure 3.3 Experiment 1 relative reach and lateral bias: Directional lateral bias in ΔX is plotted as a function of relative reach, calculated as the post-movement head-to-placement distance divided by participant arm length, separately for left-to-right self-motion (L2R) and right-to-left self-motion (R2L). Points show individual participant-level placements, with target positions indicated by shape. Solid black lines show linear mixed-model trends from the combined model. All observed reaches fell within participants' arm length, and relative reach did not reliably predict lateral bias in either movement direction.

3.2 Precision

3.2.1 Precision of Controls

Stationary control trials were first examined to determine whether starting stance alone influenced precision, analogous to the initial control analysis for lateral bias. Precision did not differ reliably among centre no self-motion (CNSM), left no self-motion (LNSM), and right no self-motion (RNSM), as seen in Table 3.4. At 15 cm depth, mean within-participant variability across the stationary control conditions ranged from 2.38 to 4.07 cm, with SEMs ranging from 0.19 to 0.55 cm. At 30 cm depth, mean variability ranged from 2.99 to 4.32 cm, with SEMs ranging from 0.27 to 0.44 cm. All pairwise comparisons

among the stationary control conditions were non-significant after Holm correction. Thus, stationary starting stance alone did not systematically influence precision across the control conditions, although one localized across-position difference was observed within CNSM at 15 cm depth, where variability differed between the -15 cm and 15 cm target positions, Holm-adjusted p = 0.0416. This isolated target-position effect did not indicate a broader systematic influence of stationary starting stance on precision.

Table 3.4: Experiment 1 stationary-control precision across target positions :Values show mean within-participant endpoint variability ± SEM in centimetres for each stationary control condition. Larger values indicate lower precision. Pairwise p-values are Holm-adjusted estimated marginal mean comparisons from the linear mixed-effects model fitted to log-transformed precision. All stationary control contrasts were non-significant.

Target position	CNSM precision	LNSM precision	RNSM precision	CNSM vs RNSM pHolm	CNSM vs LNSM pHolm	RNSM vs LNSM pHolm
-15, 15 □	3.60 ± 0.32	4.07 ± 0.55	3.10 ± 0.33	0.568 (ns)	0.592 (ns)	0.324 (ns)
0, 15 ○	2.78 ± 0.19	2.84 ± 0.28	2.77 ± 0.29	1.000 (ns)	1.000 (ns)	1.000 (ns)
15,15 △	2.38 ± 0.24	3.08 ± 0.29	3.06 ± 0.32	0.374 (ns)	0.374 (ns)	0.884 (ns)
-15, 30 ■	3.12 ± 0.27	3.75 ± 0.44	4.32 ± 0.43	0.0784 (ns)	0.455 (ns)	0.455 (ns)
0, 30 ●	3.02 ± 0.30	3.50 ± 0.42	3.49 ± 0.39	0.929 (ns)	0.929 (ns)	0.929 (ns)
15, 30 ▲	3.22 ± 0.34	4.12 ± 0.36	2.99 ± 0.29	0.794 (ns)	0.223 (ns)	0.165 (ns)

3.2.2 Precision Post-Self-Motion Left/Right

Precision was generally lower following self-motion than in the corresponding stance-matched stationary control conditions. As shown in Fig. 3.3 and summarized in Table 3.5, within-participant endpoint variability was consistently higher after left-to-right self-motion (L2R; 4.78-6.82 cm) than in left no self-motion (LNSM; 2.84-4.12 cm), and likewise higher after right-to-left self-motion (R2L; 5.12-7.71 cm) than in right no self-motion (RNSM; 2.77-4.32 cm). Thus, lateral self-motion generally reduced precision. Unlike lateral bias, however, this reduction did not show a clear or systematic spatial pattern across target positions, as the magnitude of the self-motion-related increase in variability did not change in a consistent way across lateral position or depth. This descriptive pattern was confirmed by the linear mixed-effects model fitted to log-transformed precision.

Table 3.5: Experiment 1 self-motion versus stationary-control precision contrasts: Mean within-participant endpoint variability for each self-motion condition and its stance-matched stationary control across all target positions in Experiment 1. Variability is expressed in centimetres as the mean Euclidean distance between individual placements

and each participant's mean placement within the same condition × target position. Larger values indicate lower precision. Holm-adjusted p-values indicate the significance of the difference in precision between each self-motion condition and its corresponding stationary control, based on estimated marginal mean contrasts from the linear mixed-effects model fitted to log-transformed precision.

Comparison	Target position (X,Z)	Mean self-motion variability (cm)	Mean stationary-control variability (cm)	Holm Adjusted p-value
L2R vs LNSM	-15, 15 □	5.74 ± 0.65	4.07 ± 0.55	0.0270 (*)
	0, 15 ○	6.46 ± 0.50	2.84 ± 0.28	1.31 × 10^-8 (***)
	15,15 △	6.21 ± 0.82	3.08 ± 0.29	2.59 × 10^-5 (***)
	-15, 30 ■	4.78 ± 0.46	3.75 ± 0.44	0.0596 (ns)
	0, 30 ●	6.82 ± 0.62	3.50 ± 0.42	2.92 × 10^-6 (***)
	15, 30 ▲	6.19 ± 0.79	4.12 ± 0.36	0.0115 (*)
R2L vs RNSM	-15, 15 □	7.71 ± 0.89	3.10 ± 0.33	9.50 × 10^-8 (***)
	0, 15 ○	7.58 ± 1.19	2.77 ± 0.29	6.78 × 10^-9 (***)
	15,15 △	5.45 ± 0.52	3.06 ± 0.32	1.88 × 10^-4 (***)
	-15, 30 ■	5.12 ± 0.49	4.32 ± 0.43	0.246 (ns)
	0, 30 ●	6.13 ± 0.71	3.49 ± 0.39	1.16 × 10^-4 (***)
	15, 30 ▲	5.17 ± 0.67	2.99 ± 0.29	6.02 × 10^-4 (***)

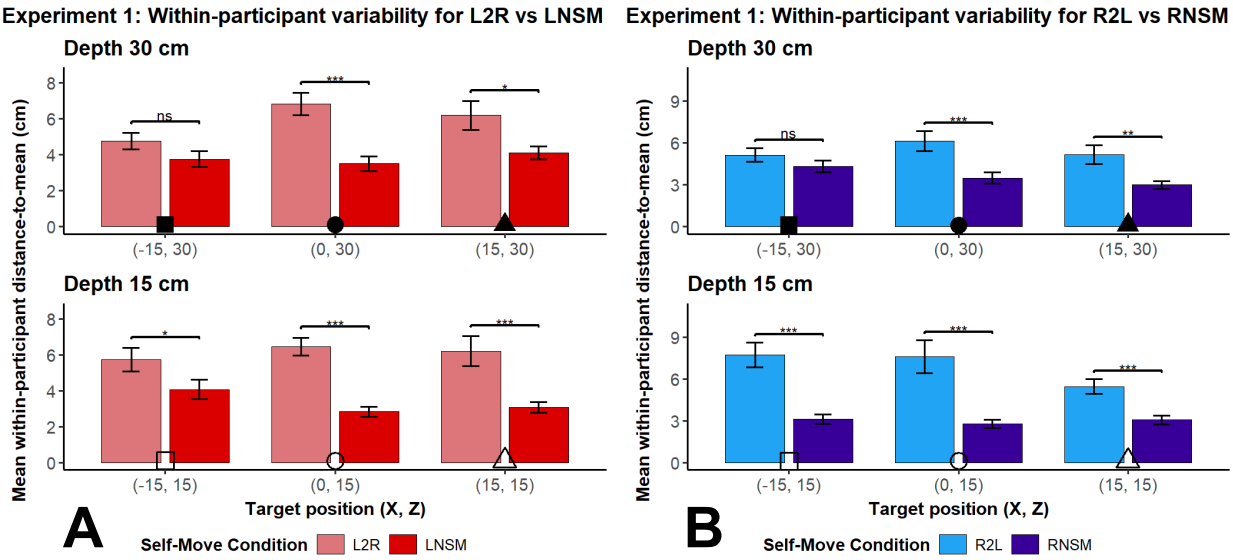

Figure 3.4: Experiment 1 stance-matched contrasts in endpoint variability: Within-participant endpoint variability is shown for all target locations, separately for left-to-right self-motion (L2R, panel A) contrasted with its stance-matched stationary control (LNSM) and right-to-left self-motion (R2L, panel B) contrasted with its stationary control (RNSM). Variability was calculated as the mean Euclidean distance between individual placements and each participant's mean placement within the same condition × target position. Bars show means ± SEM. Target locations are indicated on the x-axis by their (X, Z) coordinates, with shape and colour coding matched to Fig. 3.1.

The linear mixed-effects model fitted to log-transformed precision confirmed that self-motion condition influenced precision overall (Methods 2.5.4, Equation 2). Specifically, there was a significant main effect of self-motion, $F(4, 394.95) = 57.80$, $p < 2 \times 10^{-16}$, indicating that variability differed across the movement and stationary conditions. By contrast, there was no overall main effect of target lateral position, $F(2, 388.06) = 1.79$, $p = 0.169$, and no overall main effect of target depth, $F(1, 387.43) = 0.41$, $p = 0.522$, suggesting that precision did not simply increase or decrease as a function of target location alone. This was reflected in a significant interaction between self-motion and lateral position, $F(8, 388.02) = 2.38$, $p = 0.016$, and a significant interaction between self-motion and target depth, $F(4, 387.62) = 3.04$, $p = 0.017$. The interaction between lateral position and depth was not significant, $F(2, 387.95) = 2.13$, $p = 0.120$, and the three-way interaction among self-motion, lateral position, and depth was also not significant, $F(8, 387.66) = 1.07$, $p = 0.385$. Overall, self-motion reduced precision, but this reduction varied locally across the target array without forming a clear, monotonic spatial pattern.

3.3 Summary

In Experiment 1, lateral self-motion reliably altered haptic object replacement. Stationary starting stance alone did not influence either signed lateral bias or precision. By contrast, after self-motion, participants systematically misplaced objects in the direction opposite to travel: left-to-right self-motion produced a leftward bias, whereas right-to-left self-motion produced a rightward bias. This effect was evident across all target positions and increased with lateral target eccentricity but was not affected by the depth of the target position. This bias was not explained by relative reach, as all placements remained within each participant's arm length and relative reach did not reliably predict lateral bias.

Self-motion also reduced precision overall relative to the stance-matched stationary controls, although this loss of precision did not follow a clear or strongly systematic spatial pattern. Taken together, these findings indicate that lateral self-motion systematically biases haptic object replacement opposite to the direction of movement and reduces precision.

4.0 Experiment 2 Anteroposterior self-motion (one step)

Experiment 2 examined whether an anteroposterior self-motion step (40 cm) altered the ability to replace haptically explored objects accurately and precisely. Participants memorized one of six target locations. In contrast to Experiment 1, where target layout varied across two depth levels, Experiment 2 used two lateral positions relative to the participant (15 and 30 cm) and three depth positions from the forward most edge the participant travelled (15, 30, and 45 cm; see Chapter 2, Figure 2.1, for a schematic of the layout). Before replacing the object, participants either remained stationary at the front no self-motion position (FNSM), remained stationary at the back no self-motion position (BNSM), translated from front to back (F2B), or translated from back to front (B2F).

4.1 Accuracy

4.1.1 Accuracy of Control Conditions

Signed anteroposterior bias was similar across the two stationary control conditions, front no self-motion (FNSM) and back no self-motion (BNSM), as shown in Table 4.1. These comparisons were necessary to determine whether standing position alone, in the absence of self-motion, influenced anteroposterior bias during replacement, and therefore whether participant position relative to the object contributed to baseline bias. At the 15 cm laterality, stationary control mean signed anteroposterior bias remained modest, ranging from -2.48 to 3.06 cm, with SEMs of 0.88-1.43 cm. At the 30 cm laterality, stationary-control bias ranged from -5.16 to 1.46 cm, with SEMs of 0.85-1.19 cm. Pairwise EMM contrasts between BNSM and FNSM showed no reliable differences at any target position, with EMM differences ranging from 0.85 to 4.03 cm and all Holm-adjusted p-values non-significant. Across-depth contrasts within the stationary conditions were also non-significant. These contrasts ranged from -0.17 to -4.83 cm across FNSM and BNSM, with all Holm-adjusted p-values ≥ 0.279. Thus, there was no reliable evidence that stationary front versus back stance influenced anteroposterior bias, nor that baseline anteroposterior bias varied systematically across target depth in the absence of self-motion.

Table 4.1: Experiment 2 stationary-control anteroposterior bias across target positions: Mean signed anteroposterior bias (cm) ± SEM for the stationary control conditions, front no self-motion (FNSM) and back no self-motion (BNSM), at each target position. Negative values indicate forward bias, whereas positive values indicate backward bias. Pairwise p-values are Holm-adjusted estimated marginal mean (EMM) contrasts between FNSM and BNSM from the linear mixed-effects model fitted to signed anteroposterior error (see Methods 2.5.4, Equation 1). No stationary-control comparisons were significant.

Target position	FNSM bias (cm)	BNSM bias (cm)	EMM difference	Holm Adjusted p-value
(15, 15) □	-2.48 ± 0.98	-1.71 ± 0.88	0.85	1.000 (ns)
(15, 30) ○	-1.14 ± 0.89	0.29 ± 1.08	1.43	1.000 (ns)
(15, 45) △	-0.97 ± 1.28	3.06 ± 1.43	4.03	0.291 (ns)
(30, 15) ■	-5.16 ± 0.87	-3.38 ± 0.99	1.79	0.871 (ns)
(30, 30) ●	-2.85 ± 0.85	-0.96 ± 1.10	1.89	0.871 (ns)
(30, 45) ▲	-2.04 ± 1.19	1.46 ± 0.98	3.50	0.448 (ns)

4.1.2 Accuracy Post Anteroposterior Self-Motion

Given that baseline anteroposterior bias was similar across the two stationary control conditions, each self-motion condition was compared with its stance-matched stationary control, with back to front self-motion (B2F) compared against back no self-motion (BNSM) and front to back self-motion (F2B) compared against front no self-motion (FNSM). Across both comparisons, object replacement was biased in the direction opposite to self-motion, much like in Experiment 1. In Fig. 4.1A, the replacement vectors following B2F are consistently shifted downward, indicating that responses were displaced backward after forward self-motion. In Fig. 4.1B, this backward bias ranged from 9.87 to 24.1 cm at the 15 cm laterality and from 6.58 to 16.4 cm at the 30 cm laterality, with SEMs ranging from 2.32 to 3.76 cm and from 1.71 to 3.59 cm, respectively, and all six stance-matched comparisons were significant. By contrast, in Fig. 4.1C, the replacement vectors following F2B are shifted upward relative to their matched stationary bias by target position, indicating that responses were displaced forward relative to the true target locations. In Fig. 4.1D, this forward bias ranged from -17.2 to -3.36 cm at the 15 cm laterality and from -15.4 cm to near zero (0.12 cm) at the 30 cm laterality, with SEMs ranging from 1.28 to 2.28 cm and from 1.56 to 2.22 cm, respectively. Only four of the six stance-matched comparisons were significant, with no reliable differences at the farthest depth targets ((15, 45) and (30, 45)) relative to the corresponding stationary condition. Together, these findings show that anteroposterior self-motion shifted object replacement opposite to the direction of travel, particularly during forward movement.

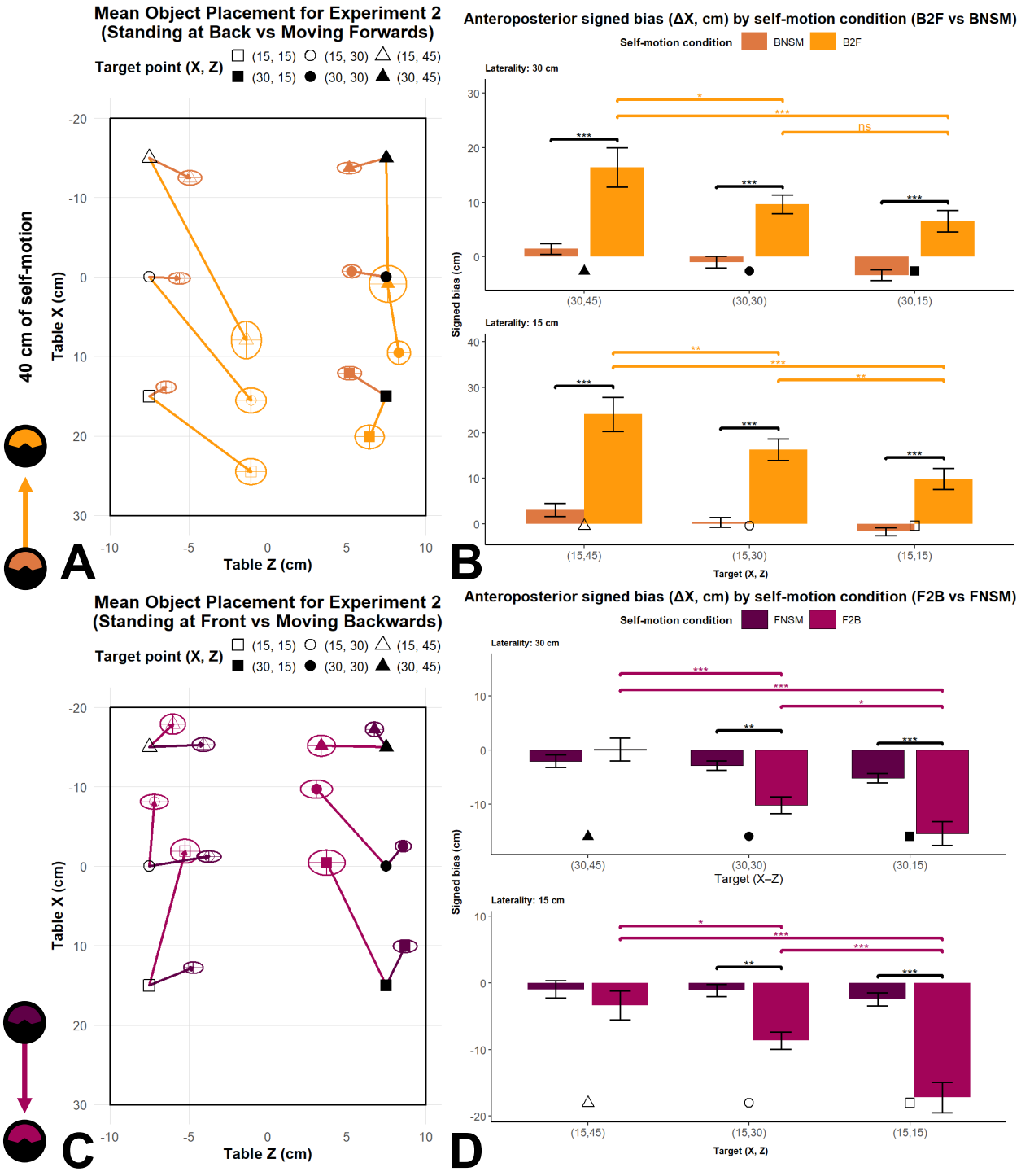

Figure 4.1: Experiment 2 object placements and anteroposterior bias:Panel A shows mean object replacement locations for back-to-front self-motion (B2F; light orange) and its stance-matched stationary control, back no self-motion (BNSM; dark orange). Panel C shows mean object replacement locations for front-to-back self-motion (F2B; light magenta) and its stance-matched stationary control, front no self-motion (FNSM; dark magenta). Error bars indicate SEM along the table X- and Z-axes. Panels B and D show

mean signed anteroposterior bias for each target position at the two lateral positions, 30 cm and 15 cm. Black horizontal brackets indicate within-position contrasts between each self-motion condition and its stance-matched stationary control, whereas coloured brackets indicate across-target-position contrasts within a movement condition. All contrasts are based on estimated marginal means from the linear mixed-effects model with Holm-adjusted inferences; asterisks indicate corrected significance levels. Consistent with the model and pairwise contrasts, B2F produced reliable positive/backward shifts across the full target array, whereas F2B produced reliable negative/forward shifts at all but the farthest target positions.

This pattern of object replacement opposite to the direction of self-motion was systematic rather than random, as confirmed by the linear mixed-effects model fitted to signed anteroposterior bias in Experiment 2 (see Methods 2.5.4, Equation 1) and further supported by the pairwise contrasts indicated by the black comparison brackets in Fig. 4.1B and D. The model showed a significant main effect of self-motion, $F(3, 411.08) = 199.60$, $p < 2.2 \times 10^{-16}$, as well as significant main effects of lateral target position, $F(1, 411.08) = 8.20$, $p = 4.40 \times 10^{-3}$, and anteroposterior target position, $F(2, 411.02) = 51.65$, $p < 2.2 \times 10^{-16}$. There was also a significant interaction between self-motion condition and lateral target position, $F(3, 411.07) = 4.45$, $p = 4.325 \times 10^{-3}$, and between self-motion condition and anteroposterior target position, $F(6, 411.01) = 6.28$, $p = 2.505 \times 10^{-6}$. By contrast, the interaction between lateral and anteroposterior target position was not significant, $F(2, 411.01) = 0.34$, $p = 0.713$, nor was the three-way interaction among self-motion condition, lateral target position, and anteroposterior target position, $F(6, 411.01) = 0.60$, $p = 0.733$. Together, these findings show that self-motion reliably altered anteroposterior bias, and that the magnitude of this effect varied across the target array. Follow-up EMM contrasts were therefore used to decompose these effects. Within-position contrasts tested whether each self-motion direction differed from its stance-matched stationary control at each target location, whereas across-depth contrasts tested whether self-motion-induced bias varied with anteroposterior target position.

Table 4.2 summarizes the contrasts between each self-motion condition and its corresponding stationary baseline at each target position. These same comparisons are shown by the black brackets in Fig. 4.1B and D. For self-motion forwards (B2F) versus BNSM, self-motion produced backward displacement at all six target locations, with mean bias ranging from 9.87 to 24.10 cm at the 15 cm lateral position (SEMs: 2.32-3.76 cm)

and from 6.58 to 16.40 cm at the 30 cm lateral position (SEMs: 1.71-3.59 cm). All six B2F contrasts were significant from the stationary control. For self-motion backwards (F2B) versus FNSM, self-motion produced forward displacement, with mean bias ranging from -17.20 to -3.36 cm at the 15 cm lateral position (SEMs: 1.28-2.28 cm) and from -15.40 to 0.12 cm at the 30 cm lateral position (SEMs: 1.56-2.22 cm). Four of the six F2B contrasts were significant, with only the farthest targets, (15, 45) and (30, 45), remaining non-significant. Thus, anteroposterior self-motion shifted object replacement opposite to the direction of travel, although this effect weakened at the farthest depth in the F2B condition.

Table 4.2: Experiment 2 stance-matched contrasts in signed anteroposterior bias: Signed anteroposterior bias contrasts between each self-motion condition and its stance-matched stationary control in Experiment 2, based on estimated marginal means from the linear mixed-effects model. Descriptive mean signed anteroposterior bias values for the stationary and self-motion conditions are also shown for each target location. Negative values indicate forward bias, whereas positive values indicate backward bias. Estimated marginal mean differences are reported as stationary minus self-motion. P-values are Holm-adjusted; significance levels are denoted as p ≤ .05 (*), p ≤ .01 (**), p ≤ .001 (***), and non-significant (ns)

Comparison	Target position	Stationary mean bias (cm)	Self-motion mean bias (cm)	EMM difference	Adjusted p
F2B vs FNSM	(15, 15) □	-2.48 ± 0.98	-17.20 ± 2.28	14.62	1.66 × 10^-8 (***)
	(15, 30) ○	-1.14 ± 0.89	-8.65 ± 1.28	7.51	0.00408 (**)
	(15, 45) △	-0.97 ± 1.28	-3.36 ± 2.16	2.39	0.324 (ns)
	(30, 15) ■	-5.16 ± 0.87	-15.40 ± 2.22	10.25	8.39 × 10^-5 (***)
	(30, 30) ●	-2.85 ± 0.85	-10.20 ± 1.56	7.31	0.00535 (**)
	(30, 45) ▲	-2.04 ± 1.19	0.12 ± 2.11	-2.16	0.373 (ns)
B2F vs BNSM	(15, 15) □	-1.71 ± 0.88	9.87 ± 2.32	-11.57	2.40 × 10^-6 (***)
	(15, 30) ○	0.29 ± 1.08	16.30 ± 2.39	-15.99	2.36 × 10^-10 (***)
	(15, 45) △	3.06 ± 1.43	24.10 ± 3.76	-21	2.53 × 10^-16 (***)
	(30, 15) ■	-3.38 ± 0.99	6.58 ± 1.98	-9.96	4.68 × 10^-5 (***)
	(30, 30) ●	-0.96 ± 1.10	9.61 ± 1.71	-10.75	3.03 × 10^-5 (***)
	(30, 45) ▲	1.46 ± 0.98	16.40 ± 3.59	-15.1	5.44 × 10^-9 (***)

To determine whether anteroposterior bias changed across depth, the across depth contrasts were examined within each lateral position for forward self-motion (B2F) and backward self-motion (F2B) only, as summarized in Table 4.3. The two movement directions showed opposite depth gradients. During forward self-motion (B2F), anteroposterior bias was smallest at the nearest targets and largest at the farthest targets.

During backward self-motion (F2B), the reverse pattern was observed, with anteroposterior bias largest at the nearest targets and weakening as target depth increased. Numerically, for forward self-motion (B2F), mean signed anteroposterior bias at the 15 cm lateral position increased from 9.87 cm at (15, 15), to 16.30 cm at (15, 30), and 24.10 cm at (15, 45). At the 30 cm lateral position, bias increased from 6.58 cm at (30, 15), to 9.61 cm at (30, 30), and 16.40 cm at (30, 45). For backward self-motion (F2B), mean signed anteroposterior bias at the 15 cm lateral position changed from -17.20 cm at (15, 15), to -8.65 cm at (15, 30), and -3.36 cm at (15, 45). A similar pattern was observed at the 30 cm lateral position, where bias changed from -15.40 cm at (30, 15), to -10.20 cm at (30, 30), and 0.12 cm at (30, 45). Thus, the across-depth contrasts in Table 4.3 evaluate a clear directional pattern in the means; forward self-motion (B2F) bias increased with target depth, whereas backward self-motion (F2B) bias was strongest at nearer targets and weakened with distance.

Table 4.3: Experiment 2 across-depth contrasts in signed anteroposterior bias: Pairwise contrasts in signed anteroposterior bias (cm) between target depths within each self-motion condition and laterality, based on estimated marginal means from the anteroposterior bias linear mixed-effects model for Experiment 2. Only the self-motion conditions are shown. Values represent model-estimated differences in signed anteroposterior bias between the two depth positions listed in the comparison column, rather than mean differences. P-values are Holm-adjusted; significance levels are denoted as, p ≤ .05 (*) p ≤ .01 (**), p ≤ .001 (***) and non-significant (ns).

Condition	Laterality	Depth comparison	Difference in mean bias (cm)	Holm Adjusted p-value
F2B	15	15 vs 30	-8.53	9.45 x 10^-4 (***)
		15 vs 45	-13.82	6.35 x 10^-8 (***)
		30 vs 45	-5.29	2.94 x 10^-2 (*)
	30	15 vs 30	-5.25	3.05 x 10^-2 (*)
		15 vs 45	-15.54	1.09 x 10^-9 (***)
		30 vs 45	-10.28	5.32 x 10^-5 (***)
B2F	15	15 vs 30	-6.41	8.45 x 10^-3 (**)
		15 vs 45	-14.19	2.75 x 10^-8 (***)
		30 vs 45	-7.78	2.81 x 10^-3 (**)
	30	15 vs 30	-3.22	1.912 x 10^-1 (ns)
		15 vs 45	-9.98	1.75 x 10^-4 (***)
		30 vs 45	-6.76	1.38 x 10^-2 (*)

4.1.3 Across lateralities

Finally, because the linear mixed model for anteroposterior bias showed a significant interaction between self-motion condition and lateral target position, across-laterality comparisons were examined at each depth to determine whether

anteroposterior bias differed between the 15 cm and 30 cm lateral positions within each self-motion condition, shown in Fig. 4.2. In F2B, signed anteroposterior bias did not differ reliably between the two lateral positions at any depth, with means remaining broadly similar at 15 cm depth (-17.2 vs -15.4 cm), 30 cm depth (-8.65 vs -10.2 cm), and 45 cm depth (-3.36 vs 0.12 cm), and all Holm-adjusted comparisons non-significant. In B2F, by contrast, laterality effects emerged more clearly. Although the near depth did not differ reliably between lateral positions (9.87 vs 6.58 cm, adjusted p = 0.175), bias was significantly larger at the 15 cm than at the 30 cm lateral position at the 30 cm depth (16.3 vs 9.80 cm, adjusted p = 0.0174) and at the 45 cm depth (24.1 vs 16.6 cm, adjusted p = 7.26×10^{-3}). Thus, lateral target position did not reliably modulate anteroposterior bias in F2B, but in B2F the 15 cm laterality produced larger positive biases than the 30 cm laterality at the middle and far depths, consistent with the significant self-motion interaction with lateral target position.

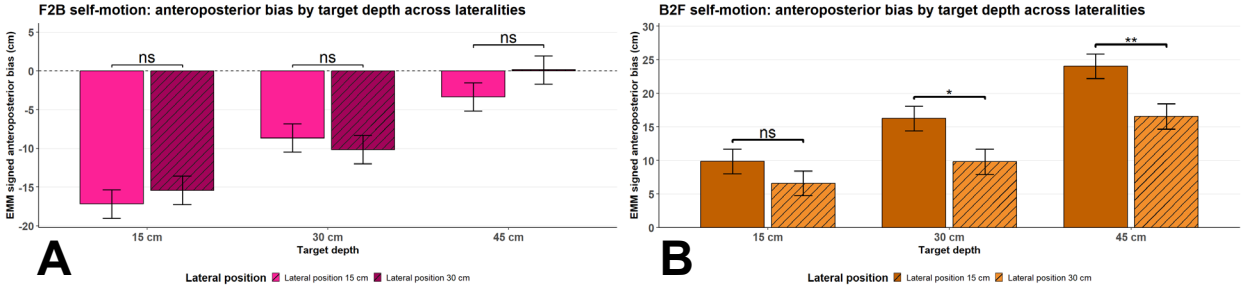

Figure 4.2: Experiment 2 across-laterality contrasts in signed anteroposterior bias: Mean signed anteroposterior bias shown for each target depth across lateralities (15 and 30 cm), separately for front-to-back self-motion (F2B; Panel A) and back-to-front self-motion (B2F; Panel B). Error bars represent means ± SEM. Black horizontal brackets indicate across-laterality contrasts at the same depth, based on EMM from the linear mixed-effects model with Holm-adjusted comparisons with asterisks indicating p ≤ .05 (*) p ≤ .01 (**).

4.1.4 Relative Reach and Anteroposterior Bias

To assess whether anteroposterior bias was influenced by effective reaching demands, signed anteroposterior bias was plotted as a function of relative reach, defined as the post-movement head-to-placement distance divided by participant arm length (Fig. 4.3). In the F2B condition, some responses required relatively extended reaches, with several observations approaching or exceeding a relative reach of 1.0 and extending to approximately 1.25. However, a linear mixed model fitted to the F2B condition showed no

evidence that relative reach predicted anteroposterior bias, slope = 2.41, SE = 6.92, t(103.14) = 0.35, p = 0.728. The marginal R^2 was .001, indicating that relative reach explained virtually none of the variance in F2B bias, while the conditional R^2 was .228.

For B2F, the relationship between relative reach and anteroposterior bias was statistically significant. The estimated slope was negative, slope = -23.94, SE = 9.03, t(105.99) = -2.65, p = 0.009, indicating that larger relative-reach values were associated with reduced positive/backward bias. However, the marginal R^2 of 0.062 shows that relative reach explained only a modest amount of the variance in bias and therefore did not account for the majority of the observed bias pattern. In contrast, the higher conditional R^2 of 0.556 indicates that the full model captured additional variance due to participant-level differences. Thus, relative reach was related to B2F bias, but it did not provide a sufficient explanation for the overall anteroposterior bias pattern.

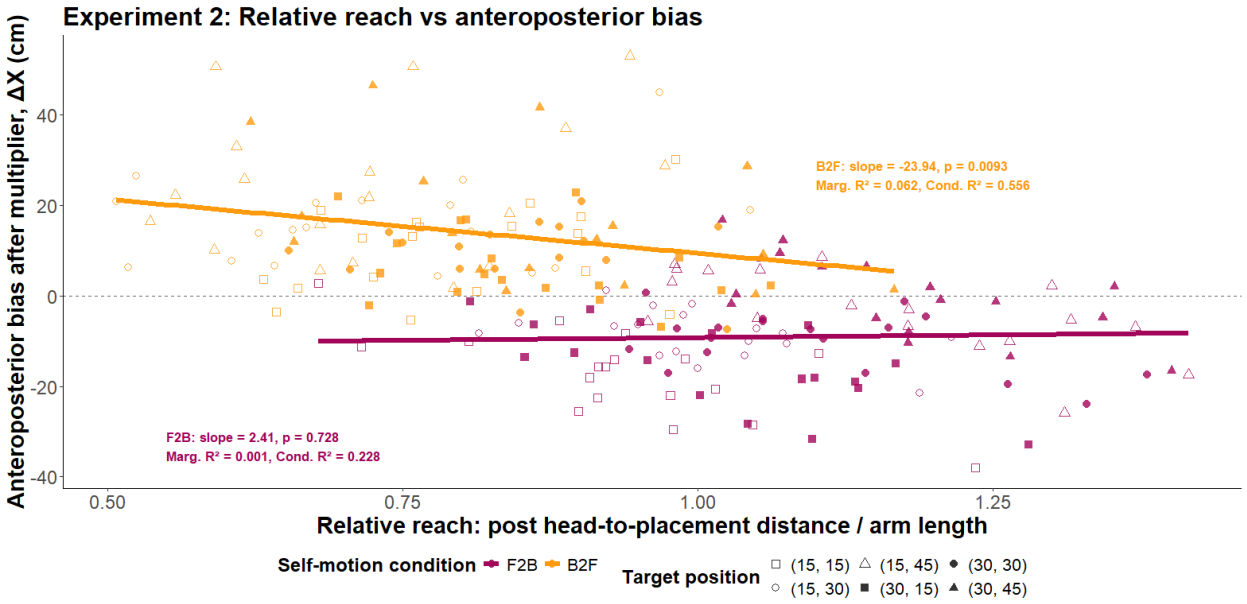

Figure 4.3: Experiment 2 Relative Reach and Anteroposterior Bias: Signed anteroposterior bias is plotted as a function of relative reach, calculated as the post-movement head-to-placement distance divided by participant arm length, separately for front-to-back self-motion (F2B) and back-to-front self-motion (B2F). Points show individual placements, with target positions indicated by shape. Solid black lines show linear mixed-model trends. Relative reach did not significantly predict anteroposterior bias in F2B, but showed a significant negative relationship in B2F; however, this relationship explained only a modest proportion of the variance and did not account for the overall bias pattern.

4.2 Precision

4.2.1 Precision of Controls

Stationary control trials were first examined to determine whether starting position alone influenced precision, in a similar fashion to the initial analysis of anteroposterior bias. Precision did not differ reliably between front no self-motion (FNSM) and back no self-motion (BNSM), as shown in Table 4.4. At the 15 cm lateral position, mean within-participant variability ranged from 3.76 to 4.37 cm in FNSM (SEMs: 0.35-0.73 cm) and from 3.83 to 4.04 cm in BNSM (SEMs: 0.36-0.47 cm). At the 30 cm lateral position, variability ranged from 3.68 to 4.73 cm in FNSM (SEMs: 0.33-0.62 cm) and from 3.87 to 5.06 cm in BNSM (SEMs: 0.39-0.65 cm). All pairwise EMM contrasts between BNSM and FNSM were non-significant after Holm correction. Thus, there was no reliable evidence that standing at the front versus the back of the table systematically affected baseline precision.

Table 4.4: Experiment 2 stationary-control precision across target positions: Mean within-participant endpoint variability ± SEM in centimetres for the stationary control conditions, front no self-motion (FNSM) and back no self-motion (BNSM), at each target position in Experiment 2. Holm-adjusted p-values indicate the significance of the within-position comparison between the two stationary control conditions, based on estimated marginal mean contrasts from the linear mixed-effects model fitted to log-transformed precision.

Target position	FNSM variability (cm)	BNSM variability (cm)	Holm Adjusted p-value
(15, 15) □	3.78 ± 0.35	3.83 ± 0.47	0.941 (ns)
(15, 30) ○	3.76 ± 0.44	4.01 ± 0.36	0.704 (ns)
(15, 45) △	4.37 ± 0.73	4.04 ± 0.44	1.00 (ns)
(30, 15) ■	4.73 ± 0.62	5.06 ± 0.65	1.00 (ns)
(30, 30) ●	3.95 ± 0.33	3.90 ± 0.42	0.702 (ns)
(30, 45) ▲	3.68 ± 0.38	3.87 ± 0.39	0.793 (ns)

4.2.2 Precision Post Anteroposterior Self-Motion

Precision differed following self-motion relative to the corresponding stationary control conditions. Fig. 4.4 shows within-participant endpoint variability for each target position in the front-to-back self-motion (F2B) versus front no self-motion (FNSM) comparison and the back-to-front self-motion (B2F) versus back no self-motion (BNSM)

comparison. Across both movement directions, self-motion generally reduced precision, with mean variability in the F2B condition ranging from 4.68 to 6.98 cm compared with 3.68 to 4.73 cm in FNSM, and in the B2F condition ranging from 5.96 to 7.23 cm compared with 3.83 to 5.06 cm in BNSM, which is further elucidated in Table 4.5. Unlike anteroposterior bias, however, these increases in variability did not show a clear spatial progression across the target array. In F2B, the reduction in precision was modest and none of the stance-matched contrasts reached significance after Holm correction. In B2F, the reduction in precision was larger overall and reached significance at three target locations: (15,15), (30,30), and (30,45). Taken together, these findings indicate that anteroposterior self-motion tended to reduce precision, with the clearest effects observed following back-to-front rather than front-to-back translation.

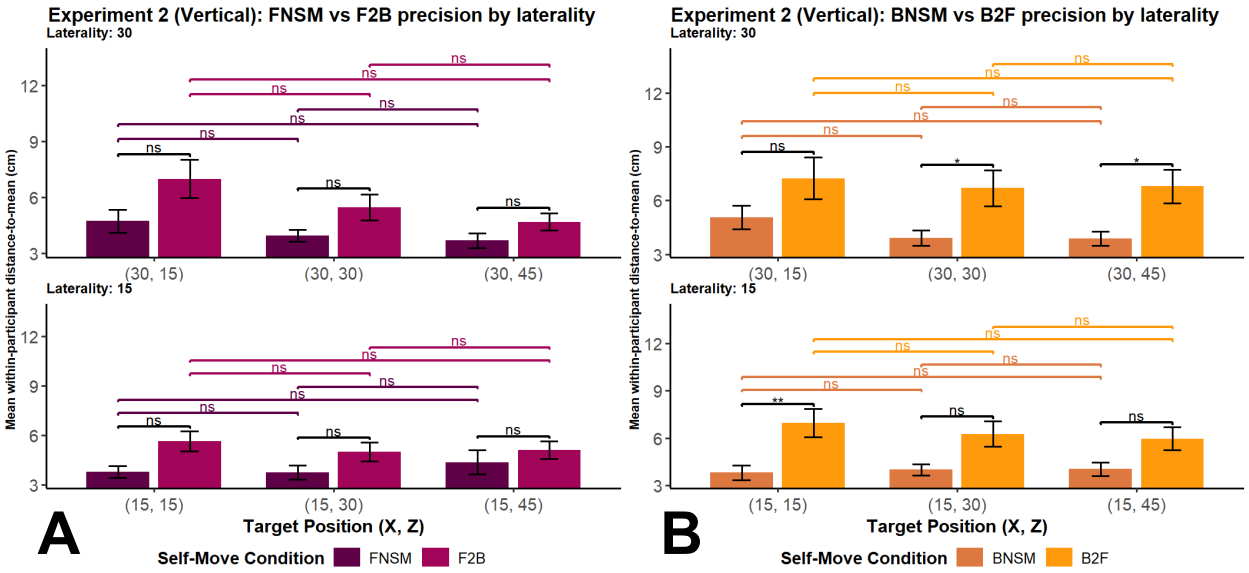

Figure 4.4: Experiment 2 stance-matched contrasts in endpoint variability: Within-participant endpoint variability (precision; cm) is shown for all target locations. In Panel A, front-to-back self-motion (F2B) is contrasted with its stance-matched stationary control (FNSM). In Panel B, back-to-front self-motion (B2F) is contrasted with its stationary control (BNSM). Within each panel, the upper subplot shows the 30 cm lateral position, and the lower subplot shows the 15 cm lateral position. Bars represent means ± SEM, with larger values indicating lower precision. Black horizontal brackets indicate within-position contrasts between each self-motion condition and its stance-matched stationary control, whereas coloured brackets indicate across-target-position contrasts within a movement condition. All contrasts are based on estimated marginal means from the log-transformed precision linear mixed-effects model with Holm-adjusted inferences; asterisks indicate corrected significance levels: p ≤ .05 (*), p ≤ .01 (**).

Table 4.5: Experiment 2 self-motion versus stationary-control precision contrasts: Mean within-participant endpoint variability (precision; cm) for the self-motion conditions and their stance-matched stationary controls at each target location in Experiment 2. Variability is expressed as the mean Euclidean distance between individual placements and each participant's mean placement within the same condition × target position. Holm-adjusted p-values indicate the significance of the within-position self-motion versus stationary-control comparisons, based on estimated marginal mean contrasts from the linear mixed-effects model fitted to log-transformed precision.

Comparison	Target position (X,Z)	Mean self-motion variability (cm)	Mean stationary-control variability (cm)	Adjusted p
F2B vs FNSM	(15, 15) □	5.65 ± 0.60	3.78 ± 0.35	0.0808 (ns)
	(15, 30) ○	4.99 ± 0.57	3.76 ± 0.44	0.466 (ns)
	(15, 45) △	5.11 ± 0.54	4.37 ± 0.73	1.000 (ns)
	(30, 15) ■	6.98 ± 1.03	4.73 ± 0.62	0.206 (ns)
	(30, 30) ●	5.46 ± 0.70	3.95 ± 0.33	0.486 (ns)
	(30, 45) ▲	4.68 ± 0.45	3.68 ± 0.38	0.673 (ns)
B2F vs BNSM	(15, 15) □	6.96 ± 0.89	3.83 ± 0.47	0.00892 (**)
	(15, 30) ○	6.27 ± 0.80	4.01 ± 0.36	0.123 (ns)
	(15, 45) △	5.96 ± 0.72	4.04 ± 0.44	0.465 (ns)
	(30, 15) ■	7.23 ± 1.17	5.06 ± 0.65	0.206 (ns)
	(30, 30) ●	6.68 ± 1.01	3.90 ± 0.42	0.0262 (*)
	(30, 45) ▲	6.79 ± 0.93	3.87 ± 0.39	0.0419 (*)

The linear mixed-effects model fitted to log-transformed precision confirmed that self-motion influenced precision overall (Methods 2.5.4, Equation 2). Specifically, there was a significant main effect of self-motion, $F(3, 316.95) = 17.71$, $p = 1.182 \times 10^{-10}$, indicating that variability differed across the movement and stationary conditions. By contrast, there was no overall main effect of lateral target position, $F(1, 314.94) = 0.94$, $p = 0.334$, and no significant main effect of anteroposterior target position, $F(2, 315.57) = 2.32$, $p = 0.099$, suggesting that precision did not simply increase or decrease as a function of target location alone. Unlike the anteroposterior bias, this reduction in precision was not reliably modulated by target position. The interaction between self-motion and lateral position was not significant, $F(3, 316.61) = 0.07$, $p = 0.975$, nor was the interaction between self-motion and anteroposterior position, $F(6, 315.91) = 0.26$, $p = 0.956$. The interaction between lateral position and anteroposterior position was also non-significant, $F(2, 316.55) = 1.22$, $p = 0.297$, and there was no three-way interaction among self-motion, lateral position, and anteroposterior position, $F(6, 316.06) = 0.27$, $p = 0.953$.

Overall, self-motion reduced precision, but this reduction did not vary systematically across the target position set.

4.3 Summary

In Experiment 2, anteroposterior self-motion reliably altered haptic object replacement. Stationary front versus back stance did not influence signed anteroposterior bias or precision. However, after self-motion, participants showed systematic displacement along the anteroposterior axis. Forward self-motion (B2F) produced a reliable backward bias at all six target locations, whereas backward self-motion (F2B) produced a reliable forward bias at four of the six locations, with the effect weakening at the farthest depth. These bias effects were not uniform across the target array. Forward self-motion (B2F) bias increased with target depth, whereas backward self-motion (F2B) bias was strongest at nearer targets and weakened with distance. Lateral position also contributed to the pattern, with larger B2F biases at the 15 cm laterality than the 30 cm laterality at middle and far depths. Although some F2B placements involved extended reaches that approached or exceeded a relative reach of 1.0, relative reach did not predict bias in F2B. In B2F, relative reach was significantly related to bias, with larger relative reaches associated with reduced positive/backward bias; however, this relationship explained only a modest proportion of the variance and therefore did not account for the overall bias pattern. Thus, reaching demands may have contributed to the B2F pattern, but they did not provide a sufficient explanation for the anteroposterior self-motion biases observed in Experiment 2.

Self-motion also reduced precision overall, but these precision effects were less pronounced and less spatially systematic than the bias effects. Although variability generally increased after movement, significant losses of precision were localized to specific target positions, particularly in B2F, rather than showing a consistent lateral- or depth-dependent pattern. Overall, Experiment 2 shows that anteroposterior self-motion strongly biases object replacement along the movement axis, while producing a more modest and spatially irregular reduction in precision.

5.0 Experiment 3 - Lateral self-motion (multistep)

Experiment 3 examined lateral self-motion, as in Experiment 1 (Chapter 3), but varied both total distance travelled and step count. Whereas Experiment 1 used a single 60 cm lateral step, Experiment 3 compared a single 30 cm step with two successive 30 cm steps, yielding either 30 cm or 60 cm of total displacement. Target position was also coded differently. In Experiment 1, lateral position was defined relative to the participant's midline, with the central targets labelled as 0 cm laterality. In Experiment 3, target position was defined from the left edge of the table; because the table was approximately 120 cm wide, the 60 cm target corresponded to the table midpoint and therefore to the same central lateral location as the 0 cm targets in Experiment 1. The Experiment 3 targets were placed at 40, 60, and 80 cm from the left edge, all at a constant depth of 20 cm, meaning that targets were separated by 20 cm rather than the 15 cm spacing used in Experiment 1. This arrangement allowed a 30 cm step left or right from the centre position to move the participant across or away from a target position. For the analyses below, movement direction and starting position were combined into a composite variable referred to as motion condition.

5.1 Accuracy

5.1.1 Accuracy of Control Conditions

Signed lateral bias did not differ reliably among the three stationary control conditions in Experiment 3, as shown in Table 5.1. These comparisons were required to establish whether stationary changes in body position relative to the target array influenced lateral replacement performance, as in Experiment 1. Across the stationary control conditions at various target positions, mean lateral bias remained small in magnitude, ranging from -3.71 to 2.43 cm, with SEMs ranging from 0.54 to 1.44 cm. Pairwise EMM contrasts among stationary left, stationary middle, and stationary right, derived from the linear mixed-effects model fitted to lateral bias (see Methods 2.5.4, Equation 3), were all non-significant after Holm correction at each target position. In addition, none of the stationary control conditions showed reliable changes in lateral bias across the 40, 60, and 80 cm target positions. Thus, stationary starting position alone did

not systematically influence lateral bias, and baseline lateral bias did not vary reliably across the target array.

Table 5.1: Experiment 3 stationary-control lateral bias across target positions: Mean signed lateral bias ± SEM in centimetres for the stationary control conditions in Experiment 3, shown separately for each target position along the table X-axis. The stationary conditions correspond to standing on the left side of the table, middle of the table, or right side of the table without self-motion. The p-value columns report Holm-adjusted pairwise estimated marginal mean contrasts between stationary conditions from the linear mixed-effects model fitted to signed lateral bias

Target position	Stationary on left bias (cm)	Stationary in middle bias (cm)	Stationary on right bias (cm)	Right vs left pHolm	Right vs middle pHolm	Left vs middle pHolm
40 cm	0.57 ± 1.18	-0.92 ± 0.89	2.43 ± 1.44	0.934 (ns)	0.575 (ns)	0.934 (ns)
60 cm	-0.06 ± 0.93	-0.60 ± 0.54	-1.12 ± 0.70	1.000 (ns)	1.000 (ns)	1.000 (ns)
80 cm	-3.71 ± 1.21	0.40 ± 1.14	-2.58 ± 0.81	0.661 (ns)	0.489 (ns)	0.329 (ns)

5.1.2 Accuracy Post Multistep Self-Motion Left/Right

Relative to the stationary controls, lateral self-motion resulted in a lateral bias opposite to the direction of travel, consistent with the pattern observed in Experiment 1 (Chapter 3). As shown in Fig. 5.1A, leftward movements were generally associated with rightward bias, whereas in Fig. 5.1B rightward movements were generally associated with leftward bias. Unlike Experiment 1, however, this pattern was not expressed uniformly across all motion conditions and target positions. The linear mixed-effects model for lateral bias showed a significant main effect of the motion condition, $F(8, 468) = 51.36$, $p < 2.2 \times 10^{-16}$, a significant main effect of target position, $F(2, 468) = 55.08$, $p < 2.2 \times 10^{-16}$, and a significant interaction between motion condition and target position, $F(16, 468) = 2.72$, $p = 3.671 \times 10^{-4}$. Thus, self-motion systematically altered signed lateral bias, but the magnitude of that bias depended on both the motion condition and the target's position on the table.

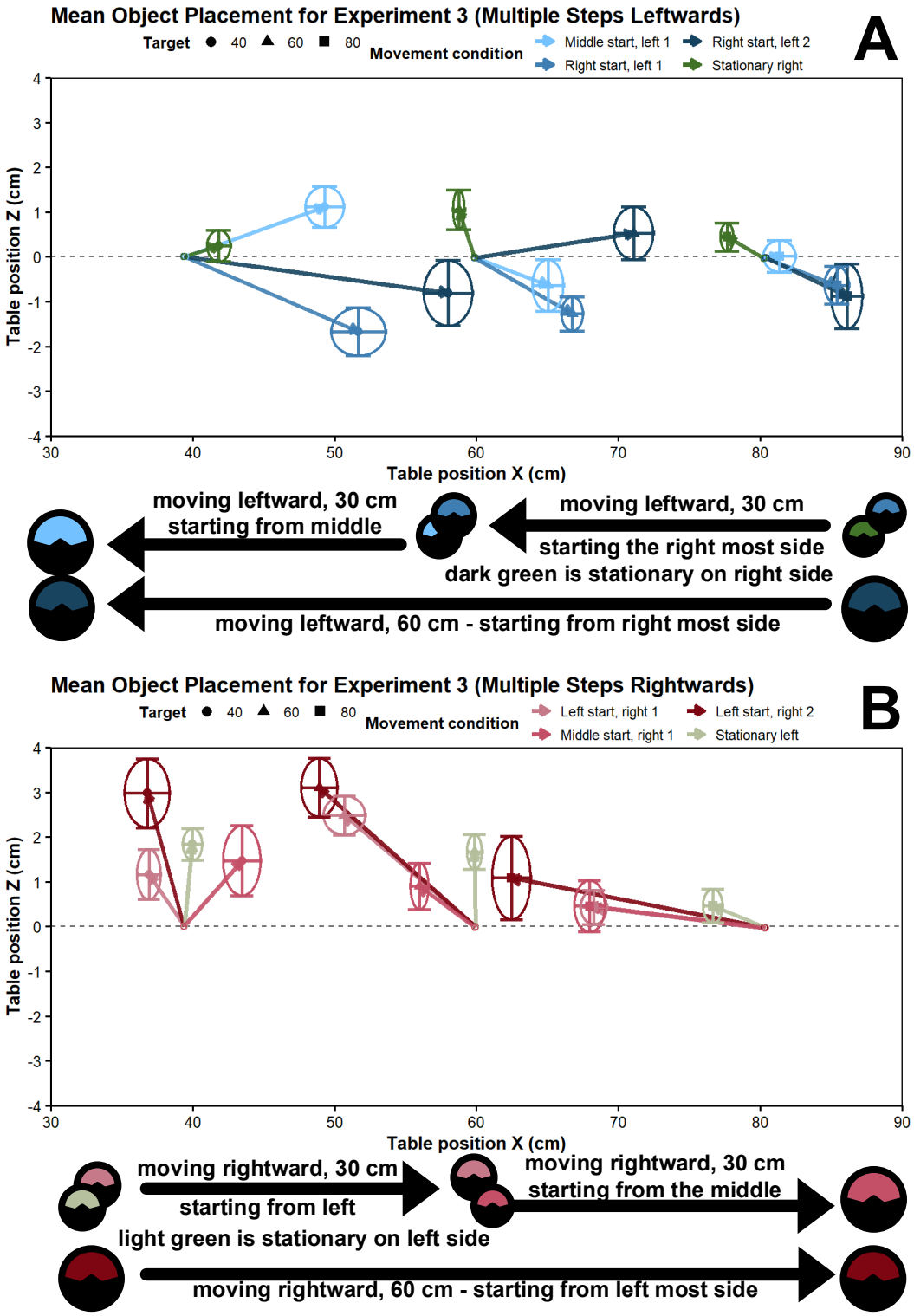

Figure 5.1: Experiment 3 object placements and lateral bias : Panel A shows mean object replacement locations for leftward self-motion conditions and their corresponding stationary controls, and Panel B shows mean object replacement locations for rightward self-motion conditions and their corresponding stationary controls. Target positions were

located at 40, 60, and 80 cm along the table X-axis. Error bars indicate SEM along the table X-axis.

5.1.2.1 Effect of Target Position on Lateral Bias

The linear mixed-effects model fitted to signed lateral bias in Experiment 3 indicated that post-self-motion lateral bias depended on both motion condition and target position (see Methods 2.5.4, Equation 3). This means that lateral bias changed depending on how far participants moved and where they began relative to the target array, as illustrated in Fig. 5.1A and Fig. 5.2A, where the leftward motion conditions generally began closest to the 80 cm target position. As shown in Table 5.2, lateral bias generally increased as the target became more eccentric relative to the participant's starting position. For leftward motion conditions, which produced rightward bias, the smallest biases occurred at the 80 cm target and the largest at the 40 cm target. In the middle-start left 1 condition, mean bias increased from 1.01 ± 2.02 cm at 80 cm, to 9.78 ± 2.40 cm at 40 cm. In the right-start left 1 condition, bias increased from 5.04 ± 1.51 cm at 80 cm, to 12.26 ± 2.76 cm at 40 cm. In the right-start left 2 condition, bias increased from 5.69 ± 1.95 cm at 80 cm, to 18.62 ± 3.04 cm at 40 cm.

The same relationship was reversed for rightward movement conditions, as illustrated in Fig. 5.1B and Fig. 5.2B, where participants generally began closest to the 40 cm target position. For rightward movement conditions, which produced leftward bias, the smallest biases occurred at the 40 cm target and the largest at the 80 cm target. In the middle-start right 1 condition, mean bias changed from 4.09 ± 1.91 cm at 40 cm, to -12.39 ± 1.89 cm at 80 cm. In the left-start right 1 condition, bias increased in leftward magnitude from -2.52 ± 1.47 cm at 40 cm, to -12.07 ± 1.63 cm at 80 cm. In the left-start right 2 condition, bias increased in leftward magnitude from -2.61 ± 2.79 cm at 40 cm, to -17.85 ± 1.92 cm at 80 cm. Thus, lateral bias increased as targets were positioned farther from the participant's starting side and closer to the side toward which the participant moved, with the largest gradients generally observed in the two-step motion conditions.

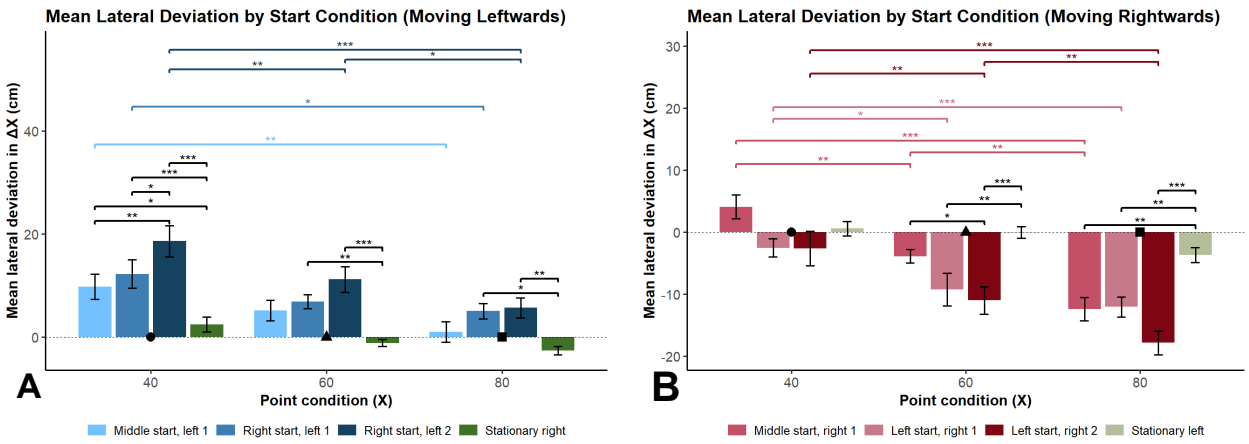

Figure 5.2: Experiment 3 lateral bias after self-motion: Panel A shows mean signed lateral bias (ΔX; cm) for leftward self-motion conditions and their corresponding stationary controls, and Panel B shows mean signed lateral bias for rightward self-motion conditions and their corresponding stationary controls. Bias is shown separately for the 40, 60, and 80 cm target positions. Positive values indicate rightward bias, and negative values indicate leftward bias. Black horizontal brackets indicate within-position contrasts between each self-motion condition and its corresponding stationary control or paired comparison of interest, whereas coloured brackets indicate across-target-position contrasts within a motion condition. All contrasts are based on estimated marginal means from the linear mixed-effects model with Holm-adjusted inferences; asterisks indicate corrected significance levels.

*Table 5.2: Experiment 3 across-target contrasts in signed lateral bias: Pairwise contrasts in signed lateral bias between target positions within each self-motion condition in Experiment 3. mean signed lateral bias ± SEM is shown for the 40, 60, and 80 cm target positions, together with Holm-adjusted within-condition comparisons across target position. Positive values indicate rightward bias and negative values indicate leftward bias. ns denotes non-significant comparisons; * denotes p ≤ .05, ** denotes p ≤ .01, and *** denotes p ≤ .001.*

Motion condition	40 cm mean bias	60 cm mean bias	80 cm mean bias	40 vs 60 pHolm	60 vs 80 pHolm	40 vs 80 pHolm
Middle start, left 1	9.78 ± 2.40	5.17 ± 1.96	1.01 ± 2.02	0.1453 (ns)	0.1453 (ns)	0.0020 (**)
Right start, left 1	12.26 ± 2.76	6.88 ± 1.34	5.04 ± 1.51	0.0722 (ns)	0.4736 (ns)	0.0151 (*)
Right start, left 2	18.62 ± 3.04	11.19 ± 2.47	5.69 ± 1.95	0.0078 (**)	0.0325 (*)	1.91 × 10^-6 (***)
Middle start, right 1	4.09 ± 1.91	-3.89 ± 1.11	-12.39 ± 1.89	0.0019 (**)	0.0019 (**)	8.79 × 10^-10 (***)
Left start, right 1	-2.52 ± 1.47	-9.25 ± 2.60	-12.07 ± 1.63	0.0178 (*)	0.2719 (ns)	6.52 × 10^-4 (***)
Left start, right 2	-2.61 ± 2.79	-11.01 ± 2.23	-17.85 ± 1.92	0.0022 (**)	0.0079 (**)	1.53 × 10^-8 (***)

5.1.2.2 Effect of Starting Position on Lateral Bias at Each Target Position

After establishing that lateral bias varied across target position within each motion condition, a second follow-up analysis examined whether starting position itself contributed to this pattern. Because motion condition combined movement direction, step magnitude, and starting position, one-step movements were compared within the same movement direction while holding step count constant. Specifically, middle-start one-step movements were compared with side-start one-step movements at each target position. This tested whether beginning from the middle versus from the side of the walking platform altered post-self-motion lateral bias for the same movement direction and target location.

Table 5.3: Experiment 3 starting-position contrasts in signed lateral bias :One-step starting-position comparisons of signed lateral bias in Experiment 3, contrasting middle-start and side-start movements in the same direction. Descriptive mean bias values and model-estimated differences are shown for each target position. Unadjusted and Holm-adjusted p-values are reported. Positive values indicate rightward bias and negative values indicate leftward bias.

Motion condition comparison	Target position (cm)	Middle start mean bias (cm)	Side-start mean bias (cm)	EMM difference	Unadjusted p-value	Holm-adjusted p-value
Middle start, left 1 vs Right start, left 1	40	9.78 ± 2.40	12.26 ± 2.76	-2.48	0.3339 (ns)	0.3339 (ns)
	60	5.17 ± 1.96	6.88 ± 1.34	-1.7	0.5065 (ns)	0.5065 (ns)
	80	1.01 ± 2.02	5.04 ± 1.51	-4.03	0.1166 (ns)	0.3498 (ns)
Middle start, right 1 vs Left start, right 1	40	4.09 ± 1.91	-2.52 ± 1.47	6.61	0.0101 (*)	0.0554 (ns)
	60	-3.89 ± 1.11	-9.25 ± 2.60	5.36	0.0369 (*)	0.1108 (ns)
	80	-12.39 ± 1.89	-12.07 ± 1.63	-0.33	0.8990 (ns)	0.8990 (ns)

As shown in Table 5.3, the mean values differed modestly between middle-start and side-start movements, but none of these comparisons remained significant after Holm correction. For leftward movement, middle-start trials generally showed smaller rightward bias than right-start trials, with the two conditions spanning 1.01-9.78 cm and 5.04-12.26 cm, respectively. For rightward movement, middle-start trials generally showed smaller leftward bias than left-start trials at the 40 and 60 cm targets, although the two conditions were nearly identical at the 80 cm target. Across target positions, the middle-start rightward condition ranged from 4.09 to -12.39 cm, whereas the left-start

rightward condition ranged from -2.52 to -12.07 cm. However, none of the middle-start versus side-start comparisons remained significant after Holm correction. Thus, starting position relative to the target produced modest descriptive shifts in one-step post-self-motion bias, but did not reliably alter lateral bias after correction for multiple comparisons.

5.1.2.3 Effect of Step Magnitude on Lateral Bias

To assess whether step magnitude contributed to signed lateral bias, a follow-up analysis was conducted using the model described in Methods 2.5.4, Equation 4. Unlike the primary motion condition analysis above, this model grouped movements by movement direction and step magnitude while collapsing across starting position. This allowed one-step and two-step movements in the same direction to be compared more directly (see Fig. 5.3). This follow-up approach was appropriate because the preceding starting-position analysis showed that middle-start and side-start one-step movements did not differ reliably after Holm correction. Therefore, collapsing across starting position provided a simpler way to examine whether a larger total displacement was associated with greater post-self-motion lateral bias. The linear mixed-effects model showed a significant main effect of movement family, $F(6, 378) = 60.19$, $p < 2.2 \times 10^{-16}$, a significant main effect of target position, $F(2, 378) = 42.45$, $p < 2.2 \times 10^{-16}$, and a significant interaction between movement family and target position, $F(12, 378) = 3.29$, $p = 1.515 \times 10^{-4}$. Thus, under this follow-up model, the effect of step magnitude on signed lateral bias varied across target position.

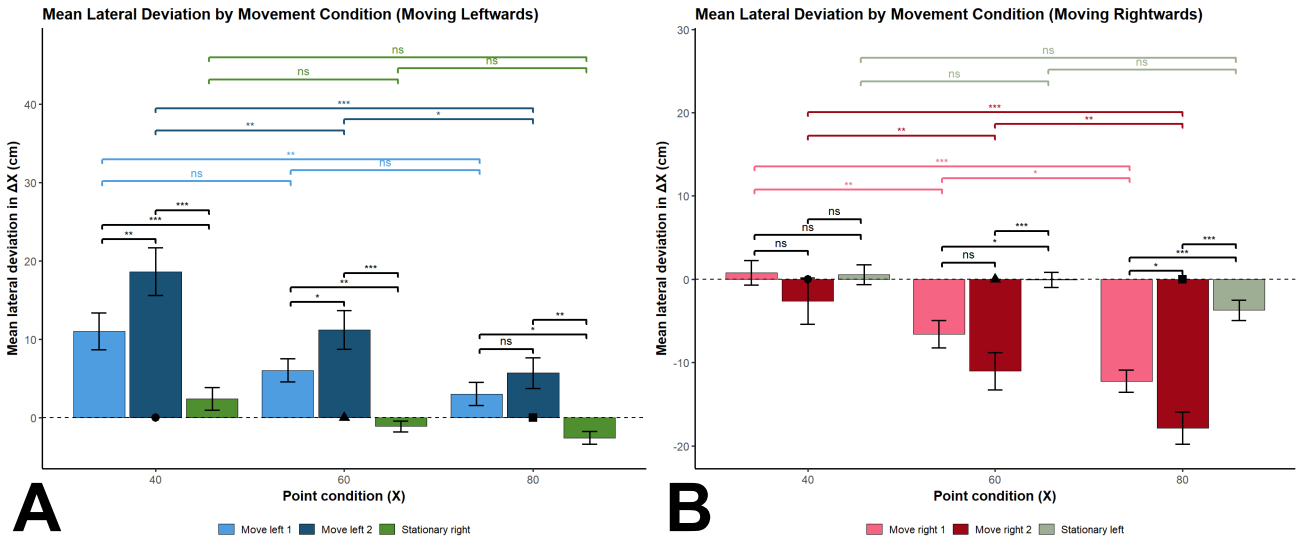

Figure 5.3: Experiment 3 step-magnitude contrasts in signed lateral bias: Panel A shows mean signed lateral bias (ΔX; cm) for the leftward movement families collapsed across starting position (move left 1, move left 2, and stationary right), and Panel B shows the corresponding rightward movement families (move right 1, move right 2, and stationary left). Error bars indicate SEM. Black horizontal brackets indicate within-target-position pairwise contrasts among the movement families, whereas coloured brackets indicate across-target-position contrasts within a movement family. All contrasts are based on estimated marginal means from the follow-up linear mixed-effects model described in Methods 2.5.4, Equation 1, with Holm-adjusted inferences; asterisks indicate corrected significance levels. Positive values indicate rightward bias, and negative values indicate leftward bias.

The significant interaction between movement family and target position was reflected in the fact that the one-step versus two-step difference was not uniform across the target array. As shown in Table 5.4, greater self-motion magnitude generally produced larger biases opposite to the direction of travel, but the location of this magnitude effect differed for leftward and rightward movements.

For leftward movement, the clearest one-step versus two-step difference occurred at the 40 cm target, where rightward bias increased from 11.02 ± 2.36 cm in the one-step condition to 18.62 ± 3.04 cm in the two-step condition, $p = 0.0018$. At the 80 cm target, the same direction of effect was present but smaller and non-significant, with bias increasing from 3.03 ± 1.48 cm to 5.69 ± 1.95 cm, $p = 0.2706$.

For rightward movement, the pattern was reversed across the array. At the 40 cm target, the one-step and two-step conditions did not differ significantly, with mean bias changing from 0.78 ± 1.46 cm to -2.61 ± 2.79 cm, $p = 0.4855$. At the 80 cm target, however, the two-step condition produced significantly greater leftward bias than the one-step condition, with bias changing from -12.23 ± 1.32 cm to -17.85 ± 1.92 cm, $p = 0.0207$. Thus, greater self-motion magnitude was associated with stronger opposite-direction bias, but this effect depended on where the target was located, consistent with the significant interaction between movement family and target position.

Table 5.4: Experiment 3 step-magnitude contrasts in signed lateral bias: Pairwise comparisons of signed lateral bias between one-step and two-step movements in the same direction in Experiment 3, based on the follow-up model described in Methods 2.5.4, Equation 1. Mean signed lateral bias is shown for each movement family at the 40, 60, and 80 cm target positions, together with Holm-adjusted pairwise comparisons

between one-step and two-step conditions. Positive values indicate rightward bias, and negative values indicate leftward bias.

Movement-family comparison	Target position (cm)	One-step mean bias (cm)	Two-step mean bias (cm)	EMM difference (cm)	Holm-adjusted p-value
Move left 1 VS Move left 2	40●	11.02 ± 2.36	18.62 ± 3.04	-7.6	0.0018 (**)
	60▲	6.03 ± 1.47	11.19 ± 2.47	-5.16	0.0335 (*)
	80■	3.03 ± 1.48	5.69 ± 1.95	-2.67	0.2706 (ns)
Move right 1 VS move right 2	40●	0.78 ± 1.46	-2.61 ± 2.79	3.39	0.4855 (ns)
	60▲	-6.57 ± 1.63	-11.01 ± 2.23	4.44	0.0671 (ns)
	80■	-12.23 ± 1.32	-17.85 ± 1.92	5.62	0.0207 (*)

5.1.3 Relative Reach and Lateral Bias

To assess whether the lateral bias observed after multistep self-motion was related to participants' effective reaching demands, directional lateral bias was plotted as a function of relative reach, defined as the post-movement head-to-placement distance divided by participant arm length (Fig. 5.4). Separate linear mixed models were fitted for the rightward and leftward movement families. These analyses showed no evidence that relative reach reliably predicted lateral bias in either movement direction. For rightward movements, the estimated slope was positive but non-significant, slope = 6.36, SE = 4.66, $t(161.50) = 1.37$, $p = 0.174$, with a marginal R^2 of 0.012 and a conditional R^2 of 0.164. For leftward movements, the estimated slope was also non-significant, slope = -1.14, SE = 3.88, $t(153.71) = -0.29$, $p = 0.770$, with a marginal R^2 below 0.001 and a conditional R^2 of 0.401. Thus, although Experiment 3 showed clear effects of target position and self-motion magnitude on lateral bias, these effects were not explained by how far participants reached relative to their arm length.

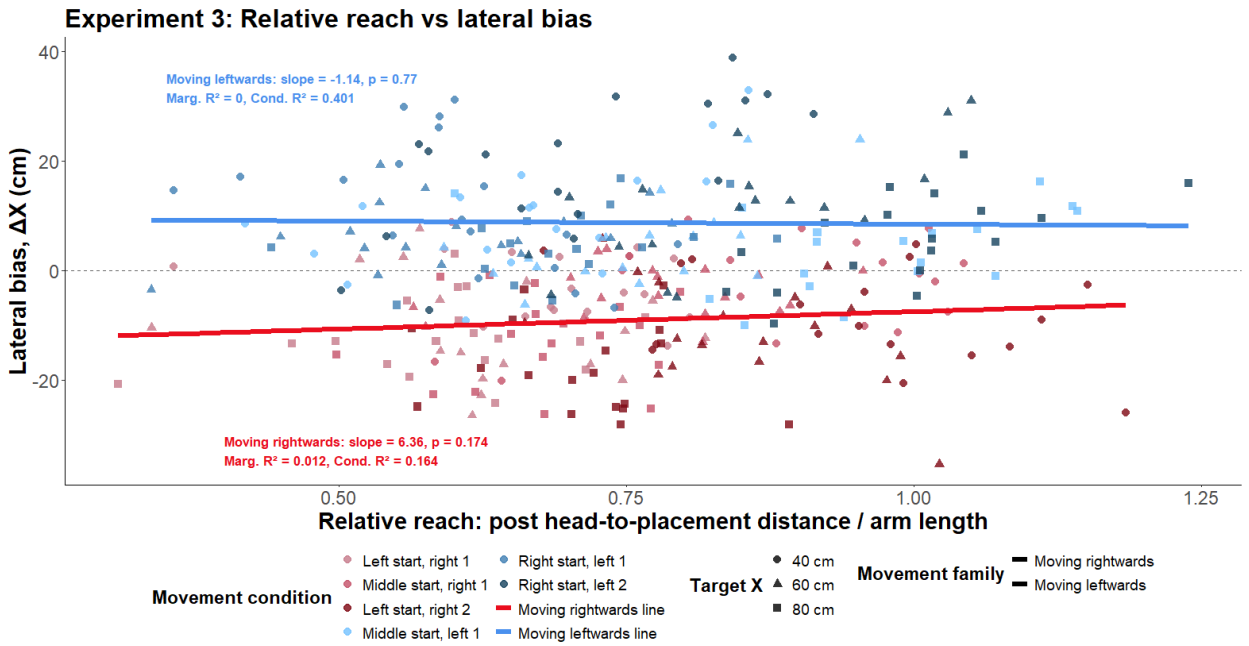

Figure 5.4: Experiment 3 Relative Reach and Lateral Bias: Directional lateral bias in ΔX is plotted as a function of relative reach, calculated as the post-movement head-to-placement distance divided by participant arm length, grouped by movement family. Movement-right and movement-left trials are shown separately to assess whether lateral bias varied systematically with effective reaching demands across movement direction. Points show individual participant-level placements, with target positions indicated by shape. Solid lines show linear mixed-model trends for each movement family. Relative reach did not reliably account for the observed lateral bias pattern for either movement family/direction, indicating that the displacement biases following self-motion were not primarily explained by how far participants reached relative to their arm length.

5.2 Precision

5.2.1 Precision of Controls

Stationary starting position did not reliably influence precision in Experiment 3, as seen in Table 5.5. Mean within-participant variability across stationary left, stationary middle, and stationary right ranged from 2.70 to 6.16 cm, with SEMs ranging from 0.29 to 0.68 cm. After Holm correction, all pairwise comparisons among the stationary conditions were non-significant at the 40 and 60 cm target positions. The only significant contrast occurred at 80 cm, where stationary left was more variable than stationary middle (Holm-adjusted p = 0.0111), although stationary left did not differ significantly from stationary right at the same target position. Thus, control precision was largely uniform across the array, with only one small, localized difference at the 80 cm target position.

*Table 5.5: Experiment 3 stationary-control precision across target positions: Mean within-participant endpoint variability ± SEM in centimetres for the stationary control conditions in Experiment 3, shown separately for each target position along the table X-axis. The stationary conditions correspond to standing on the left side, middle, or right side of the table without self-motion. Holm-adjusted p-values report pairwise comparisons among stationary conditions at each target position. ns denotes non-significant comparisons; * denotes p ≤ 0.05.*

Target position	Stationary on left variability (cm)	Stationary in middle variability (cm)	Stationary on right variability (cm)	Right vs left pHolm	Right vs middle pHolm	Left vs middle pHolm
40 cm	4.29 ± 0.68	3.66 ± 0.31	4.22 ± 0.43	1.000 (ns)	1.000 (ns)	1.000 (ns)
60 cm	4.28 ± 0.50	2.70 ± 0.29	3.55 ± 0.46	1.000 (ns)	1.000 (ns)	0.466 (ns)
80 cm	6.16 ± 0.60	3.12 ± 0.35	3.89 ± 0.42	0.0899 (ns)	1.000 (ns)	0.0111 (*)

5.2.2 Precision Post-Self-Motion Left/Right

Relative to the corresponding stationary controls, lateral self-motion generally reduced precision, producing greater endpoint variability after movement as seen in Figure 5.5. The linear mixed-effects model fitted to log-transformed precision (see Methods 2.5.4, Equation 5) showed a significant main effect of self-motion condition, $F(8, 360.36) = 17.66$, $p < 2 \times 10^{-16}$, but no main effect of target position, $F(2, 360.35) = 1.73$, $p = 0.179$, and only a marginal interaction between self-motion condition and target position, $F(16, 360.39) = 1.50$, $p = 0.096$. Thus, precision differed reliably across self-motion conditions, but these differences were not strongly or consistently organized by target position across the array.

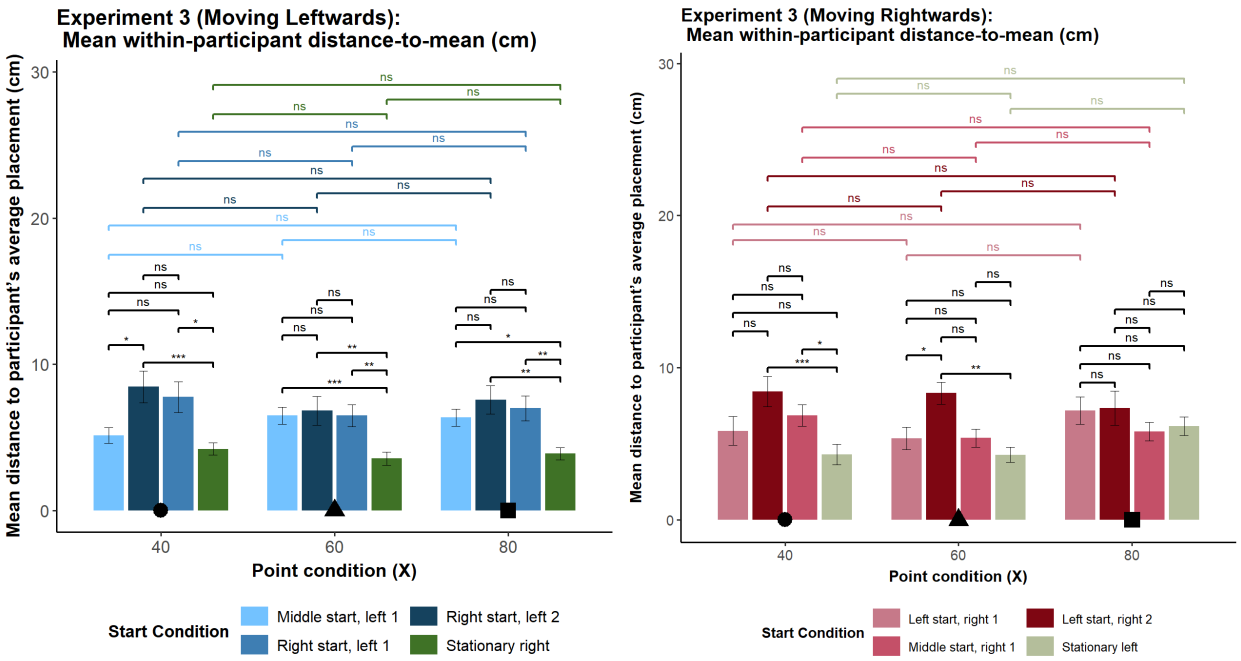

Figure 5.5: Experiment 3 self-motion versus stationary-control endpoint variability: Within-participant endpoint variability (precision; mean Euclidean distance to each participant's condition by target-position mean; cm) is shown for the lateral self-motion conditions and corresponding stationary controls in Experiment 3, separately for leftward movement conditions (Panel A) and rightward movement conditions (Panel B). Target locations are indicated on the x-axis by their 40, 60, and 80 cm positions. Bars represent means plus or minus SEM, with larger values indicating lower precision. Black brackets indicate within-position comparisons among the plotted conditions. Statistics are based on the Experiment 3 precision linear mixed-effects model.

Although the interaction between self-motion and target position was only marginal, the within-position contrasts in Table 5.6 indicate that some precision reductions were localized to specific motion conditions and target positions. These effects were most evident in the two-step conditions, which differed from their stationary controls more often than the one-step conditions. In the leftward two-step condition, endpoint variability ranged from 6.83 to 8.47 cm (SEMs: 0.97-1.08 cm), compared with 3.55 to 4.22 cm in the stationary right control (SEMs: 0.42-0.46 cm). In the rightward two-step condition, variability ranged from 7.35 to 8.44 cm (SEMs: 0.73-1.12 cm), compared with 4.28 to 6.16 cm in the stationary left control (SEMs: 0.50-0.68 cm). By contrast, one-step movements showed a less consistent pattern of precision loss. Thus, self-motion generally increased endpoint variability, but the target-position dependence of this effect was weak and should be interpreted cautiously.

*Table 5.6: Experiment 3 self-motion versus stationary-control precision contrasts: Mean within-participant endpoint variability ± SEM in centimetres for each lateral self-motion condition and its corresponding stationary control in Experiment 3. Each cell reports self-motion variability versus stationary-control variability at the same target position. Leftward movements are compared with the stationary right control, and rightward movements are compared with the stationary left control. Larger values indicate lower precision. Significance labels show Holm-adjusted within-position contrasts from the log-transformed precision linear mixed-effects model. ns denotes non-significant comparisons; * denotes p ≤ .05, ** denotes p ≤ .01, and *** denotes p ≤ .001.*

Movement direction	Motion Condition Comparisons	40 cm target (●)	60 cm target (▲)	80 cm target (■)
Leftward	Middle start, left 1 vs stationary right	5.13 ± 0.53 vs 4.22 ± 0.43 (*)	6.49 ± 0.59 vs 3.55 ± 0.46 (***)	6.36 ± 0.58 vs 3.89 ± 0.42 (*)
Leftward	Right start, left 1 Vs stationary right	7.76 ± 1.04 vs 4.22 ± 0.43 (*)	6.50 ± 0.74 Vs 3.55 ± 0.46 (**)	6.99 ± 0.85 vs 3.89 ± 0.42 (**)
Leftward	Right start, left 2 vs stationary right	8.47 ± 1.08 vs 4.22 ± 0.43 (***)	6.83 ± 1.00 vs 3.55 ± 0.46 (**)	7.58 ± 0.97 vs 3.89 ± 0.42 (**)
Rightward	Left start, right 1 vs stationary left	5.85 ± 0.94 vs 4.29 ± 0.68 (ns)	5.37 ± 0.74 Vs 4.28 ± 0.50 (ns)	7.18 ± 0.90 Vs 6.16 ± 0.60 (ns)
Rightward	Middle start, right 1 vs stationary left	6.86 ± 0.71 vs 4.29 ± 0.68 (*)	5.37 ± 0.60 vs 4.28 ± 0.50 (ns)	5.80 ± 0.61 vs 6.16 ± 0.60 (ns)
Rightward	Left start, right 2 vs stationary left	8.44 ± 1.00 vs 4.29 ± 0.68 (***)	8.33 ± 0.73 Vs 4.28 ± 0.50 (**)	7.35 ± 1.12 vs 6.16 ± 0.60 (ns)

Another notable pattern was that some two-step movements were descriptively more variable than comparable one-step movements. After Holm correction, only two such contrasts remained significant: at the 40 cm target position, right start, left 2 was more variable than middle start, left 1 (8.47 vs 5.13 cm, p = 0.0122), and at the 60 cm target position, left start, right 2 was more variable than left start, right 1 (8.33 vs 5.37 cm, p = 0.0253), with the rest of the comparisons being non-significant as described in Table 5.7. No other one-step versus two-step comparisons were significant. Thus, although larger lateral displacements sometimes appeared to reduce precision, the evidence for a general step-magnitude effect on precision remained limited.

Table 5.7: Experiment 3 step-magnitude contrasts in precision : Mean within-participant endpoint variability ± SEM in centimetres for selected comparisons involving one-step and two-step lateral self-motion conditions in Experiment 3. EMM differences are reported

*on the log-transformed precision scale from the linear mixed-effects model. Holm-adjusted p-values are shown for the corresponding comparisons. Middle-start versus side-start one-step comparisons were all non-significant and are therefore not shown. ns denotes non-significant comparisons; * denotes p ≤ 0.05.*

Motion condition comparison	Target position (cm)	One-step variability (cm)	Two-step variability (cm)	EMM difference	Holm-adjusted p-value
Middle start, left 1	40●	5.13 ± 0.53	8.47 ± 1.08	-0.51	0.0122 (*)
vs	60▲	6.49 ± 0.59	6.83 ± 1.00	0.05	ns
Right start, left 2	80■	6.36 ± 0.58	7.58 ± 0.97	-0.1	ns
Right start, left 1	40●	7.76 ± 1.04	8.47 ± 1.08	-0.15	ns
Vs	60▲	6.50 ± 0.74	6.83 ± 1.00	0.03	ns
Right start, left 2	80■	6.99 ± 0.85	7.58 ± 0.97	-0.07	ns
Left start, right 1	40●	5.85 ± 0.94	8.44 ± 1.00	-0.38	ns
Vs	60▲	5.37 ± 0.74	8.33 ± 0.73	-0.51	0.0253 (*)
Left start, right 2	80■	7.18 ± 0.90	7.35 ± 1.12	0.00	ns
Middle start, right 1	40●	6.86 ± 0.71	8.44 ± 1.00	-0.18	ns
vs	60▲	5.37 ± 0.60	8.33 ± 0.73	-0.43	ns
Left start, right 2	80■	5.80 ± 0.61	7.35 ± 1.12	-0.22	ns

5.3 Summary

In Experiment 3, lateral self-motion again altered haptic object replacement, broadly replicating the central directional pattern observed in Experiment 1. Stationary starting position alone did not systematically influence signed lateral bias, and baseline lateral bias did not vary reliably across the target array. After self-motion, participants generally misplaced objects opposite to the direction of travel, with leftward movements producing rightward bias, and rightward movements producing leftward bias. However, unlike Experiment 1, this effect depended strongly on both target position and self-motion magnitude. Bias increased as targets were positioned farther from the starting side of the movement, with the largest gradients generally observed in the two-step movement conditions. Direct comparisons between one-step and two-step movements further indicated that greater self-motion magnitude produced larger opposite-direction bias, although this effect varied by target position. By contrast, one-step movements that differed only in starting position showed modest numerical differences, but none remained significant after correction. Relative reach also did not reliably predict lateral bias in either movement family, indicating that the observed bias pattern was not explained by how far participants reached relative to their arm length. Thus, post-self-motion lateral bias in Experiment 3 was shaped primarily by target position and self-motion magnitude, whereas starting position alone had a weaker and non-reliable effect.

Precision showed a related but less systematic pattern. Stationary starting position did not meaningfully affect baseline precision. After self-motion, endpoint variability generally increased relative to stationary controls, indicating reduced precision after movement. These precision reductions were most evident in the two-step conditions and were significant at several specific target positions, but the interaction between self-motion and target position was only marginal. Direct one-step versus two-step comparisons provided limited evidence that larger movements further reduced precision, with only two contrasts remaining significant after correction.

Overall, Experiment 3 shows that lateral self-motion had a robust effect on lateral bias during object replacement, with bias occurring opposite to the direction of movement, especially when movement magnitude was larger and when targets were positioned farther from the starting side of the movement. Precision was also reduced, but more modestly and less consistently.

6.0 Experiment 4 - Anteroposterior Self-motion (multistep)

Experiment 4 examined anteroposterior self-motion using a design that extended the simpler arrangement of Experiment 2 (Chapter 4). In Experiment 2, participants moved only toward or away from the target locations, whereas Experiment 4 varied starting position so that movement could occur toward, away from, or across the target positions. In this respect, Experiment 4 served as the anteroposterior analogue of Experiment 3 (Chapter 5), because both experiments varied the relationship between starting position, movement direction, and target position. As in Experiment 3, movement direction and starting position were combined into a composite variable referred to as motion condition. However, not all target positions were tested for every motion condition. For safety reasons, the 80 cm target was not tested from the front starting position in the backward-motion conditions, as described in Methods 2.4.4.4.

6.1 Accuracy

6.1.1 Accuracy of Control Conditions

Signed anteroposterior bias did not differ reliably among the stationary control conditions or across target positions in Experiment 4. For the available stationary controls, mean signed bias remained small, ranging from -6.10 to 2.47 cm, with SEMs ranging from 0.82 to 1.51 cm. No pairwise comparisons among the stationary control conditions were significant after Holm correction, and no stationary condition showed significant changes in signed anteroposterior bias across target position. Thus, stationary starting position alone did not systematically influence signed anteroposterior bias in Experiment 4, and the control conditions showed no meaningful directional bias differences across the tested spatial layout.

Table 6.1: Experiment 4 stationary-control anteroposterior bias across target positions: Mean signed anteroposterior bias ± SEM in centimetres for the stationary control conditions in Experiment 4, shown separately for each target position. The stationary conditions correspond to standing at the front, middle, or back of the table without self-motion. Negative values indicate forward bias, whereas positive values indicate backward bias. Holm-adjusted p-values report pairwise comparisons among stationary conditions

at each target position. The front stationary condition was not tested at the 80 cm target position. ns denotes non-significant comparisons.

Target position	Stationary at front bias (cm)	Stationary in middle bias (cm)	Stationary at back bias (cm)	Front vs middle pHolm	Front vs back pHolm	Middle vs back pHolm
40 cm	2.47 ± 1.51	-0.54 ± 1.50	-0.86 ± 1.24	0.644 (ns)	0.644 (ns)	0.905 (ns)
60 cm	-2.23 ± 0.99	-3.24 ± 1.33	-3.75 ± 0.82	1.000 (ns)	1.000 (ns)	1.000 (ns)
80 cm	not tested	-4.23 ± 1.11	-6.10 ± 0.93	—	—	0.436 (ns)

6.1.2 Accuracy Post Anteroposterior Self-motion

Viewed across all layouts in Fig. 6.1, Experiment 4 did not show the clear, uniform post-self-motion directional pattern observed in the earlier experiments. In both Fig. 6.1A, showing forward self-motion, and Fig. 6.1C, showing backward self-motion, the mean replacement vectors were heterogeneous across target positions, with both forward and backward biases evident rather than a single consistent directional shift. However, the linear mixed-effects model fitted to signed anteroposterior bias (see Methods 2.5.4, Equation 3) showed a significant main effect of motion condition, $F(8, 412.03) = 9.43$, $p = 5.37 \times 10^{-12}$, a significant main effect of target position, $F(2, 412.03) = 53.13$, $p < 2.2 \times 10^{-16}$, and a significant interaction between motion condition and target position, $F(13, 412.02) = 1.80$, $p = 0.040$. These effects indicate that post-self-motion bias in Experiment 4 was not absent, but varied as a function of both motion condition and target position, as shown more clearly in Fig. 6.1B and D. Accordingly, the findings are considered separately for the forward- and backward-motion conditions, with the former showing clearer and more coherent effects and the latter appearing less stable across the tested layouts.

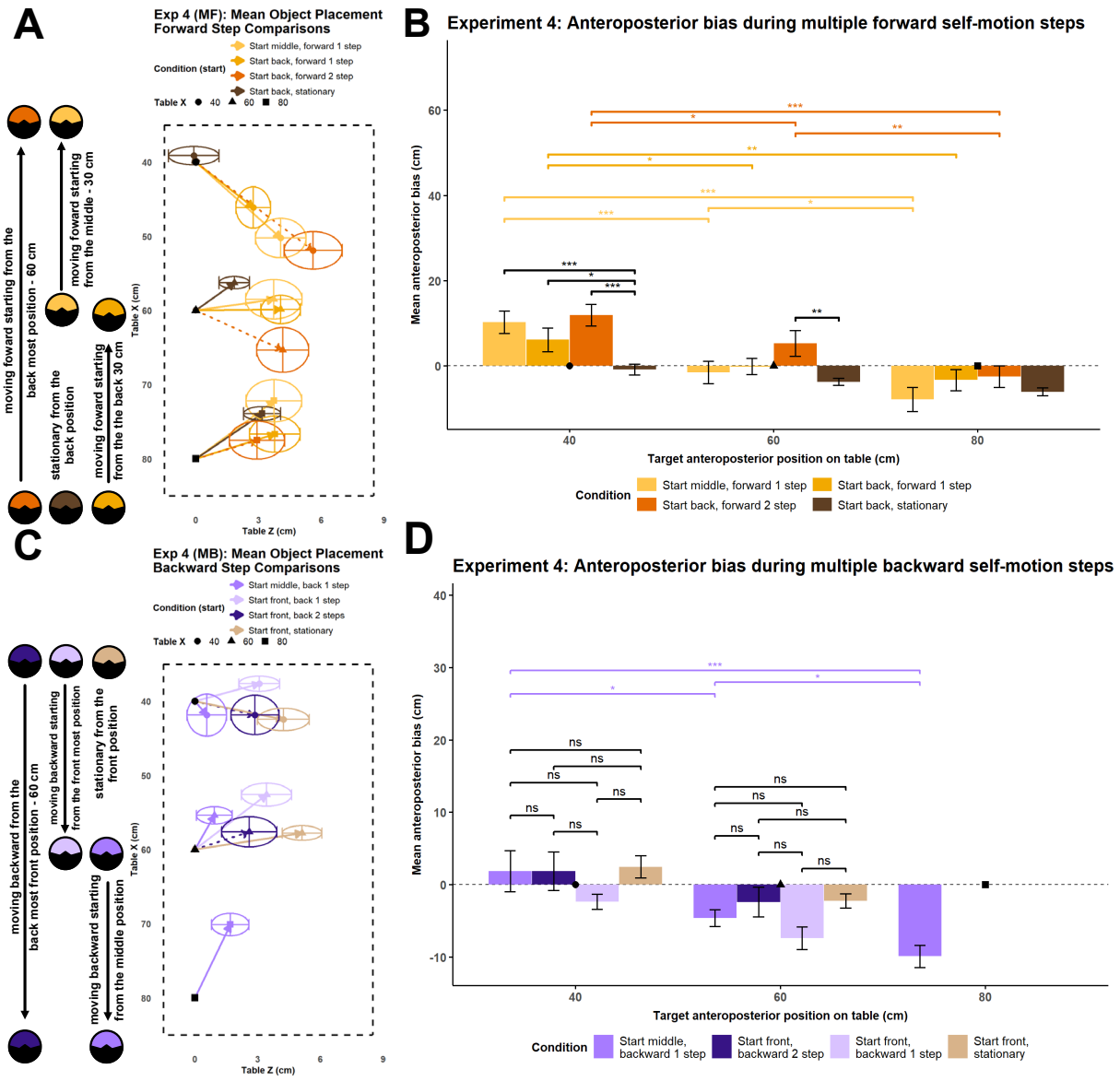

Figure 6.1: Experiment 4 object placements and anteroposterior bias: Panel A shows mean object replacement locations for the forward self-motion conditions and their corresponding stationary control, and Panel B shows mean signed anteroposterior bias for those same forward conditions at the 40, 60, and 80 cm target positions, with positive values indicating backward bias and negative values indicating forward bias. Panel C shows mean object replacement locations for the backward self-motion conditions and their corresponding stationary control, and Panel D shows mean signed anteroposterior bias for the backward conditions, using the same sign convention (positive is backwards, negative is forwards). Error bars/ellipses indicate SEM. Black horizontal brackets indicate within-position contrasts between movement conditions and their corresponding stationary controls or paired comparisons of interest, whereas coloured brackets indicate across-target-position contrasts within a movement condition. All contrasts are based on estimated marginal means from the linear mixed-effects model with Holm-adjusted inferences; asterisks indicate corrected significance levels. Forward self-motion showed

clearer target-dependent modulation of anteroposterior bias, whereas backward self-motion produced weaker and less spatially consistent effects.

6.1.2.1 Forward Self-motion Anteroposterior Bias

The forward self-motion conditions shown in Fig. 6.1B produced the clearest and most spatially structured evidence of anteroposterior self-motion bias. At the 40 cm target position, all three forward self-motion conditions differed reliably from the stationary at back control condition. Mean signed anteroposterior bias in the forward self-motion conditions ranged from 6.12 ± 2.78 cm to 11.90 ± 2.53 cm, indicating a backward bias, as seen in Chapter 4 (Experiment 2), whereas the stationary at back condition showed a small forward bias of -0.86 ± 1.24 cm. At 60 cm, this pattern weakened, with only the two-step forward condition remaining reliably different from the stationary bias. This two-step condition showed a backward bias of 5.33 ± 3.03 cm compared with a forward bias of -3.75 ± 0.82 cm in the stationary at back condition, $p = 4.69 \times 10^{-3}$. By 80 cm, none of the forward self-motion conditions differed reliably from stationary performance. At this target position, all forward self-motion conditions shifted into forward bias, with means ranging from -7.83 ± 2.85 cm to -2.50 ± 2.57 cm, compared with -6.10 ± 0.93 cm in the stationary at back condition. Thus, forward self-motion produced the clearest positive, backward bias relative to stationary performance at the 40 cm target position, a weaker positive/backward effect at 60 cm, and no reliable difference from stationary performance at 80 cm, where the forward-motion means were negative and therefore reflected forward bias.

*Table 6.2: Experiment 4 (forward) anteroposterior bias contrasts: Mean signed anteroposterior bias ± SEM in centimetres for the forward self-motion conditions in Experiment 4, shown separately for each target position. Holm-adjusted p-values compare each forward self-motion condition with the stationary at back control at the same target position. Negative values indicate forward bias, whereas positive values indicate backward bias. ns denotes non-significant comparisons; * denotes p ≤ .05, ** denotes p ≤ .01, and *** denotes p ≤ .001.*

Target position	Start middle, forward 1 step	vs stationary pHolm	Start back, forward 1 step	vs stationary pHolm	Start back, forward 2 steps	vs stationary pHolm
40●	10.20 ± 2.66	2.10×10^-4(***)	6.12 ± 2.78	0.0383(*)	11.90 ± 2.53	1.61 × 10^-5 (***)
60▲	-1.51 ± 2.65	0.810(ns)	-0.13 ± 1.91	0.535(ns)	5.33 ± 3.03	0.00469(**)
80■	-7.83 ± 2.85	1.000(ns)	-3.32 ± 2.44	0.800(ns)	-2.50 ± 2.57	0.632(ns)

Despite the weakening of the within-position contrasts across the target positions, the forward-motion conditions still showed clear across-target differences, as summarized in Table 6.3. Relative to the true target position, bias shifted progressively in the forward direction from the 40 cm to the 80 cm target position in all three forward-motion conditions, moving from positive/backward values at 40 cm toward negative/forward values at 80 cm. For the middle start, one-step forward condition, mean signed bias shifted from a backward bias of 10.20 ± 2.66 cm at 40 cm to a forward bias of -7.83 ± 2.85 cm at 80 cm, with all across-target contrasts significant. A similar pattern was observed for the back start, one-step forward condition, where bias shifted from a backward bias of 6.12 ± 2.78 cm at 40 cm to a forward bias of -3.32 ± 2.44 cm at 80 cm, although the 60 versus 80 cm comparison was not significant. The two-step forward condition also decreased across the target array, from a backward bias of 11.90 ± 2.53 cm at 40 cm to a forward bias of -2.50 ± 2.57 cm at 80 cm, with all across-target contrasts significant. Thus, the forward-motion conditions showed the most coherent anteroposterior bias pattern in Experiment 4: differences from stationary performance were strongest at 40 cm, weakened at 60 cm, and were no longer reliable at 80 cm, even though bias still changed reliably across target position within the forward-motion conditions.

*Table 6.3: Experiment 4 (forward) across-target contrasts in anteroposterior bias: Across-target-position contrasts in signed anteroposterior bias for the forward self-motion conditions in Experiment 4. EMM differences are reported from the linear mixed-effects model fitted to signed anteroposterior bias and compare the target positions listed in each column. Positive EMM differences indicate that the first target position showed a more positive, backward bias, or a less negative, forward bias, than the second target position. Holm-adjusted p-values are shown for each comparison. ns denotes non-significant comparisons; * denotes p ≤ .05, ** denotes p ≤ .01, and *** denotes p ≤ .001.*

Movement condition	40 vs 60 EMM difference	40 vs 60 pHolm	60 vs 80 EMM difference	60 vs 80 pHolm	40 vs 80 EMM difference	40 vs 80 pHolm
Start middle, forward 1 step	11.75	3.00 × 10^-5 (***)	6.32	0.0189 (*)	18.08	1.56 × 10^-10 (***)
Start back, forward 1 step	6.25	0.0408 (*)	3.2	0.234 (ns)	9.45	0.00144 (**)
Start back, forward 2 steps	6.57	0.0148 (*)	7.84	0.00737 (**)	14.41	3.91 × 10^-7 (***)

6.1.2.2 Backward Self-motion Anteroposterior Bias

The backward self-motion conditions shown in Fig. 6.1D were less consistent and provided weaker evidence of anteroposterior self-motion bias, as summarized in Table 6.4. At the 40 cm target position, none of the backward self-motion conditions differed reliably from the stationary at front control condition. The stationary at front condition showed a backward bias of 2.47 ± 1.51 cm, whereas the backward self-motion conditions ranged from a forward bias of -2.35 ± 1.03 cm to a backward bias of 1.88 ± 2.83 cm. At the 60 cm target position, the stationary at front condition showed a forward bias of -2.23 ± 0.99 cm, while the backward self-motion conditions also showed forward bias, with means ranging from -7.40 ± 1.56 cm to -2.39 ± 2.04 cm. None of these backward self-motion conditions differed reliably from the stationary at front control. Thus, backward self-motion produced negative, forward bias in several conditions, consistent with the opposite-to-motion direction observed in Chapter 4 (Experiment 2), but these effects were not reliably different from stationary performance in Experiment 4. At 80 cm, only the middle start one-step backward condition was available, which showed a forward bias of -9.90 ± 1.52 cm; therefore, movement versus stationary comparisons could not be evaluated at that target position.

Table 6.4: Experiment 4 (backward) anteroposterior bias contrasts: Mean signed anteroposterior bias ± SEM in centimetres for the backward self-motion conditions in Experiment 4, shown separately for each target position. Holm-adjusted p-values compare each backward self-motion condition with the stationary at front control at the same target position. The 80 cm target position was not tested for the stationary at front, start front backward 1 step, or start front backward 2 step conditions. Negative values indicate forward bias, whereas positive values indicate backward bias. ns denotes non-significant comparisons.

Target position	Start middle, backward 1 step	vs stationary pHolm	Start front, backward 1 step	vs stationary pHolm	Start front, backward 2 steps	vs stationary pHolm
40●	1.88 ± 2.83	1.000 (ns)	-2.35 ± 1.03	0.438 (ns)	1.86 ± 2.66	1.000 (ns)
60▲	-4.61 ± 1.17	1.000 (ns)	-7.40 ± 1.56	0.362 (ns)	-2.39 ± 2.04	1.000 (ns)
80■	-9.90 ± 1.52	—	not tested	—	not tested	—

Despite the absence of reliable movement versus stationary differences, the clearest across-position change was observed for the middle start, one-step backward condition. Mean signed anteroposterior bias shifted from a small positive/backward bias of 1.88 ±

2.83 cm at 40 cm to negative/forward biases of -4.61 ± 1.17 cm at 60 cm and -9.90 ± 1.52 cm at 80 cm. Across-position contrasts confirmed this progression, with significant differences between 40 and 60 cm, EMM difference = 6.50, p = 0.0319; between 60 and 80 cm, EMM difference = 5.29, p = 0.0496; and between 40 and 80 cm, EMM difference = 11.80, p = 4.28 × 10^-5. The remaining backward-motion conditions showed weaker across-position change, with no reliable 40 versus 60 cm differences for start front, backward 2 steps, EMM difference = 4.25, p = 0.114, or start front, backward 1 step, EMM difference = 5.05, p = 0.0608. Because the 80 cm target position was unavailable for the front start backward conditions and the stationary at front condition, across-position comparisons for the backward-motion family were necessarily more limited.

6.1.3 Relative Reach and Anteroposterior Bias

To assess whether the anteroposterior bias observed after multistep self-motion was related to participants' effective reaching demands, signed anteroposterior bias was plotted as a function of relative reach, defined as the post-movement head-to-placement distance divided by participant arm length (Fig. 6.2). Separate linear mixed models were fitted for the forward and backward movement families. These analyses showed no evidence that relative reach reliably predicted anteroposterior bias in either movement direction. For forward movements, the estimated slope was non-significant, slope = -0.49, SE = 4.66, t(160.90) = -0.10, p = 0.917, with a marginal R^2 below .001 and a conditional R^2 of 0.399. For backward movements, the estimated slope was also non-significant, slope = -1.63, SE = 5.60, t(105.35) = -0.29, p = 0.772, with a marginal R^2 of 0.001 and a conditional R^2 of 0.209. Thus, although Experiment 4 showed condition- and target-dependent changes in anteroposterior bias, these effects were not explained by how far participants reached relative to their arm length.

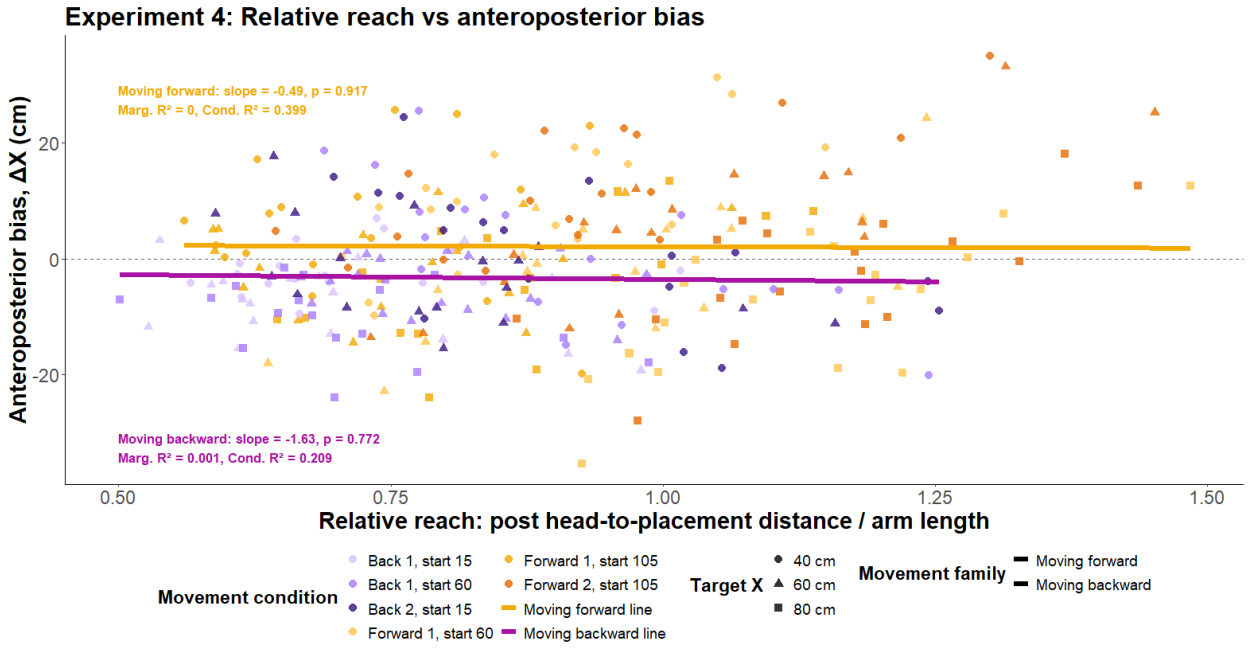

Figure 6.2: Relative Reach and Anteroposterior Bias: Signed anteroposterior bias is plotted as a function of relative reach, calculated as the post-movement head-to-placement distance divided by participant arm length, grouped by movement family. Forward and backward movement trials are shown separately to assess whether anteroposterior bias varied systematically with effective reaching demands across movement direction. Points show individual participant-level placements, with target positions indicated by shape. Solid lines show linear mixed-model trends for each movement family. Relative reach did not reliably account for the observed anteroposterior bias pattern in either movement family, indicating that the displacement biases following self-motion were not primarily explained by how far participants reached relative to their arm length.

6.2 Precision

6.2.1 Precision of Controls

Mean variability across the available stationary controls remained within a relatively narrow range, from 4.05 to 5.46 cm, with SEMs ranging from 0.38 to 0.69 cm. Pairwise comparisons among the stationary control conditions at shared target positions revealed no significant differences in variability, and comparisons across target positions within each stationary condition were likewise non-significant. Thus, unlike the localized precision changes observed in some self-motion conditions, the stationary controls did not show reliable modulation of precision. This indicates that baseline response variability

was generally uniform across the available control array, providing a stable reference against which post-self-motion changes in precision could be interpreted.

Table 6.5: Experiment 4 stationary-control precision across target positions: Mean within-participant endpoint variability ± SEM in centimetres for the stationary control conditions in Experiment 4. The front, middle, and back stationary control conditions are shown separately at each target position. The three rightmost columns report within-target pairwise comparisons among stationary controls; all available comparisons were non-significant. Comparisons involving the front stationary control at 80 cm were not tested because this condition was unavailable at that target position.

Target position	Stationary at front mean (cm)	Stationary at middle (cm)	Stationary at back mean (cm)	Front vs middle pHolm	Front vs back pHolm	Middle vs back pHolm
40 cm	5.46 ± 0.57	4.53 ± 0.52	4.05 ± 0.39	0.955	0.531	1.000
60 cm	4.19 ± 0.50	4.19 ± 0.38	5.20 ± 0.59	1.000	1.000	1.000
80 cm	Not tested	4.53 ± 0.69	4.64 ± 0.42	Not tested	Not tested	1.000

6.2.2 Precision Post Anteroposterior Self-Motion

The linear mixed-effects model fitted to log-transformed precision revealed a significant main effect of motion condition, $F(8, 318.59) = 10.37$, $p = 6.49 \times 10^{-13}$, indicating that precision differed across self-motion and stationary conditions. The main effect of target position was only marginal, $F(2, 318.91) = 2.37$, $p = 0.095$, and the interaction between motion condition and target position was not significant, $F(13, 318.50) = 1.14$, $p = 0.321$. Thus, any changes in precision were attributable primarily to condition, rather than to a consistent spatial modulation across the tested target positions.

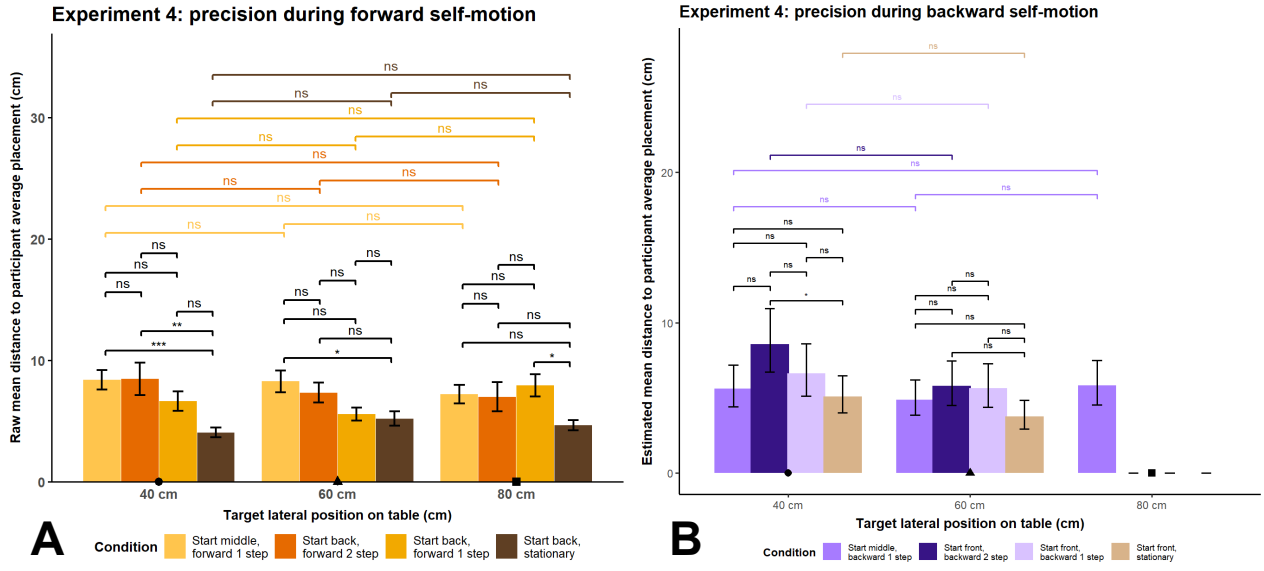

Figure 6.3: Experiment 4 endpoint variability: Panel A shows precision for the forward self-motion conditions, and Panel B shows precision for the backward self-motion

conditions. Precision is plotted as mean within-participant endpoint variability at the 40, 60, and 80 cm target positions, with larger values indicating lower precision. Most comparisons were non-significant, with only a few isolated significant contrasts marked by asterisks. Black brackets indicate within-position comparisons, coloured brackets indicate across-target-position comparisons within a condition, and all contrasts are based on estimated marginal means from the log-transformed precision linear mixed-effects model with Holm-adjusted inferences.

As shown in Table 6.6, the forward-motion conditions showed several localized reductions in precision relative to the stationary back-start control. Variability was generally higher after forward self-motion than in the stationary condition, especially at the 40 cm target position, where the forward-motion means ranged from 6.63 to 8.46 cm compared with 4.05 cm in the stationary back-start control. At 60 cm, variability remained elevated most clearly for the middle start one-step forward condition, which was significantly more variable than stationary performance. At 80 cm, only the back-start one-step forward condition differed reliably from stationary performance. Thus, forward self-motion tended to reduce precision, but this effect was not uniform across motion conditions or target positions. The forward-motion conditions did not differ significantly from one another at any target position, and no across-target comparisons within any forward-motion condition reached significance.

*Table 6.6: Experiment 4 (forward) precision contrasts: Mean within-participant endpoint variability ± SEM in centimetres for the forward-motion conditions in Experiment 4. The rightmost columns report Holm-adjusted p-values for within-target comparisons between each forward-motion condition and the stationary back control. Larger values indicate lower precision. Significance labels are shown in brackets; * denotes p ≤ .05, ** denotes p ≤ .01, and *** denotes p ≤ .001. All forward-motion conditions were also compared with one another within each target position, but these comparisons were non-significant and are not shown.*

Target position	Start middle, forward 1 step mean (cm)	Start back, forward 2 steps mean (cm)	Start back, forward 1 step mean (cm)	Middle 1-step vs stationary back pHolm	Back 2-step vs stationary back pHolm	Back 1-step vs stationary back pHolm
40 cm	8.39 ± 0.81	8.46 ± 1.34	6.63 ± 0.79	2.42 × 10^-4 (***)	0.003 (**)	0.066 (ns)
60 cm	8.26 ± 0.91	7.34 ± 0.83	5.56 ± 0.53	0.016 (*)	0.176 (ns)	1.000 (ns)
80 cm	7.20 ± 0.78	6.99 ± 1.19	7.93 ± 0.91	0.290 (ns)	0.599 (ns)	0.029 (*)

The backward-motion conditions showed a weaker pattern than the forward-motion conditions. As shown in Table 6.7, only the two-step backward condition starting from the front showed significantly reduced precision relative to the stationary front control, and this effect was limited to the 40 cm target position, where mean variability was 8.96 ± 0.83 cm compared with 5.46 ± 0.57 cm in the stationary condition. The remaining backward-motion comparisons with the stationary front control were non-significant at both 40 cm and 60 cm. At 80 cm, only the one-step backward condition beginning from the middle was available, so movement-versus-control comparisons could not be tested at that target position. As with the forward-motion conditions, there was no evidence of reliable across-target changes in precision within a given backward-motion condition. Taken together, these results indicate that self-motion affected precision in selected cases, but these effects were localized and condition-specific rather than reflecting a robust global spatial dependence.

*Table 6.7: Experiment 4 (backward) precision contrasts: Mean within-participant endpoint variability ± SEM in centimetres for the backward-motion conditions and the stationary front control in Experiment 4. The rightmost columns report Holm-adjusted p-values for within-target comparisons between each backward-motion condition and the stationary front control. Larger values indicate lower precision. Significance labels are shown in brackets; * denotes p ≤ .05, ** denotes p ≤ .01, and *** denotes p ≤ .001. Comparisons at 80 cm involving the front start backward conditions and the stationary front control were not tested because these conditions were unavailable at that target position.*

Target position	Start middle, backward 1 step mean (cm)	Start front, backward 2 steps mean (cm)	Start front, backward 1 step mean (cm)	Middle 1-step vs stationary front pHolm	Front 2-step vs stationary front pHolm	Front 1-step vs stationary front pHolm
40 cm	6.36 ± 0.82	8.96 ± 0.83	7.18 ± 0.96	1.000 (ns)	0.013 (*)	0.852 (ns)
60 cm	5.23 ± 0.55	6.66 ± 0.93	5.87 ± 0.67	0.852 (ns)	0.095 (ns)	0.130 (ns)
80 cm	6.16 ± 0.59	Not tested	Not tested	Not tested	Not tested	Not tested

6.3 Summary

In Experiment 4, anteroposterior self-motion produced weaker and less uniform effects than those observed in Experiment 2. Stationary starting position alone did not systematically influence signed anteroposterior bias or precision across the available target positions. After self-motion, there was some evidence of anteroposterior bias opposite to the direction of travel, but this pattern was strongly dependent on motion

condition and target position. Forward self-motion produced the clearest positive/backward bias relative to stationary performance at the 40 cm target position, a weaker positive/backward effect at 60 cm, and no reliable difference from stationary performance at 80 cm, where the means were negative and therefore reflected forward bias. Backward self-motion showed weaker evidence of bias, with no reliable movement-versus-stationary differences at the shared target positions, although the middle start backward condition showed a clear across-target shift from a small positive/backward bias at 40 cm to negative/forward bias at 60 and 80 cm. Relative reach did not reliably predict anteroposterior bias in either movement family, indicating that the Experiment 4 bias pattern was not explained by how far participants reached relative to their arm length. Thus, unlike Experiment 2, anteroposterior self-motion in Experiment 4 did not produce a uniform directional bias across the full target array.

7.0 Discussion

7.1 General Summary of Findings

This thesis examined haptic spatial updating by testing how accurately (bias) and precisely (variability) participants could replace a previously explored object at its original position after either remaining stationary or actively translating via self-generated steps of different directions and magnitudes. In the stationary control conditions, replacement was relatively veridical and variability remained minimal, with little evidence that different starting positions produced systematic bias or increased variability.

7.1.1 Bias Findings

Once participants moved, object replacements were systematically displaced opposite to the direction of travel. This meant that object placements were displaced away from their true locations by as much as 20 cm, depending on the experiment and condition. Specifically, after leftward movement, objects were replaced too far to the right of the true location, after rightward movement, objects were replaced too far to the left. After forward movement, objects tended to be replaced too far backward, whereas after backward movement, objects tended to be replaced too far forward. This pattern was clearest in the lateral movement experiments, whereas the anteroposterior experiments showed the same general tendency but with greater variation across target position, and occasional reversals in the tendencies depending on distance from the participant.

Movement magnitude, or the total distance travelled, also contributed to the magnitude of the directional bias. Larger translations tended to produce larger displacement errors, particularly in the lateral multistep experiment (Exp. 3), where two-step movements generally produced a larger bias than one-step movements. However, in the multistep anteroposterior experiment (Exp. 4), there was some evidence that two-step forward movements produced larger biases than one-step forward movements for targets located in front of the participant, but not behind the participant. These findings suggest that the relationship between distance travelled and haptic replacement bias was not strictly linear but varied with movement direction and target position.

Additionally, bias magnitude was systematically modulated by the object's initial distance from the participant. Replacement errors were largest for targets encoded farther away and smallest for targets encoded nearer to the body, indicating that self-motion did not affect all remembered haptic locations equally. Restated relative to the participant's final position, the largest biases often occurred for targets that were closest after self-motion. This suggests that the effect may have been constrained by the reachable workspace: when the remembered location fell directly within arm's reach, participants had greater freedom to express the full displacement bias, whereas farther targets may have been limited by arm-extension constraints.

7.1.2 Precision Findings

Active self-motion generally reduced precision of placements. Participants' replacement responses were more variable following movement than in the stationary control conditions, indicating that haptic spatial updating increased uncertainty in the remembered object location. However, this reduction in precision was less spatially organized than the bias effects. Whereas bias varied systematically with movement direction and target position, precision did not consistently depend on target location, initial distance, or movement geometry. Moreover, precision differences were less apparent at the farthest target locations, possibly because arm-length constraints limited the range over which response variability could be expressed.

Experiment 3 provided partial evidence for a movement-magnitude effect on precision. Two-step movements were more consistently associated with reduced precision relative to stationary controls, whereas one-step movements were sometimes closer to stationary performance. However, because one-step and two-step movements did not always differ reliably, the effect should be interpreted cautiously: larger self-motion appeared to reduce precision, but not in a strictly linear stepwise manner.

7.2 Evaluation of the Hypotheses

7.2.1 Bias Hypotheses (H1 and H2)

H1 predicted that self-motion would displace object placements in the direction of travel. This hypothesis was not supported. Instead, active self-motion produced systematic replacement errors opposite to the direction of movement. This reversal was most robust in the lateral experiments (Experiments 1 and 3). The anteroposterior experiments showed a similar general tendency, particularly in Experiment 2, although the effect was more condition-dependent in Experiment 4. In that experiment, posterior reach geometry likely constrained performance where participants may not have been able to express the full bias. In the frontal response regions, however, the same opposite-direction pattern was more apparent. Thus, H1 was contradicted in its predicted direction, although the results nevertheless showed that self-motion systematically altered haptic object-location updating. Importantly, the direction of this alteration was opposite to that reported in comparable visual updating studies.

H2 predicted that larger movements would produce larger directional biases. This hypothesis was partially supported. Two-step translations produced larger opposite-direction biases than one-step translations most clearly in the lateral multistep experiment, suggesting that movement magnitude contributed to the size of the updating error. In the anteroposterior multistep experiment, however, this effect was weaker and more dependent on movement direction and target position. Therefore, movement magnitude influenced bias, but not as a simple linear function of distance travel.

7.2.2 Precision Hypotheses (H3 and H4)

H3 predicted that active self-motion would reduce response precision relative to stationary control trials. This hypothesis was broadly supported. Across the experiments, movement conditions were generally associated with greater response variability than stationary conditions, indicating that haptic spatial updating introduced additional uncertainty into the remembered object location. However, these precision effects were less spatially systematic than the bias effects and were not consistently present at every target position.

H4 predicted that larger self-motion magnitudes would produce further reductions in precision. This hypothesis received weaker support. In Experiment 3, two-step movements were more consistently associated with reduced precision relative to stationary controls, whereas one-step movements were sometimes closer to stationary performance. However, one-step and two-step movements did not always differ reliably from each other. Thus, movement magnitude appeared to contribute to precision loss, but the evidence did not support a strictly linear relationship in which precision declined reliably from no movement to one step, to two steps.

The degree of support for each hypothesis is summarized in Table 7.1.

Table 7.1: Summary of the outcomes of the original hypotheses: Yellow highlights denote bias-related hypotheses. Aqua shading denotes precision-related hypotheses.

Hypothesis	Result Found
H1 – Self-motion produces bias along axis of motion	Not supported as predicted; bias was opposite to the direction of travel.
H2 – More self-motion produces larger biases	Partially supported; clearest in the lateral experiments.
H3 – Self-motion increases response variability	Supported; movement generally reduced precision.
H4 – More self-motion produces larger variability	Weak support; variability sometimes increased with movement magnitude, but not consistently.

7.3 Direction of Bias and the Transformation of the Haptic Reference Frame After Self-Motion

7.3.1 Stationary haptic replacement was relatively stable

The stationary control conditions suggest that the large biases observed after self-motion cannot be attributed to a poor haptic localisation ability. When participants remained stationary, object replacement was relatively stable, indicating that the initial haptic encoding of object location was preserved with reasonable accuracy across the 5 second delay. This pattern is consistent with previous works showing small haptic localisation or replacement errors in the frontal peripersonal workspace, typically on the order of a few centimeters (Darling & Miller, 1993; Giudice et al., 2013; Sheth & Shimojo, 2001; Wako & Ayabe-Kanamura, 2016; Wilson et al., 2010). Although other studies report haptic performance in angular, gain-based, or relational terms rather than direct

centimeter error, they converge on the same general conclusion; haptic spatial representations remain relatively stable when the observer does not move (Hollins & Kelley, 1988; Zanini et al., 2021). Therefore, the present movement-related biases are unlikely to reflect a general failure of haptic object-location encoding but instead appear to emerge when that encoded location must be updated after active self-motion.

7.3.2 Active self-motion introduced a directional updating error

Relative to the stationary controls, the self-motion conditions produced a clear directional updating error. Participants generally replaced objects beyond their true locations in the direction opposite to their own movement, indicating that the remembered object location had been reconstructed too far relative to the new body position. Importantly, this directional bias was not well explained by relative reach or by simple arm-length limitations. Although reachable workspace geometry may have influenced how strongly the bias could be expressed at particular target locations, the relative-reach analyses provide little evidence that the bias itself was driven by biomechanical reach constraints. Behaviourally, the pattern therefore appears as an apparent overcompensation of self-motion rather than as a failure to reach the intended location.

Only a limited number of studies have examined haptic spatial updating after self-motion. The closest comparison is Hollins and Kelley (1988), who asked participants to encode haptic locations around a table and then rotate (90 degrees clockwise) to a new position before responding. Their results showed relatively accurate stationary performance, but systematic distortions after rotation around the table that resemble an overcompensatory updating pattern. Hollins and Kelley described these errors as distortions in haptic memory rather than as an overestimation of travelled distance. In the present experiments, however, the stationary control conditions provide little evidence for a generalized distortion or instability of haptic object-location memory itself. Instead, the errors emerged primarily after self-motion, suggesting that the critical source of distortion was the post-movement updating or reconstruction of the remembered haptic location.

Importantly, Hollins & Kelley (1988) also found that allowing participants to re-examine the table after movement reduced these errors, suggesting that renewed haptic

contact can recalibrate the spatial representation. Other haptic spatial-updating studies have focused more on allocentric layout reconstruction than on signed bias at a single remembered location, showing that haptic arrays can be maintained across rotations or changes in observer position (Giudice et al., 2017; Martolini et al., 2021). However, these studies primarily examined rotational viewpoint changes and relational spatial memory, rather than active linear translation and direct object replacement. The present thesis therefore extends this literature by showing that haptic object-location updating after linear self-motion produces an apparent overcompensatory bias. Before interpreting this pattern as self-motion overestimation, however, it is necessary to consider whether the broader walking and path-integration literature supports such an explanation.

7.3.3 Self-Motion Overestimation Is a Useful but Insufficient Explanation

Although the present bias pattern seen above resembles self-motion overestimation, it is important to distinguish this behavioural appearance from a direct perceptual claim. In one sense, the present results provide the complementary pattern to visual self-motion updating studies in which biases in the direction of travel have been interpreted as evidence that participants underestimated their displacement, see Fig. 1.2C (Kim & Harris, 2024; Medendorp et al., 1999). Here, participants showed the opposite pattern: object replacements were displaced opposite the direction of travel, as though the remembered object location had been updated too far relative to the new body position (Fig. 1.2D). This makes self-motion overestimation a useful descriptive account of the results. However, this account is incomplete for several reasons. The broader walking and path-integration literature generally shows that short-distance walking without vision can be relatively stable, particularly when participants walk to previously encoded targets. Thus, although the replacement pattern appears behaviourally consistent with overcompensation, it cannot by itself establish that the underlying cause was a simple overestimation of travelled distance (Ellard & Shaughnessy, 2003; Piekarski et al., 2018; Rieser et al., 1990; Thomson, 1983). Although locomotor distance perception is not perfectly veridical, and can vary with cue availability, response method, and movement context (Schwartz, 1999), these studies suggest that short-distance active

walking is not usually grossly overestimated. Therefore, the present opposite-direction bias is unlikely to reflect a simple locomotor-distance error alone.

However, errors in travelled-distance perception do occur, but their direction depends strongly on the task and available self-motion cues. Some walking studies report overestimation (Philbeck & Loomis, 1997) and underestimation (Böök & Gärling, 1981) at short distances under unfamiliar or reduced cue environments. Optic-flow studies often report overestimation when visual motion is presented without the normal proprioceptive, vestibular, and efference-copy cues of active walking (Bansal et al., 2024; Campos et al., 2010; Redlick et al., 2001). Passive whole-body motion can also distort perceived distance, producing underestimation in some contexts (Siegle et al., 2009) and overestimation in others (Hecht et al., 2018). More closely related blindfolded-movement studies also show direction and distance-dependent errors, including overshooting during backward walking over larger distances (Marlinsky, 1999) and underestimations during lateral blind walking (Paquet et al., 2007). Thus, travelled-distance perception is not perfectly veridical, but neither does the literature indicate a consistent tendency to overestimate short active translations of less than one meter without vision. This makes a simple locomotor-distance account insufficient for explaining the present haptic replacement biases.

Thus, the present bias likely reflects more than a simple gain error in perceived travel distance. Instead, it appears to arise when a haptically encoded target location is combined with active self-motion information and transformed into a new haptic response position. This motivates a broader account in which error emerges from the transformation of spatial information across haptic, body-centered, and movement-based reference frames (Hollins & Kelley, 1988).

7.3.3.1 Constraints on a Simple Self-Motion Overestimation Account

The structure of the present data also argues against a pure self-motion overestimation account. If the bias primarily reflected a simple, uniform gain error in perceived travel distance, equivalent movements should have produced broadly similar replacement errors across target positions, and larger movements should have generated

proportionally larger errors. The observed pattern did not follow that prediction. Bias magnitude varied with the target location being updated. Target positions initially located near the participant were often replaced with relatively small errors after self-motion, whereas targets initially located farther away, particularly those that became nearer to the participant after movement, showed the largest displacement errors. Such target dependence indicates that the effect was not a single overarching overestimation applied uniformly to the whole workspace. Rather, self-motion information appears to have been combined with the remembered haptic target representation in a position-dependent manner.

Conversely, different movement magnitudes (1 step vs 2 steps) sometimes produced relatively similar biases for initially near targets, whereas larger differences between one-step and two-step movements emerged more clearly at spatial extremities. This target-dependent effect also cannot be reduced to a simple arm length limitation. Most replacements remained within participants' measured arm length, and even when the remembered location approached or exceeded this range, participants were not mechanically prevented from completing the response. Instead, they could lean slightly forward and place the object at the location they judged to be correct. Thus, arm length did not impose a hard ceiling on the observed displacement. Rather, the relative-reach analysis indicates that biomechanical reach constraints did not generally determine the magnitude or direction of the updating bias.

7.3.4 Comparison to Visual Experiments

7.3.4.1 – Comparison to Spatiotopic Visual studies

The present findings contrast with the most comparable spatiotopic visual self-motion updating studies. Studies that specifically allowed participants to see a room or arm position generally report biases in the direction of motion. In visual object-location updating, participants often behave as though they have underestimated their displacement. This pattern has been reported after active stepping and pointing to remembered visual targets (Medendorp et al., 1999; Van Pelt & Medendorp, 2007), passive lateral translation with visual localisation responses (Kim & Harris, 2024), and visually simulated perspective shifts or rotations in virtual reality (Segen et al., 2023).

The comparison with Medendorp et al. (1999) is especially important because their task also involved active self-motion, followed by a manual pointing response to a remembered visual target within peripersonal space. Although pointing and direct placement are not identical response modes, prior work suggests that manual pointing and reaching/placement responses can yield broadly comparable spatial localisation patterns within and across vision and haptics (Adamovich et al., 1998; Darling & Miller, 1993; Hollins & Kelley, 1988; Perdreau et al., 2019; Soechting & Flanders, 1989). Therefore, this contrast is theoretically important because it suggests that the direction of spatial updating error may depend not only on self-motion itself, but on the sensory reference frame in which the target is initially encoded and later reconstructed.

7.3.4.2 – Comparison with gaze and head-centered sensorimotor updating

An important distinction is that not all visually related sensorimotor updating studies show the same undercompensatory pattern observed in large-scale or spatiotopic visual updating. Studies involving gaze and reaching show remembered target locations are often systematically mislocalized farther away than should be after changes in eye or head rotation. For example, when participants view or remember a target, make an intervening saccade, and then reach or point to the remembered location, responses can be displaced in a manner consistent with an overestimation of the target's position relative to gaze (Bharmauria et al., 2025; Henriques et al., 1998, 2003; Klier et al., 2008; Medendorp, Tweed, et al., 2003; Mueller & Fiehler, 2014). Related studies using head rotation or vestibular stimulation similarly show that remembered tactile or visual target locations must be updated across changes in head-centered or vestibular reference frames, and that this updating process can introduce systematic spatial biases that resemble the transformation errors observed in gaze-centered reaching. (Reuschel et al., 2012; Van Pelt & Medendorp, 2007). Thus, the present findings do not simply oppose visual or sensorimotor updating more generally. Instead, they diverge most clearly from spatiotopic or allocentric visual self-motion studies, while paralleling a broader class of gaze- and head-centered transformation errors in which remembered locations are reconstructed after the observer's egocentric reference frame has changed through eye, head, or whole-body movement.

A methodological caveat is that head orientation and eye position were not strictly controlled in the present experiments. Participants were instructed to face straight ahead and avoid swaying, but small head rotations, such as looking toward the target positions, or eye movements underneath the blindfold may have occurred. This is relevant because gaze and head-centered updating studies show that eccentric eye or head positions can bias remembered target localisation; for example, 15° head-orientation shifts can produce reaching errors of several centimeters (Reuschel et al., 2012). However, these effects are unlikely to explain the present findings. The replacement biases observed here often exceeded 5 cm and reached approximately 20 cm, whereas controlled gaze- and head-centered updating studies typically report smaller biases of only a few centimeters from 20° of eye rotation (Henriques et al., 1998; Medendorp, Goltz, et al., 2003; Medendorp, Tweed, et al., 2003). Thus, uncontrolled eye or head movements may have added variability, but they cannot fully explain the systematic displacement observed here. Additionally, It has been shown that saccade-related localisation errors vary in magnitude and direction across the retina and with spatial context (Szinte & Cavanagh, 2011).

Furthermore, uncontrolled gaze or head orientation would not readily explain the forward and backward biases observed in the anteroposterior experiments. In those experiments, targets were arranged along the anteroposterior axis on the right side of the table, so any horizontal gaze eccentricity toward the workspace would likely have been relatively similar across target positions. The relevance of the gaze- and head-centered literature is therefore not that eye or head movements caused the present effect, but that spatial memory can become biased when remembered locations must be transformed across changing sensory-motor reference frames.

7.3.5 Transformations of Reference Frames

The divergence between the present findings and spatiotopic visual updating studies, together with their closer resemblance to gaze- and head-centred transformation errors, suggests that the present task is best understood as a problem of reference-frame transformation. Participants first encoded the object through active touch, forming a haptic representation based on tactile and proprioceptive information; they then translated their body through space, generating a self-motion estimate from vestibular, proprioceptive,

and efference-copy cues; finally, they had to reconstruct the remembered object location from a new body position. The critical feature of the task is that participants were not allowed to re-explore the table after moving, meaning that they could not rebuild the haptic frame from the new position. Instead, they had to transform the original haptic representation using self-motion information. This interpretation is consistent with Hollins and Kelley (1988), who found that distortions after rotation around a table were reduced when participants re-examined the workspace, suggesting that renewed haptic exploration can recalibrate the spatial representation. In the present experiments, no such recalibration was available, so responses depended on an internally transformed representation rather than a newly sampled haptic frame.

This interpretation shifts the origin of the bias away from a simple self-motion error and toward an error in reference frame transformations. The issue now becomes how a remembered haptic location was combined with self-motion information and reconstructed for action. This framing is consistent with broader accounts in which perception and action depend not on a single fixed reference frame, but on transformations among eye-centered reference frames (Henriques et al., 1998; McGuire & Sabes, 2009; Medendorp, Goltz, et al., 2003), head-centered reference frames (Bakker et al., 2019; Beurze et al., 2006; Reuschel et al., 2012; Van Pelt & Medendorp, 2007), body-centered and peripersonal reference frames (Bufacchi & Iannetti, 2018; Serino, 2019), limb or hand-centered reference frames (Darling & Miller, 1993; Dupin et al., 2017; Rosenbaum et al., 1993), and external or allocentric reference frames (Noel et al., 2015; Pouget et al., 2002). This logic has been demonstrated behaviourally in several related domains: visual and proprioceptive information must be transformed for reaching and pointing (Berkinblit et al., 1995; Beurze et al., 2006; Darling & Miller, 1993), different postures and remembered target locations must be reconciled during reaching (Rosenbaum et al., 1993), and haptic perception can depend on trunk-centered rather than purely hand-centered coordinates (Dupin et al., 2018). Neural evidence is also consistent with this behavioural literature, as cortical motor areas have been described as transforming extrinsic target information into intrinsic movement commands (Kakei et al., 2003), and kinesthetically guided reaching can recruit visual cortical regions even in the absence of vision (Darling et al., 2007). Within this broader framework, the present

findings suggest that haptic object-location updating after whole-body translation is vulnerable to error at the transformation stage. When the initially encoded haptic representation had to be reconstructed from the participant's new body position, the remembered object location was not preserved veridically. Instead, it appeared to be reconstructed too far opposite the direction of travel, producing a behavioural pattern consistent with apparent overcompensation. Fig. 7.1 illustrates this proposed transformation chain.

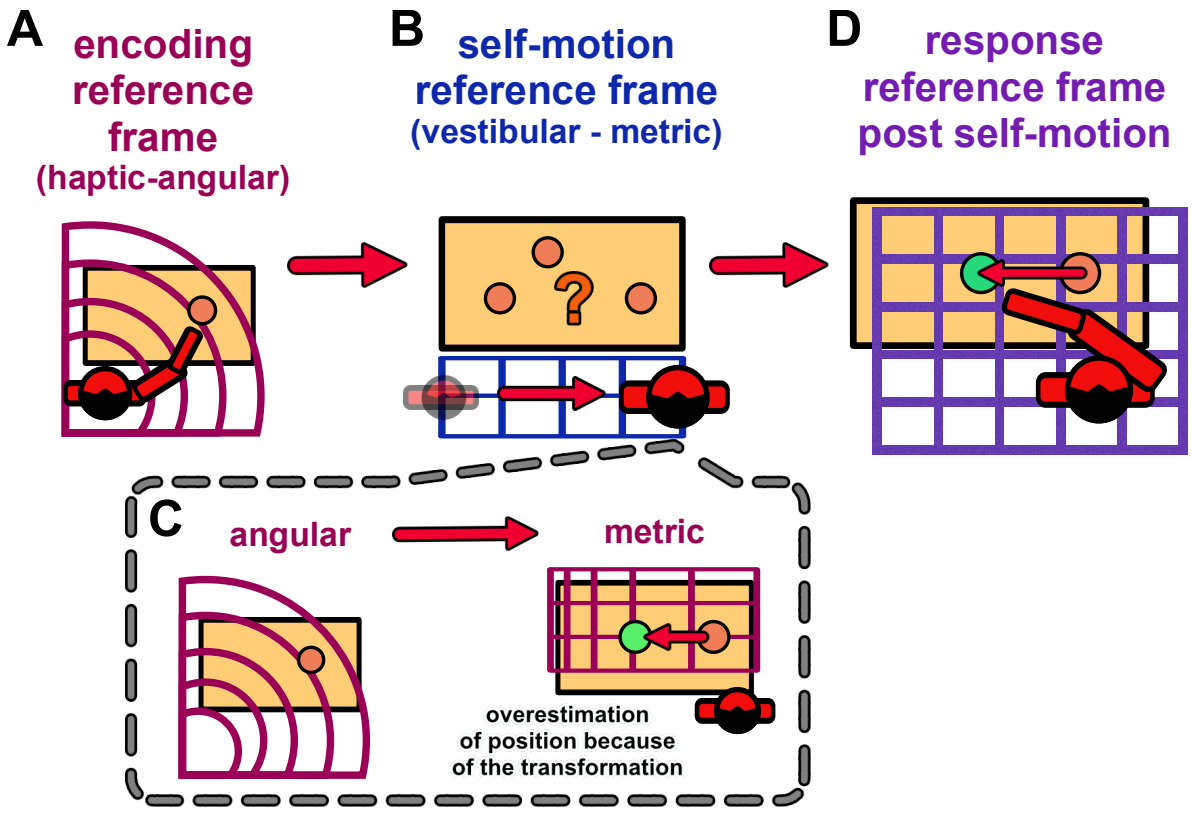

Figure 7.1: Proposed transformation-chain account of apparent overestimation during haptic spatial updating: (A) The object is initially encoded through active touch within a haptic, body-relative reference frame, based on tactile contact, limb position, and proprioceptive information. (B) After rightward self-motion, the participant's displacement is represented using self-motion cues, including vestibular, proprioceptive, and efference-copy information. At this stage, the previously felt object location is no longer directly available from the participant's new body position and must be reconstructed with respect to the estimated body displacement. (C) Because the workspace is not re-explored after movement, this reconstruction depends on an internal transformation of the original haptic representation into a post-motion body-relative response frame. The proposed distortion arises during this transformation, as a limb- and posture-based haptic representation must be converted into a metric tabletop location for action. The green circle represents the reconstructed remembered location, which is displaced from the true object location

because the transformation does not fully preserve the original spatial relation. (D) The final replacement response is generated from this transformed haptic representation. In the example shown, the remembered object location is reconstructed too far opposite the direction of travel, producing a leftward placement bias that appears behaviourally as an overestimation of self-motion.

One possible reason for this non-linear and overcompensatory distortion is that haptic object-location memory and whole-body self-motion may rely on differently parameterized reference frames. Haptic localisation depends strongly on limb configuration, joint position, and proprioceptive estimates of the hand relative to the body and has often been described in relation to rotations, angles, or limb-centered coordinates (Darling & Miller, 1993; McGuire & Sabes, 2009). In contrast, whole-body translation and visual spatial updating are often described as displacement through Cartesian or linear space (Medendorp et al., 1999; Presson & Montello, 1994; Redish & Ekstrom, 2013). The present task may therefore have required participants to transform a limb-centered haptic representation through a whole-body displacement estimate and then reconstruct that representation within a new body-relative response frame. Because joint rotations, limb posture, and external linear displacement do not map onto one another in a simple one-to-one manner (Dupin et al., 2018; Kesner & Creem-Regehr, 2013; Lederman & Klatzky, 2009; McGuire & Sabes, 2009; Medendorp et al., 1999; Pezzulo et al., 2022; Presson & Montello, 1994; Volcic & Kappers, 2008), this transformation may have produced a non-linear distortion of the remembered haptic workspace. More specifically, the reconstructed haptic frame may have remained anchored to the region closest to the participant's original body position, such that nearby targets were preserved more veridically, whereas farther or more obliquely encoded targets were transformed with greater error. Under this account, the apparent overcompensatory bias does not reflect a literal expansion of haptic space, but a contraction or warping of the remembered haptic frame with fewer distortions near the initially stable region after self-motion. As a result, when the participant responded from the new body position, the remembered object location was reconstructed too far opposite the direction of travel. In natural viewing conditions, stable visual landmarks and spatiotopic visual information may help constrain or recalibrate this transformation (Ciucurel & Iconaru, 2026; Souman et al., 2009), even non-informative visual information has been shown to provide such a "stabilizing effect"

(Newport et al., 2002). In the present experiments, however, such visual anchoring cues were absent, allowing the internally transformed haptic representation to guide the response without external correction. This account remains speculative, because the experiments measured behavioural replacement errors rather than the underlying coordinate transformations directly.

Accordingly, the opposing bias observed across haptic and visual updating tasks may reflect differences in the transformations required by each modality. Visual updating may be more easily constrained by stable external landmarks and spatiotopic cues, whereas haptic updating after self-motion requires a remembered limb-based location to be transformed through body displacement and reconstructed in a new action-oriented frame. This does not mean that over-updating should be dismissed entirely: behaviourally, the present responses still appeared as though the remembered object location had been updated too far relative to the participant's new body position. However, the findings suggest that this apparent over-updating may be deeper than a simple overestimation of travelled distance. In the absence of renewed haptic exploration or visual anchoring, the internally transformed haptic representation may persist, producing the apparent overcompensatory bias observed in the present experiments.

7.4 Bias's Magnitude

Self-motion produced a bias opposite to the direction of travel. A separate question is why the magnitude of this bias varied across target positions and movement conditions. This difference in bias across target position was not initially predicted by any hypothesis, but it is theoretically informative because it suggests that the updating error was not applied uniformly across the workspace. Instead, the size of the bias appeared to depend on where the object was initially encoded, where it had to be reconstructed after movement, and how much the initial and final haptic workspaces overlapped.

7.4.1 Initial Position

One explanation is that target position affected the stability of the initial haptic representation and the difficulty of reconstructing that representation after movement. Targets encoded closer to the participant may have been represented more robustly

within the initial haptic frame, whereas farther targets may have required greater extrapolation from limb position and proprioceptive information. At the same time, initial and final target distance were partly confounded by the task's geometry: targets that were farther from the participant before movement could become closer after movement. Therefore, the position effect cannot be attributed exclusively to either encoding or response reconstruction. A more plausible interpretation is that both contributed: self-motion required the original haptic representation to be transformed into a new response frame, and this transformation was shaped by the limits of the reachable workspace. Biases may have been expressed most fully when the remembered location fell within comfortable arm's reach, whereas farther locations may have been constrained by arm-extension limits.

7.4.2 Movement Magnitude

Movement magnitude provides a related constraint. Larger translations likely reduced the overlap between the initial and final haptic frames, increasing the transformation required before the object could be replaced. However, if this transformation is non-linear, larger movements should not necessarily produce uniformly larger biases across all target positions. Instead, the effect of movement magnitude should depend on where the target falls within the reachable workspace. In more stable or comfortably reachable regions of the workspace, one-step and two-step movements may produce similar replacement performance. In contrast, differences between movement magnitudes should emerge more clearly at the edges of the workspace, where the remembered location must be reconstructed across a larger or less stable transformation. This was observed statistically in Experiment 3, where one-step and two-step lateral movements differed most clearly at the outer target positions, and appeared descriptively in Experiment 4. Thus, movement magnitude increased transformation demand, but the resulting bias was shaped by target position and workspace geometry rather than by a simple linear effect of distance travelled.

7.4.3 Relative Reach's Contribution

Relative reach should nevertheless not be dismissed entirely. It remains plausible that some aspects of the observed bias pattern were shaped by the limits of the reachable

arm length, especially because several responses approached, and in some cases exceeded, participants' measured arm length. This should have been more tightly controlled experimentally. However, the relative-reach analyses argue against a simple reach-limitation account: across most movement conditions, relative reach did not significantly predict bias, suggesting that participants were not merely placing the object incorrectly because they could not physically reach the remembered location.

The main exception was the backward-to-forward condition in Experiment 2. This condition is informative because it likely involved targets that were initially encoded near the participant's maximum arm length, possibly with some forward sway, and then replaced after the participant had moved forward toward the remembered object location. The significant relationship between increased relative reach and reduced bias suggests that targets near the edge of reachable space may have provided a useful spatial anchor, allowing participants to preserve the object's location as being near maximum arm length after moving forward. Thus, the one reliable relative-reach effect does not suggest that reach limitation caused the bias; instead, it suggests that, in this specific forward-updating case (where the object is always anterior to the body), the edge of the reachable workspace may have helped constrain the reconstructed object's location. Reach geometry may have modulated how the bias was expressed, but it did not provide a sufficient explanation for the direction or magnitude of the bias.

7.5 Precision Loss After Self-Motion

The reduction in precision after self-motion provides a complementary consequence of the proposed transformation bias idea. Whereas the directional bias indicates that remembered haptic locations were systematically reconstructed in the wrong position, the precision effects suggest that this reconstruction was not applied identically on every trial. This is in contrast to the stationary conditions, where the participant, table, and target remained in a fixed spatial relation after 5 s of waiting, allowing replacement to be guided by a comparatively stable haptic reference frame. No remapping of the remembered target location was required, resulting in nonsignificant and high precision.

Following self-motion, by contrast, the remembered location had to be transformed into a new body-relative response frame. This transformation depended on combining the initial haptic representation with an internal estimate of body displacement derived from proprioceptive, vestibular, and efference-copy signals. Non-visual self-motion estimation is not perfectly stable and can vary significantly (Campos et al., 2010; Durgin et al., 2005), and any trial-to-trial uncertainty in that displacement estimate could propagate into the reconstructed haptic target location. When this uncertain self-motion information was integrated with the remembered haptic position, the resulting post-motion location may therefore have varied more across trials, increasing response variability. In addition, participants had neither online visual information nor an opportunity to re-explore the tabletop after moving, which could otherwise have corrected or stabilized the reconstructed target location before replacement.

Thus, movement may have reduced precision because it added uncertainty to an already uncertain memory-guided response. Along with the post-motion replacement requiring the initial haptic reference frame memory to be combined with an internally estimated body displacement magnifying any starting uncertainties of position. Resulting in an increase in variability consistent with the broader interpretation that self-motion introduced a noisy reconstruction process.

7.6 Limitations

A primary limitation of the present experiments is also one of their main strengths: participants moved actively and naturally. Active self-motion was necessary because the task was intended to include the proprioceptive, vestibular, and efference-copy signals normally available during self-generated movement. However, this also introduced variability in the exact execution of each step. Although participants were instructed to move along the required axis, small deviations in step length and minor off-axis movements occurred across trials. These deviations were generally small and averaged towards the intended movement distances, but they nevertheless added variability that would not be present in a fully constrained passive-motion design.

A related limitation is that perceived travelled distance was not measured independently. The observed replacement pattern appeared behaviourally consistent with overcompensatory updating, but the experiments did not directly ask participants to estimate how far they had moved. Therefore, the results cannot determine whether participants explicitly overestimated their self-motion, or whether the apparent overestimation emerged during the transformation of the remembered haptic location into a new response frame. A future version of the task could include explicit distance-estimation trials or a continuous self-motion report to separate perceived travel distance from haptic spatial updating.

Another limitation concerns arm-movement recording during haptic exploration. More complete kinematic tracking of the exploring arm would have allowed a stronger analysis of whether exploration strategy influenced later replacement bias. In Experiment 1, rudimentary arm-tracking data allowed several exploratory measures to be examined, including bounding-box area, average speed, peak velocity, exploration duration, and total arm-path distance during search. These measures did not show a clear relationship with lateral bias, suggesting that the observed updating errors were unlikely to be driven simply by how extensively or quickly participants explored the object before movement. However, because comparable tracking measures were not available across all experiments, the present thesis cannot fully rule out a contribution of individual differences in haptic exploration strategy.

Finally, head orientation, eye position, and postural sway were minimized but not strictly controlled. Participants were instructed to face forward and avoid swaying, but small head, eye, or body-position changes may still have occurred. These factors may have contributed to response variability, although they are unlikely to explain the systematic movement-direction-dependent biases observed across experiments. Rare nonspecific cues were also reported, including subtle auditory information during placement by a few participants and perceived air displacement from the experimenter's movement by one participant. These cues were not common or consistent enough to explain the main findings, but they remain minor methodological limitations.

Overall, these limitations do not undermine the central finding that active self-motion produced systematic haptic replacement biases. Rather, they define the boundary of the present interpretation. The experiments demonstrate a robust behavioural updating error, but they do not isolate the precise contributions of perceived travel distance, haptic exploration strategy, eye/head position, or reference-frame transformation. The findings nevertheless suggest that haptic spatial updating is not a simple linear remapping of object positions across body movement. Instead, when visual or spatiotopic anchoring cues are absent, remembered haptic locations may be reconstructed through a non-uniform transformation that warps the remembered haptic frame toward its initially stable region, producing systematic overcompensatory bias.

7.7 General Conclusion

Therefore, this thesis establishes that active self-motion systematically alters haptic object-location updating. In a blindfolded pick-up, move, and replace task, participants placed objects beyond their true locations in the direction opposite to travel. This overcompensatory pattern was contrary to the original prediction and contrasts with comparable visual self-motion studies, which often report undercompensatory updating errors.

The present findings further suggest that initial haptic localisation was relatively stable across a wide range of starting positions, as stationary replacement remained largely veridical when participants stood at different locations along the table edge. The overcompensatory effect also cannot be reduced to a simple overestimation of travelled distance, because the broader self-motion literature does not show a consistent tendency to overestimate short active translations. Instead, the bias appears to emerge when a haptically encoded location must be transformed across self-motion and reconstructed from a new body position. This thesis therefore identifies an unexpected and novel feature of haptic spatial updating. After self-motion, remembered haptic targets were repositioned in a manner consistent with overcompensatory updating. The present results suggest that this effect may arise from a previously unaccounted for transformation bias, in which the reconstruction of haptically encoded space is sufficiently non-uniform to displace remembered locations beyond their true positions. Importantly, this haptic

overcompensatory tendency may stand in contrast to the undercompensatory pattern often reported in visually guided spatial updating. More broadly, these findings contribute to the study of haptic spatial perception, and spatial updating in general, by suggesting that transformations between reference frames may shape not only the magnitude and variability of updating errors, but also their direction.

7.8 Future Directions

Future work should first compare haptic and visual spatial updating within the same experimental design. A key question that remains unanswered is whether the opposite bias patterns observed across haptic and visual studies reflect differences in target modality, or the self-motion estimation. Participants could encode targets visually, haptically, or visuo-haptically, then translate to a new position under different cue conditions, including active walking with vision, blind walking, passive body movement in darkness, or optic-flow-based simulated self-motion. This would test whether visual self-motion cues tend to produce under-updating, whereas nonvisual or dark movement conditions produce over-updating, even when the target modality and response mode are held constant, or not.

A second priority is to manipulate re-exploration after movement. The present task prevented participants from rebuilding the haptic workspace after self-motion. Allowing brief re-exploration of the table or target region would test to what extent renewed haptic contact recalibrates the post-movement reference frame and allow an exploration into the degree of how much of a reduction in overcompensatory bias will be observed, if any, would be observed if the haptic frame can be reupdated. Continuous pointing or tracking during movement would also be useful, as it could reveal whether the bias accumulates during translation, as a function of speed of the update or emerges primarily during the final response, or even changes over time.

Finally, future studies should examine factors that may stabilize or destabilize haptic updating, including visual feedback of the acting limb, head and gaze stabilization, target position height, movement speed, further granularity in the step sizes, and individual differences in sensorimotor expertise. Comparing trained musicians, athletes,

professional gamers, and untrained participants could determine whether long-term motor experience reduces transformation error, possibly lending this study to a more empirical measurement of high-performance activities and training therein. .

Lastly, a virtual- or augmented-reality version of the task could further dissociate visual scene motion, visible limb position, physical haptic contact, and proprioceptive versus tactile feedback, allowing the contribution of each cue to the updating bias to be tested more directly. A variation where the participants are asked to move, then move back to the original spot, or past the original spot in the opposite direction and greater magnitude could help uncover these transformation biases in further depth. Furthermore, a variation in which both the left and right hands, or dominant and non-dominant hands would also shed further insights into the nature of the haptic spatial sense. These extensions would clarify whether the present bias reflects a general property of haptic spatial updating or a specific consequence of reconstructing a remembered limb-based location after blind active self-motion.

References

Adamovich, S. V., Berkinblit, M. B., Fookson, O., & Poizner, H. (1998). Pointing in 3D Space to Remembered Targets. I. Kinesthetic Versus Visual Target Presentation. *Journal of Neurophysiology*, *79*(6), 2833–2846. https://doi.org/10.1152/jn.1998.79.6.2833

Adamovich, S. V., Berkinblit, M. B., Hening, W., Sage, J., & Poizner, H. (2001). (PD) The interaction of visual and proprioceptive inputs in pointing to actual and remembered targets in Parkinson's disease. *Neuroscience*, *104*(4), 1027–1041. https://doi.org/10.1016/S0306-4522(01)00099-9

Bakker, R. S., Selen, L. P. J., & Medendorp, W. P. (2019). Transformation of vestibular signals for the decisions of hand choice during whole body motion. *Journal of Neurophysiology*, *121*(6), 2392–2400. https://doi.org/10.1152/jn.00470.2018

Bansal, A., McManus, M., Jörges, B., & Harris, L. R. (2024). Perceived travel distance depends on the speed and direction of self-motion. *PloS One*, *19*(9), e0305661. https://doi.org/10.1371/journal.pone.0305661

Beek, F. E. van, Tiest, W. M. B., & Kappers, A. M. L. (2014). Haptic Discrimination of Distance. *PLOS ONE*, *9*(8), e104769. https://doi.org/10.1371/journal.pone.0104769

Bennett, C. R., Loomis, J. M., Klatzky, R. L., & Giudice, N. A. (2017). Spatial updating of multiple targets: Comparison of younger and older adults. *Memory & Cognition*, *45*(7), 1240–1251. https://doi.org/10.3758/s13421-017-0725-0

Berkinblit, MichailB., Fookson, OlgaI., Smetanin, B., Adamovich, SergeyV., & Poizner, H. (1995). The interaction of visual and proprioceptive inputs in pointing to actual and

remembered targets. *Experimental Brain Research*, *107*(2). https://doi.org/10.1007/BF00230053

Beurze, S. M., Van Pelt, S., & Medendorp, W. P. (2006). Behavioral Reference Frames for Planning Human Reaching Movements. *Journal of Neurophysiology*, *96*(1), 352–362. https://doi.org/10.1152/jn.01362.2005

Bharmauria, V., Seo, S., & Crawford, J. D. (2025). Neural integration of egocentric and allocentric visual cues in the gaze system. *Journal of Neurophysiology*, *133*(1), 109–120. https://doi.org/10.1152/jn.00498.2024

Blumenfeld, W. (1937). The relationship between the optical and haptic construction of space. *Acta Psychologica*, *2*, 125–174. https://doi.org/10.1016/S0001-6918(37)90011-8

Böök, A., & Gärling, T. (1981). Maintenance of orientation during locomotion in unfamiliar environments. *Journal of Experimental Psychology: Human Perception and Performance*, *7*(5), 995–1006. https://doi.org/10.1037/0096-1523.7.5.995

Bufacchi, R. J., & Iannetti, G. D. (2018). An Action Field Theory of Peripersonal Space. *Trends in Cognitive Sciences*, *22*(12), 1076–1090. https://doi.org/10.1016/j.tics.2018.09.004

Campos, J. L., Byrne, P., & Sun, H.-J. (2010). The brain weights body-based cues higher than vision when estimating walked distances. *European Journal of Neuroscience*, *31*(10), 1889–1898. https://doi.org/10.1111/j.1460-9568.2010.07212.x

Ciucurel, C., & Iconaru, E. I. (2026). Static Estimation of Vista-Space Egocentric Distance with Iterative Feedback: A Cognitive–Perceptual Task. *Life*, *16*(1), 173. https://doi.org/10.3390/life16010173

Darling, W. G., & Miller, G. F. (1993). Transformations between visual and kinesthetic coordinate systems in reaches to remembered object locations and orientations. *Experimental Brain Research*, *93*(3). https://doi.org/10.1007/BF00229368

Darling, W. G., Seitz, R. J., Peltier, S., Tellmann, L., & Butler, A. J. (2007). Visual cortex activation in kinesthetic guidance of reaching. *Experimental Brain Research*, *179*(4), 607–619. https://doi.org/10.1007/s00221-006-0815-x

Dassonville, P. (1995). Haptic localization and the internal representation of the hand in space. *Experimental Brain Research*, *106*(3), 434–448. https://doi.org/10.1007/BF00231066

de Grave, D. D. J., Brenner, E., & Smeets, J. B. J. (2011). Using a Stick Does Not Necessarily Alter Judged Distances or Reachability. *PLoS ONE*, *6*(2), e16697. https://doi.org/10.1371/journal.pone.0016697

Dijkerman, H. C., & Medendorp, W. P. (2021). Visuo-tactile predictive mechanisms of peripersonal space. In F. De Vignemont, A. Serino, H. Y. Wong, & A. Farnè (Eds.), *The World at Our Fingertips* (1st ed., pp. 81–100). Oxford University Press Oxford. https://doi.org/10.1093/oso/9780198851738.003.0005

Dupin, L., Hayward, V., & Wexler, M. (2017). Generalized movement representation in haptic perception. *Journal of Experimental Psychology: Human Perception and Performance*, *43*(3), 581–595. https://doi.org/10.1037/xhp0000327

Dupin, L., Hayward, V., & Wexler, M. (2018). Radial trunk-centred reference frame in haptic perception. *Scientific Reports*, *8*(1), 13550. https://doi.org/10.1038/s41598-018-32002-3

Durgin, F. H., Pelah, A., Fox, L. F., Lewis, J., Kane, R., & Walley, K. A. (2005). Self-Motion Perception During Locomotor Recalibration: More Than Meets the Eye. *Journal of Experimental Psychology: Human Perception and Performance*, *31*(3), 398–419. https://doi.org/10.1037/0096-1523.31.3.398

Ellard, C. G., & Shaughnessy, S. C. (2003). A Comparison of Visual and Nonvisual Sensory Inputs to Walked Distance in a Blind-Walking Task. *Perception*, *32*(5), 567–578. https://doi.org/10.1068/p5041

Faineteau, H., Gentaz, E., & Viviani, P. (2005). Factors affecting the size of the detour effect in the kinaesthetic perception of Euclidean distance. *Experimental Brain Research*, *163*(4), 503–514. https://doi.org/10.1007/s00221-004-2204-7

Fernández-Díaz, M., & Travieso, D. (2011). Performance in haptic geometrical matching tasks depends on movement and position of the arms. *Acta Psychologica*, *136*(3), 382–389. https://doi.org/10.1016/j.actpsy.2011.01.003

Forster, P.-P., Fiehler, K., & Karimpur, H. (2023). Egocentric cues influence the allocentric spatial memory of object configurations for memory-guided actions. *Journal of Neurophysiology*, *130*(5), 1142–1149. https://doi.org/10.1152/jn.00149.2023

Giudice, N. A., Bennett, C. R., Klatzky, R. L., & Loomis, J. M. (2017). SPATIAL UPDATING OF HAPTIC ARRAYS ACROSS THE LIFE SPAN. *Experimental Aging Research*, *43*(3), 274–290. https://doi.org/10.1080/0361073X.2017.1298958

Giudice, N. A., Betty, M. R., & Loomis, J. M. (2011). Functional equivalence of spatial images from touch and vision: Evidence from spatial updating in blind and sighted individuals. *Journal of Experimental Psychology: Learning, Memory, and Cognition*, *37*(3), 621–634. https://doi.org/10.1037/a0022331

Giudice, N. A., Klatzky, R. L., Bennett, C. R., & Loomis, J. M. (2013). Perception of 3-D location based on vision, touch, and extended touch. *Experimental Brain Research*, *224*(1), 141–153. https://doi.org/10.1007/s00221-012-3295-1

Hecht, H., Ramdohr, M., & von Castell, C. (2018). Underestimation of large distances in active and passive locomotion. *Experimental Brain Research*, *236*(6), 1603–1609. https://doi.org/10.1007/s00221-018-5245-z

Henriques, D. Y. P., Klier, E. M., Smith, M. A., Lowy, D., & Crawford, J. D. (1998). Gaze-Centered Remapping of Remembered Visual Space in an Open-Loop Pointing Task. *The Journal of Neuroscience*, *18*(4), 1583–1594. https://doi.org/10.1523/JNEUROSCI.18-04-01583.1998

Henriques, D. Y. P., Medendorp, W. P., Gielen, C. C. a. M., & Crawford, J. D. (2003). Geometric computations underlying eye-hand coordination: Orientations of the two eyes and the head. *Experimental Brain Research*, *152*(1), 70–78. https://doi.org/10.1007/s00221-003-1523-4

Hollins, M., & Kelley, E. K. (1988). Spatial updating in blind and sighted people. *Perception & Psychophysics*, *43*(4), 380–388. https://doi.org/10.3758/BF03208809

Jones, S. A. H., Cressman, E. K., & Henriques, D. Y. P. (2010). Proprioceptive localization of the left and right hands. *Experimental Brain Research*, *204*(3), 373–383. https://doi.org/10.1007/s00221-009-2079-8

Jones, S. A. H., Fiehler, K., & Henriques, D. Y. P. (2012). A task-dependent effect of memory and hand-target on proprioceptive localization. *Neuropsychologia*, *50*(7), 1462–1470. https://doi.org/10.1016/j.neuropsychologia.2012.02.031

Kakei, S., Hoffman, D. S., & Strick, P. L. (2003). Sensorimotor transformations in cortical motor areas. *Neuroscience Research*, *46*(1), 1–10. https://doi.org/10.1016/S0168-0102(03)00031-2

Kappers, A. M. L. (1999). Large systematic deviations in the haptic perception of parallelity. *Perception*, *28*(8), 1001–1012. https://doi.org/10.1068/p2802

Kappers, A. M. L. (2007). Haptic space processing—Allocentric and egocentric reference frames. *Canadian Journal of Experimental Psychology / Revue Canadienne de Psychologie Expérimentale*, *61*(3), 208–218. https://doi.org/10.1037/cjep2007022

Kappers, A. M. L., & Koenderink, J. J. (1999). Haptic Perception of Spatial Relations. *Perception*, *28*(6), 781–795. https://doi.org/10.1068/p2930

Kappers, A. M. L., & Schakel, W. B. (2011). Comparison of the haptic and visual deviations in a parallelity task. *Experimental Brain Research*, *208*(3), 467–473. https://doi.org/10.1007/s00221-010-2500-3

Kennedy, J. M. (1993). *Drawing & the blind: Pictures to touch*. Yale University Press.

Kesner, R. P., & Creem-Regehr, S. H. (2013). Parietal contributions to spatial cognition. In D. Waller & L. Nadel (Eds.), *Handbook of spatial cognition.* (pp. 35–63). American Psychological Association. https://doi.org/10.1037/13936-003

Kim, J. J. J., & Harris, L. R. (2024). Updating the remembered position of targets following passive lateral translation. *PLOS ONE*, *19*(12), e0316469. https://doi.org/10.1371/journal.pone.0316469

Klatzky, R. L., & Lederman, S. J. (1988). The Intelligent Hand. In G. H. Bower (Ed.), *Psychology of Learning and Motivation* (Vol. 21, pp. 121–151). Academic Press. https://doi.org/10.1016/S0079-7421(08)60027-4

Klatzky, R. L., & Lederman, S. J. (1993). Toward a Computational Model of Constraint-Driven Exploration and Haptic Object Identification. *Perception*, *22*(5), 597–621. https://doi.org/10.1068/p220597

Klier, E. M., Hess, B. J. M., & Angelaki, D. E. (2008). Human Visuospatial Updating After Passive Translations in Three-Dimensional Space. *Journal of Neurophysiology*, *99*(4), 1799–1809. https://doi.org/10.1152/jn.01091.2007

Kuling, I. A., Brenner, E., & Smeets, J. B. J. (2016). Proprioceptive Localization of the Hand Changes When Skin Stretch around the Elbow Is Manipulated. *Frontiers in Psychology*, *7*. https://doi.org/10.3389/fpsyg.2016.01620

Lederman, S. J., & Klatzky, R. L. (2009). Haptic perception: A tutorial. *Attention, Perception & Psychophysics*, *71*(7), 1439–1459. https://doi.org/10.3758/APP.71.7.1439

Li, N., & Angelaki, D. E. (2005). Updating Visual Space during Motion in Depth. *Neuron*, *48*(1), 149–158. https://doi.org/10.1016/j.neuron.2005.08.021

Marlinsky, V. V. (1999). Vestibular and vestibulo-proprioceptive perception of motion in the horizontal plane in blindfolded man. Estimations of linear displacement. *Neuroscience*, *90*(2), 389–394. https://doi.org/10.1016/S0306-4522(98)00450-3

Martolini, C., Cappagli, G., Saligari, E., Gori, M., & Signorini, S. (2021). Allocentric spatial perception through vision and touch in sighted and blind children. *Journal of Experimental Child Psychology*, *210*, 105195. https://doi.org/10.1016/j.jecp.2021.105195

McGuire, L. M. M., & Sabes, P. N. (2009). Sensory transformations and the use of multiple reference frames for reach planning. *Nature Neuroscience*, *12*(8), 1056–1061. https://doi.org/10.1038/nn.2357

McIntyre, J., Stratta, F., & Lacquaniti, F. (1997). Viewer-Centered Frame of Reference for Pointing to Memorized Targets in Three-Dimensional Space. *Journal of Neurophysiology*, *78*(3), 1601–1618. https://doi.org/10.1152/jn.1997.78.3.1601

McIntyre, J., Stratta, F., & Lacquaniti, F. (1998). Short-Term Memory for Reaching to Visual Targets: Psychophysical Evidence for Body-Centered Reference Frames. *The Journal of Neuroscience*, *18*(20), 8423–8435. https://doi.org/10.1523/JNEUROSCI.18-20-08423.1998

Medendorp, W. P., Goltz, H. C., Vilis, T., & Crawford, J. D. (2003). Gaze-Centered Updating of Visual Space in Human Parietal Cortex. *Journal of Neuroscience*, *23*(15), 6209–6214. https://doi.org/10.1523/JNEUROSCI.23-15-06209.2003

Medendorp, W. P., Tweed, D. B., & Crawford, J. D. (2003). Motion Parallax Is Computed in the Updating of Human Spatial Memory. *The Journal of Neuroscience*, *23*(22), 8135–8142. https://doi.org/10.1523/JNEUROSCI.23-22-08135.2003

Medendorp, W. P., Van Asselt, S., & Gielen, C. C. A. M. (1999). Pointing to remembered visual targets after active one-step self-displacements within reaching space: *Experimental Brain Research*, *125*(1), 50–60. https://doi.org/10.1007/s002210050657

Mueller, S., & Fiehler, K. (2014). Gaze-dependent spatial updating of tactile targets in a localization task. *Frontiers in Psychology*, *5*. https://doi.org/10.3389/fpsyg.2014.00066

Mugge, W., Kuling, I. A., Brenner, E., & Smeets, J. B. J. (2016). Haptic Guidance Needs to Be Intuitive Not Just Informative to Improve Human Motor Accuracy. *PLoS ONE*, *11*(3), e0150912. https://doi.org/10.1371/journal.pone.0150912

Nelson, J. S., Kuling, I. A., Gori, M., Postma, A., Brenner, E., & Smeets, J. B. J. (2018). Spatial Representation of the Workspace in Blind, Low Vision, and Sighted Human Participants. *I-Perception*, *9*(3), 2041669518781877. https://doi.org/10.1177/2041669518781877

Newport, R., Rabb, B., & Jackson, S. R. (2002). Noninformative vision improves haptic spatial perception. *Current Biology: CB*, *12*(19), 1661–1664. https://doi.org/10.1016/s0960-9822(02)01178-8

Noel, J.-P., Grivaz, P., Marmaroli, P., Lissek, H., Blanke, O., & Serino, A. (2015). Full body action remapping of peripersonal space: The case of walking. *Neuropsychologia*, *70*, 375–384. https://doi.org/10.1016/j.neuropsychologia.2014.08.030

Oldfield, R. C. (1971). The assessment and analysis of handedness: The Edinburgh inventory. *Neuropsychologia*, *9*(1), 97–113. https://doi.org/10.1016/0028-3932(71)90067-4

Oldfield, S. R., & Parker, S. P. A. (1984). Acuity of Sound Localisation: A Topography of Auditory Space. I. Normal Hearing Conditions. *Perception*, *13*(5), 581–600. https://doi.org/10.1068/p130581

Paquet, N., Rainville, C., Lajoie, Y., & Tremblay, F. (2007). Reproducibility of Distance and Direction Errors Associated with Forward, Backward, and Sideway Walking in

the Context of Blind Navigation. *Perception*, *36*(4), 525–536. https://doi.org/10.1068/p5532

Parseihian, G., Jouffrais, C., & Katz, B. F. G. (2014). Reaching nearby sources: Comparison between real and virtual sound and visual targets. *Frontiers in Neuroscience*, *8*, 269. https://doi.org/10.3389/fnins.2014.00269

Pasqualotto, A., & Newell, F. N. (2007). The role of visual experience on the representation and updating of novel haptic scenes. *Brain and Cognition*, *65*(2), 184–194. https://doi.org/10.1016/j.bandc.2007.07.009

Perdreau, F., Cooke, J. R. H., Koppen, M., & Medendorp, W. P. (2019). Causal inference for spatial constancy across whole body motion. *Journal of Neurophysiology*, *121*(1), 269–284. https://doi.org/10.1152/jn.00473.2018

Pezzulo, G., Donnarumma, F., Ferrari-Toniolo, S., Cisek, P., & Battaglia-Mayer, A. (2022). Shared population-level dynamics in monkey premotor cortex during solo action, joint action and action observation. *Progress in Neurobiology*, *210*, 102214. https://doi.org/10.1016/j.pneurobio.2021.102214

Philbeck, J. W., & Loomis, J. M. (1997). Comparison of two indicators of perceived egocentric distance under full-cue and reduced-cue conditions. *Journal of Experimental Psychology. Human Perception and Performance*, *23*(1), 72–85. https://doi.org/10.1037//0096-1523.23.1.72

Piekarski, S., Lajoie, Y., & Paquet, N. (2018). Effect of Transient Perturbations of Short-Term Memory on Target-Directed Blind Locomotion. *Journal of Motor Behavior*, *50*(1), 2–7. https://doi.org/10.1080/00222895.2016.1271301

Postma, A., Zuidhoek, S., Noordzij, M. L., & Kappers, A. M. L. (2008). Keep an eye on your hands: On the role of visual mechanisms in processing of haptic space. *Cognitive Processing*, *9*(1), 63–68. https://doi.org/10.1007/s10339-007-0201-z

Pouget, A., Deneve, S., & Duhamel, J.-R. (2002). A computational perspective on the neural basis of multisensory spatial representations. *Nature Reviews Neuroscience*, *3*(9), 741–747. https://doi.org/10.1038/nrn914

Presson, C. C., & Montello, D. R. (1994). Updating after rotational and translational body movements: Coordinate structure of perspective space. *Perception*, *23*(12), 1447–1455. https://doi.org/10.1068/p231447

R Core Team. (2021). *R* (Version 4.4) [Computer software].

Redish, A. D., & Ekstrom, A. (2013). Hippocampus and related areas: What the place cell literature tells us about cognitive maps in rats and humans. In D. Waller & L. Nadel (Eds.), *Handbook of spatial cognition.* (pp. 15–34). American Psychological Association. https://doi.org/10.1037/13936-002

Redlick, F. P., Jenkin, M., & Harris, L. R. (2001). Humans can use optic flow to estimate distance of travel. *Vision Research*, *41*(2), 213–219. https://doi.org/10.1016/S0042-6989(00)00243-1

Reuschel, J., Rösler, F., Henriques, D. Y. P., & Fiehler, K. (2012). Spatial Updating Depends on Gaze Direction Even after Loss of Vision. *The Journal of Neuroscience*, *32*(7), 2422–2429. https://doi.org/10.1523/JNEUROSCI.2714-11.2012

Rieser, J. J., Ashmead, D. H., Talor, C. R., & Youngquist, G. A. (1990). Visual Perception and the Guidance of Locomotion without Vision to Previously Seen Targets. *Perception*, *19*(5), 675–689. https://doi.org/10.1068/p190675

Rincon-Gonzalez, L., Buneo, C. A., & Helms Tillery, S. I. (2011). The Proprioceptive Map of the Arm Is Systematic and Stable, but Idiosyncratic. *PLoS ONE*, *6*(11), e25214. https://doi.org/10.1371/journal.pone.0025214

Rosenbaum, D. A., Engelbrecht, S. E., Bushe, M. M., & Loukopoulos, L. D. (1993). A model for reaching control. *Acta Psychologica*, *82*(1–3), 237–250. https://doi.org/10.1016/0001-6918(93)90014-I

Schwartz, M. (1999). Haptic perception of the distance walked when blindfolded. *Journal of Experimental Psychology: Human Perception and Performance*, *25*(3), 852–865. https://doi.org/10.1037/0096-1523.25.3.852

Segen, V., Avraamides, M. N., Slattery, T., & Wiener, J. M. (2023). Biases in object location estimation: The role of rotations and translation. *Attention, Perception, & Psychophysics*, *85*(7), 2307–2320. https://doi.org/10.3758/s13414-023-02716-2

Serino, A. (2019). Peripersonal space (PPS) as a multisensory interface between the individual and the environment, defining the space of the self. *Neuroscience & Biobehavioral Reviews*, *99*, 138–159. https://doi.org/10.1016/j.neubiorev.2019.01.016

Sheth, B. R., & Shimojo, S. (2001). Compression of space in visual memory. *Vision Research*, *41*(3), 329–341. https://doi.org/10.1016/S0042-6989(00)00230-3

Shimono, K., Higashiyama, A., & Tam, W. J. (2001). Location of the egocenter in kinesthetic space. *Journal of Experimental Psychology. Human Perception and Performance*, *27*(4), 848–861.

Siegle, J. H., Campos, J. L., Mohler, B. J., Loomis, J. M., & Bülthoff, H. H. (2009). Measurement of instantaneous perceived self-motion using continuous pointing. *Experimental Brain Research*, *195*(3), 429–444. https://doi.org/10.1007/s00221-009-1805-6

Soechting, J. F., & Flanders, M. (1989). Sensorimotor representations for pointing to targets in three-dimensional space. *Journal of Neurophysiology*, *62*(2), 582–594. https://doi.org/10.1152/jn.1989.62.2.582

Souman, J. L., Frissen, I., Sreenivasa, M. N., & Ernst, M. O. (2009). Walking straight into circles. *Current Biology: CB*, *19*(18), 1538–1542. https://doi.org/10.1016/j.cub.2009.07.053

Strong, G. W. (1994). There is no “point” to space. *Behavioral and Brain Sciences*, *17*(2), 279–279. https://doi.org/10.1017/S0140525X00034592

Szinte, M., & Cavanagh, P. (2011). Spatiotopic apparent motion reveals local variations in space constancy. *Journal of Vision*, *11*(2), 4–4. https://doi.org/10.1167/11.2.4

Szubielska, M., & Möhring, W. (2019). Adults’ spatial scaling: Evidence from the haptic domain. *Cognitive Processing*, *20*(4), 431–440. https://doi.org/10.1007/s10339-019-00920-3

Szubielska, M., Szewczyk, M., Augustynowicz, P., Kędziora, W., & Möhring, W. (2024). Adults’ spatial scaling of tactile maps: Insights from studying sighted, early and late

blind individuals. *PLOS ONE*, *19*(5), e0304008. https://doi.org/10.1371/journal.pone.0304008

Thomson, J. A. (1983). Is continuous visual monitoring necessary in visually guided locomotion? *Journal of Experimental Psychology: Human Perception and Performance*, *9*(3), 427–443. https://doi.org/10.1037/0096-1523.9.3.427

Toni, I., Gentilucci, M., Jeannerod, M., & Decety, J. (1996). Differential influence of the visual framework on end point accuracy and trajectory specification of arm movements. *Experimental Brain Research*, *111*(3). https://doi.org/10.1007/BF00228734

Van Dijk, R., Kappers, A. M. L., & Postma, A. (2013). Haptic Spatial Configuration Learning in Deaf and Hearing Individuals. *PLOS ONE*, *8*(4), e61336. https://doi.org/10.1371/journal.pone.0061336

Van Pelt, S., & Medendorp, W. P. (2007). Gaze-Centered Updating of Remembered Visual Space During Active Whole-Body Translations. *Journal of Neurophysiology*, *97*(2), 1209–1220. https://doi.org/10.1152/jn.00882.2006

Volcic, R., & Kappers, A. M. L. (2008). Allocentric and egocentric reference frames in the processing of three-dimensional haptic space. *Experimental Brain Research*, *188*(2), 199–213. https://doi.org/10.1007/s00221-008-1353-5

Volcic, R., Kappers, A. M. L., & Koenderink, J. J. (2007). Haptic parallelity perception on the frontoparallel plane: The involvement of reference frames. *Perception & Psychophysics*, *69*(2), 276–286. https://doi.org/10.3758/BF03193749

Wako, R., & Ayabe-Kanamura, S. (2016). Characteristics of Haptic Peripersonal Spatial Representation of Object Relations. *PLOS ONE*, *11*(7), e0160095. https://doi.org/10.1371/journal.pone.0160095

Weast, R. A. T., & Proffitt, D. R. (2018). Can I reach that? Blind reaching as an accurate measure of estimated reachable distance. *Consciousness and Cognition*, *64*, 121–134. https://doi.org/10.1016/j.concog.2018.02.013

Westwood, D. A., Heath, M., & Roy, E. A. (2003). No Evidence for Accurate Visuomotor Memory: Systematic and Variable Error in Memory-Guided Reaching. *Journal of Motor Behavior*, *35*(2), 127–133. https://doi.org/10.1080/00222890309602128

Wilson, E. T., Wong, J., & Gribble, P. L. (2010). Mapping Proprioception across a 2D Horizontal Workspace. *PLOS ONE*, *5*(7), e11851. https://doi.org/10.1371/journal.pone.0011851

Zanini, A., Patané, I., Blini, E., Salemme, R., Koun, E., Farnè, A., & Brozzoli, C. (2021). Peripersonal and reaching space differ: Evidence from their spatial extent and multisensory facilitation pattern. *Psychonomic Bulletin & Review*, *28*(6), 1894–1905. https://doi.org/10.3758/s13423-021-01942-9

Zuidhoek, S., Kappers, A. M. L., van der Lubbe, R. H. J., & Postma, A. (2003). Delay improves performance on a haptic spatial matching task. *Experimental Brain Research*, *149*(3), 320–330. https://doi.org/10.1007/s00221-002-1365-5

Zuidhoek, S., Visser, A., Bredero, MerleE., & Postma, A. (2004). Multisensory integration mechanisms in haptic space perception. *Experimental Brain Research*, *157*(2). https://doi.org/10.1007/s00221-004-1938-6

Appendix A: Post Experiment Surveys

Post-Study Participant Experience

Post-Study Participant Experience Survey

Thank you for completing the haptic perception task! We would appreciate your feedback on the experience. Please answer the questions below as honestly as possible.

All questions are completely optional as well as this survey, please fill out as much or as little as you'd like.

1. **How would you rate your overall experience during the haptic task?**
   (1 = Very Negative, 5 = Very Positive)
   - ○ 1
   - ○ 2
   - ○ 3
   - ○ 4
   - ○ 5

2. **How confident did you feel in your ability to perform the task?**
   (1 = Not Confident at All, 5 = Very Confident)
   - ○ 1
   - ○ 2
   - ○ 3
   - ○ 4
   - ○ 5

3. **How challenging did you find the haptic task?**
   (1 = Very Easy, 5 = Very Difficult)
   - ○ 1
   - ○ 2
   - ○ 3
   - ○ 4
   - ○ 5

4. **Did you find the task enjoyable?**
   (1 = Not Enjoyable at All, 5 = Very Enjoyable)
   - ○ 1
   - ○ 2
   - ○ 3
   - ○ 4
   - ○ 5

5. **Did you feel that the instructions were clear?**
   (1 = Not Clear at All, 5 = Extremely Clear)
   - ○ 1
   - ○ 2
   - ○ 3
   - ○ 4
   - ○ 5

6. **Do you have any feedback or suggestions for improving the haptic task or instructions?**

   (Please describe below):

Participant Background Questionnaire for Haptic Perception Study

Participant Background Questionnaire for Haptic Perception Study

Thank you for participating in our study. This questionnaire is designed to help us understand more about your background, which may help us interpret the results of the haptic task. Please answer the following questions as accurately as possible. Your responses will remain confidential and anonymous.

All questions are completely optional as well as this survey, please fill out as much or as little as you'd like.

1. Age _____ **2. Gender**:_____ **3. Sex**: _____

4. Height (cm/m or ft/in) **5. Weight (kg or lbs)**: **6. Arm length (cm)**: Ask me to measure!

7. Do you have any experience with video games?

- Yes, frequently in the present
- Yes, in the past
- Occasionally
- Rarely
- No experience

8. If yes, how many hours per week do you typically spend playing video games?

- Less than 1 hour
- 1-5 hours
- 6-10 hours
- More than 10 hours

9. Do you participate in any sports or physical activities? (e.g., tennis, swimming, yoga)

- Yes, frequently
- Occasionally
- Rarely
- No

10. If yes, which sports or physical activities do you participate in?

- (Please list all that apply): _____

11. Do you / have you played any musical instruments?

-Yes - No

12. If yes, which instruments do you play?

(Please list all that apply): _____

13. Have you had any previous experience with virtual reality (VR) or augmented reality (AR) technologies?

- Yes - No

14. If yes, how frequently do you use VR/AR technologies?

- Regularly
- Occasionally
- Rarely

15. How would you describe your spatial awareness skills?

- Excellent
- Above average
- Average
- Below average
- Poor

17. Have you ever taken part in a haptic perception study before?

- Yes - No

18. Do you have any other hobbies or activities that may involve tactile skills? (e.g., crafting, cooking, painting)

- (Please list all that apply): _____

19. Please scan the QR Code for the Edinburgh handedness inventory and state the laterality index you obtain: _____

The QR code is on your right side, on the door, you can't miss it!

Thank you for completing this questionnaire! Your responses will greatly help us in understanding individual differences that may impact performance in the haptic task.